AD-A185 466 THREE-DIMENSIONAL STRUCTURE OF BOUNDARY LAYERS IN TRANSITION TO TURBULENC (U) VIRGINIA POLYTECHNIC INST AND STATE UNIV BLACKSBURG DEPT OF E T HERBERT 1/1

UNCLASSIFIED 24 JUN 87 AFOSR-TR-87-0981 F49620-84-K-0002 F/G 20/4 NL

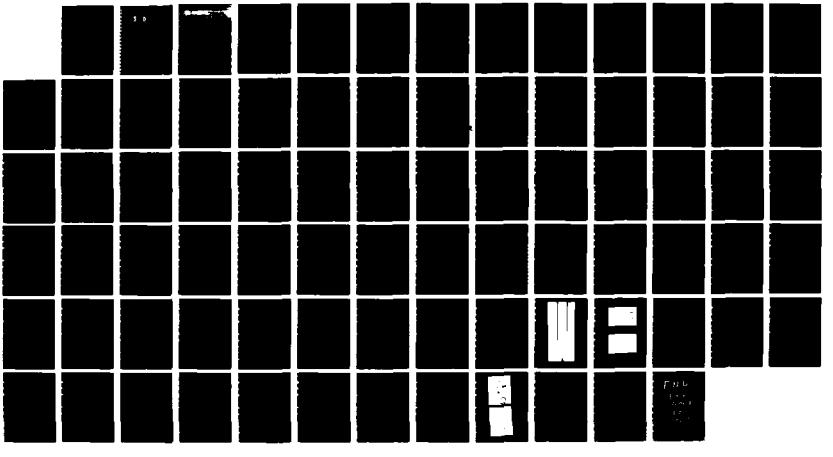

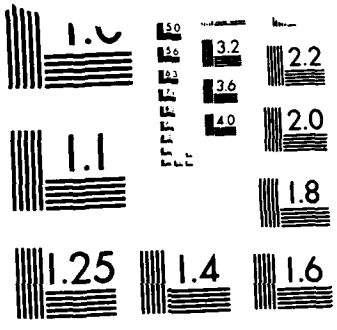

MICROCOPY RESOLUTION TEST CHART
NATIONAL BUREAU OF STANDARDS 1963-A

AD-A185 466

(2)

REPORT DOCUMENTATION PAGE

1a. REPORT SECURITY CLASSIFICATION: UNCLASSIFIED	1b. RESTRICTIVE MARKINGS:
2a. SECURITY CLASSIFICATION AUTHORITY	3. DISTRIBUTION/AVAILABILITY OF REPORT: Approved for Public Release, Distribution is Unlimited
2b. DECLASSIFICATION/DOWNGRADING SCHEDULE	
4. PERFORMING ORGANIZATION REPORT NUMBER(S)	5. MONITORING ORGANIZATION REPORT NUMBER(S): AFOSR-TR- 87-0981
6a. NAME OF PERFORMING ORGANIZATION: VPI & SU, ESM Department	6b. OFFICE SYMBOL (If applicable): CD
6c. ADDRESS (City, State and ZIP Code): Blacksburg, VA 24061	7a. NAME OF MONITORING ORGANIZATION: AFOSR/NA, Bldg 410, Bolling AFB, DC 20332
	7b. ADDRESS (City, State and ZIP Code): same as 7a
8a. NAME OF FUNDING/SPONSORING ORGANIZATION: Air Force Office of Scientific Research	8b. OFFICE SYMBOL (If applicable): NA
8c. ADDRESS (City, State and ZIP Code): Building 410, Bolling AFB DC 20332-6448	9. PROCUREMENT INSTRUMENT IDENTIFICATION NUMBER: F49620-84-K-0002
	10. SOURCE OF FUNDING NOS.

PROGRAM ELEMENT NO	PROJECT NO	TASK NO	WORK UNIT NO
61102F	2307	A2	

11. TITLE (Include Security Classification): Three-Dimensional Structure of Boundary Layers in Transition to Turbulence

12. PERSONAL AUTHOR(S): Thorwald Herbert

13a. TYPE OF REPORT	13b. TIME COVERED	14. DATE OF REPORT (Yr., Mo., Day)	15. PAGE COUNT
Final	FROM 84/02/01 TO 87/02/28	87 06 24	76

16. SUPPLEMENTARY NOTATION

17. COSATI CODES			18. SUBJECT TERMS (Continue on reverse if necessary and identify by block number)
FIELD	GROUP	SUB GR	Boundary Layer, Stability, Transition

19. ABSTRACT (Continue on reverse if necessary and identify by block number)

A unified theory of secondary instability in wall-bound shear flows has been developed. This theory rests on Floquet systems of stability equations and permits classification and quantitative analysis of different modes of secondary instability in the three-dimensional stage of laminar-turbulent transition. The catalogue of solutions is consistent with observations and predicts other phenomena that have not been identified in experiments. The theoretical results have been used to reproduce patterns in flow visualizations by computer animation. Analysis of the energy balance has shown a feedback loop between mean flow, two-dimensional, and three-dimensional disturbances that is considered key to the process of self-sustained transition. Various techniques have been developed to investigate details of the nonlinear three-dimensional processes involved in this feedback loop.

20. DISTRIBUTION/AVAILABILITY OF ABSTRACT	21. ABSTRACT SECURITY CLASSIFICATION
UNCLASSIFIED/UNLIMITED X SAME AS RPT ☐ DTIC USERS	Unclassified

22a. NAME OF RESPONSIBLE INDIVIDUAL	22b. TELEPHONE NUMBER (Include Area Code)	22c. OFFICE SYMBOL
Dr. James M. McMichael	(202) 767-4937	AFOSR/NA

DD FORM 1473, 83 APR EDITION OF 1 JAN 73 IS OBSOLETE

SECURITY CLASSIFICATION OF THIS PAGE: UNCLASSIFIED

COLLEGE OF ENGINEERING

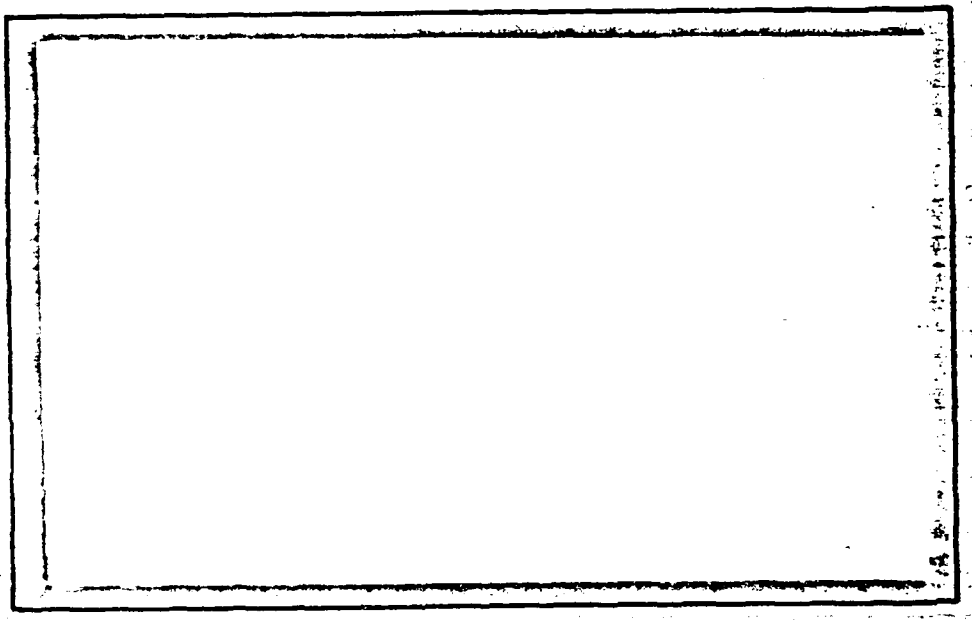

VIRGINIA POLYTECHNIC INSTITUTE AND STATE UNIVERSITY

BLACKSBURG, VIRGINIA

TABLE OF CONTENTS

Summary

A unified theory of secondary instability in wall-bound shear flows has been developed. This theory rests on Floquet systems of stability equations and permits classification and quantitative analysis of different modes of secondary instability in the three-dimensional stage of laminar-turbulent transition. The catalogue of solutions is consistent with observations and predicts other phenomena that have not been identified in experiments. The theoretical results have been used to reproduce patterns in flow visualizations by computer animation. Analysis of the energy balance has shown a feedback loop between mean-flow, two-dimensional, and three-dimensional disturbances that is considered key to the process of self-sustained transition. Various techniques have been developed to investigate details of the nonlinear three-dimensional processes involved in this feedback loop.

1. Research Objectives

The project "On the Three-Dimensional Structure of Boundary Layers in Transition to Turbulence" under AFOSR Contract F49620-84-K-0002 was originally planned as a joint theoretical - experimental effort with Thorwald Herbert and William S. Saric as principal investigators. After Dr. Saric left VPI & SU in Summer 1984, the contract was split, the research plan was rearranged, and most of the theoretical work remained at VPI & SU with Th. Herbert as principal investigator. The working period for this contract was 02/01/84 - 01/31/87 with an extension until 02/28/87.

A detailed description of the research objectives has been given in sections 2 and 3 of the original proposal. Overall, the work aimed at gaining insight into the intricate process of laminar-turbulent transition in plane shear flows, especially in boundary layers. Our research goals during the three-year period of the contract were comprised in four topics that are detailed in the following:

(1) Transition mechanisms

- (1.1) Analysis of fundamental (peak-valley splitting) modes in boundary layers
- (1.2) Analysis of combination resonance in Poiseuille flow and boundary-layer flow
- (1.3) Development of weakly nonlinear models of subharmonic instability and evaluation of their utility
- (1.4) Analysis of energy balance and vorticity dynamics for deeper understanding of transition and design of improved transition models
- (1.5) Analysis of the evolution of time-periodic and isolated wave packets in a weakly nonlinear framework.

(2) Three-dimensional flow field

- (2.1) Determine the amplitude levels for significant nonlinear interaction of three-dimensional disturbances with the modulated basic flow
- (2.2) Calculation of the three-dimensional flow field, in particular the formation of high-shear layers during peak-valley splitting
- (2.3) Analysis of the scales of the three-dimensional flow and of approximations for tertiary high-frequency instability
- (2.4)* Reproduction of smoke-flow visualizations by computer animation of theoretical data

(3) Effect of free-stream disturbances

- (3.1) Development of asymptotic or computational models for the entrainment of sound and exterior disturbances into the leading-edge flow for given contour and pressure distribution
- (3.2) Relation between phenomena in the viscous sublayer of turbulent flows and phenomena in pretransitional flows; analysis of scales and simple models of the feedback loops

(4) Nonlinear stages of three-dimensional development

- (4.1) Analysis of three-dimensional equilibrium states originating from subharmonic instability in plane Poiseuille flow

(4.2) Analysis of three-dimensional states associated with peak-valley splitting and a longitudinal vortex system

(4.3) Tracing of the most dangerous route (4.1 or 4.2) for a general parabolic velocity distribution

(4.4) Discussion of the relevance of these motions for the forced situation in the laminar sublayer of turbulent flows

The third topic, the study (3) of the effect of free-stream disturbances, especially the entrainment of exterior disturbances into the flow around the leading edge of a flat plate was adopted by W. S. Saric. This computational work is conducted at Arizona State University while the experimental facilities are under development. The flow visualizations (2.4) were not part of the original proposal. This topic has been included since the still pictures of laboratory experiments are difficult to interpret and usually show a mixture of different modes.

2. Research Achievements

Since the first description of the three-dimensional nature of boundary layer transition by Klebanoff et al. (1962), the explanation of the observed three-dimensional phenomena has been a challenge to theoreticians and stimulated the study of numerous weakly nonlinear (low order perturbation) models. Failure of these studies to provide convincing explanation and quantitative characterization of the observed phenomena can be caused by either (i) too low order of truncation, (ii) use of perturbation series outside their radii of convergence, or (iii) inappropriate choice of the primary instability modes involved in the model. The formulation of a rational perturbation approach (Herbert 1980, 1983a) allowed analysis of high-order series and led to the conclusion that previous and new models (Herbert & Morkovin 1980) of resonant or non-resonant interactions are insufficient for describing the observations of Klebanoff et al. (1962).

Guided by a revised interpretation of the observations, Herbert & Morkovin (1980) suggested that three-dimensional disturbances originate from parametric excitation in the streamwise periodic flow created by the primary TS wave. Simultaneously, Orszag & Patera (1981) found exponential growth of small 3D disturbances in transition simulations of channel flow and attributed this fact to the activity of a linear stability mechanism. Consequently, a theory of linear secondary instability based on Floquet systems of disturbance equations was formulated and first applied for studying three-dimensional disturbances in streamwise periodic equilibrium states in a plane channel (Orszag & Patera 1981, Herbert 1981, 1983b). There are four main results of this work: (i) Three-dimensional secondary instability can lead to different types of disturbances. Primary resonance with the TS wave produces peak-valley splitting as the TS amplitude exceeds some threshold. Subharmonic resonance can occur at even smaller amplitudes. (ii) Calculated disturbance velocities and growth rates are consistent with experiments. Three-dimensional modes grow on a fast convective time scale, typically by a factor of 100 within 5 cycles of the TS wave. (iii) Secondary instability originates from the redistribution of spanwise vorticity into streamwise periodic lumps near the critical layer. Growth of three-dimensional modes arises from combined vortex tilting and stretching. (iv) Analysis of the limit TS amplitude $A \to 0$ reveals the intricate connection between modes of primary and secondary

instability. This provides for the first time a rational means for evaluating existing and constructing new models of weakly nonlinear interactions.

Encouraged by the results for channel flow and guided by the nature of the secondary instability mechanism, Herbert (1983c) introduced approximations which permit application of the theory to the full class of classical stability problems, especially boundary layers. A comprehensive survey on the development and application of this approach has been given as an invited lecture at the Tenth U. S. National Congress of Applied Mechanics, June 16-20, 1986, Austin, Texas. For further information, Appendix A contains a copy of this paper. The systematic study of the various types of three-dimensional disturbances and review of experimental information has led to a broader and revised picture of transition in boundary layers. Many of these views are summarized in an article to be published in Annual Reviews of Fluid Mechanics, Vol. 20, 1988. A preprint of this article is provided as Appendix B. Here, we restrict discussion only to the main conclusions and some incomplete results.

The Floquet approach explains the linear secondary instability with respect to 3D disturbances as originating from parametric instability of a plane basic flow that is periodic in space and time. Different classes of modes are associated with different types of resonance: primary resonance results in peak-valley splitting modes; principal parametric resonance causes subharmonic modes of instability; both these classes can be considered special cases of combination resonance; vortex pairing is a degenerate (two- dimensional) case of subharmonic instability.

The theory is capable of quantitatively predicting the temporal growth rates and the spatial disturbance field up to the stages immediately preceding breakdown and transition. Comparison with the experiments of Kachanov & Levchenko (1984) has verified the results on the subharmonic instability in the Blasius flow (Herbert 1984a). Comparison with the experiments of Klebanoff et. al. (1962) has shown that the theory explains all the essential qualitative and quantitative aspects of peak-valley splitting in the Blasius flow (Herbert 1985). A detailed comparison with more recent measurements of peak-valley splitting by Cornelius (1985) will be published in the near future. Nishioka & Asai (1984) found essential agreement of their measurements on peak-valley splitting in plane Poiseuille flow with our results, even at unexpectedly large disturbance amplitudes. Recent results using the spatial (instead of the temporal) growth concept indicate further improvements in the prediction of growth rates, especially for boundary layers in adverse pressure gradients.

The development of the Floquet theory of secondary instability arising from the growth of TS waves in shear flows can well be considered a major breakthrough in hydrodynamic stability theory. Our work, although yet incompletely published, has found widespread attention. The formal classification of phenomena has provided an ordering scheme for virtually inconsistent observations. The explanation of Klebanoff's experimental results was overdue. Most important for practical purpose, however, seems to be the capability of predicting the growth rates for the various modes of secondary instability. Given the disturbance background, e.g. in a boundary layer, the amplitude of a specific disturbance as it grows in time or in the streamwise direction can be calculated. Experiments show that, as this amplitude reaches a certain level, the secondary disturbance takes over and shortly causes breakdown. Therefore, the prediction of breakdown is a matter of developing an empirical or theoretical measure for this critical amplitude level.

The close relation between the amplitude level for self-sustained growth of secondary disturbances and breakdown originates from the vortical nature of the secondary instability mechanisms. At sufficiently large amplitude, the primary TS-wave produces an array of vorticity concentrations near the critical layer. Bending, tilting, and stretching of these distributed vortices in regions of different streamwise velocity causes the strong growth of secondary disturbances on a convective (rather than viscous) time scale (Orszag & Patera 1983). As another consequence, this strong secondary instability can be considered a generic phenomenon in flows with primary TS-instability.

In a linear framework, secondary instability leads a parasitic life on the TS waves. Secondary modes may grow but will harmlessly decay as the vital vorticity concentrations fade away. However, the strong growth leads rapidly to three-dimensional amplitudes large enough to affect the two-dimensional wave development. In fact, the nonlinear self-interaction of the 3D mode may reproduce a vorticity concentration that sustains its growth. This process is key to the low subcritical transition Reynolds numbers in plane Poiseuille flow (and probably other closed flows) as well as to the self-sustained transition in boundary layers.

We have studied the nonlinear processes associated with the rapid growth of vortical disturbances on the basis of both the energy equation and the momentum equations. The analysis of the energy transfer between mean flow, TS wave, and 3D disturbances has been conducted first for plane Poiseuille flow (Croswell 1985, Herbert 1986a) and is currently adapted to boundary-layer flows. Although our approach differs in various aspects from Orszag & Patera's, we were led to essentially the same conclusions on the highly localized energy transfer from the mean flow into the 3D field, the close relation between areas of concentrated vorticity and strong energy transfer, and the catalytic role of the TS wave in this process. Beyond the concentrations in the plane of the mean flow, we also identify highly localized regions of strong energy transfer in the plane normal to the mean flow at those locations where the deflection of the spanwise vortex tubes is strongest. We also associate the areas of energy transfer with the symmetries of the various peak-valley splitting and subharmonic modes.

Analysis of the global energy transfer over a domain formed by the channel walls and the streamwise and spanwise wavelengths of the 3D disturbances reveals on one hand the different scale (convective rather than viscous) of the secondary instability, on the other hand an illuminating distribution of the transfer terms. At realistic amplitudes, typically 60% of the energy received from the mean flow provide the growth of the 3D mode, 30% are dissipated, while 10% are transferred into the 2D field. Whereas this loss is of minor importance for the 3D disturbance, the gain for the 2D field is considerable and may boost the growth or easily overweigh the (viscous) decay of the TS wave. In fact, the energy transfer from the 3D into the 2D field can be considered responsible for the observed ultimate growth of the 2D wave on a convective scale as the 3D wave attains a sufficiently high amplitude. Further considered the catalytic role of the 2D wave for the 3D growth, this energy transfer appears to be key to the feedback loop that causes self-sustained growth of the later stage of transition. We currently analyze this hypothesis for the Blasius boundary layer where some limited experimental information is available.

In addition to using the energy equation, we have pursued various approaches of solving the equations of motion. The initial attempt to study the nonlinear evolution of the 3D field in the boundary layer with perturbation methods applied to improved models of

combined primary models was largely unsuccessful. Similar experience has been reported by Nayfeh (1985) with respect to the linear secondary instability. This work has clearly shown the important role of Squire modes in the interaction indicated by dominating values of their interaction coefficients. It has not become clear, however, whether the overall failure of this approach is due to certain modes that may be missing in the model or due to lacking convergence of the series. As another suspect, the role of the continuous spectrum inherent to the primary stability equations in semi-infinite domains is unknown. In view of the numerous modes involved, a continuation of the approach to sufficiently high order for a series analysis is illusionary. The rather intricate analytical connections between numerous modes at extremely small amplitudes observed in the (linear) Floquet analysis (Herbert 1983) may well indicate a convergence problem of the weakly nonlinear method.

A more successful perturbation approach has been developed exploiting the fact that the interactions between 3D primary modes in earlier models are comprised in the modes of secondary instability readily available from Floquet analysis. As a simple case, we have developed the formulation and the numerical tools for studying the nonlinear development of a single (subharmonic or peak-valley splitting) mode of secondary instability up to reasonably high order. The most tedious task in this approach is the verification of the proper function of the computer programs. Surprisingly, the expansion in the spanwise direction is formally very similar to the expansion for 2D primary modes in the streamwise direction. The account for the streamwise periodic structure of the 3D field, however, is a non-trivial step that complicates formalism and computer programs and requires major computational efforts.

As a result of the expansion in the amplitude of a single secondary mode, we obtain at second order a modification of the mean flow, a contribution to the 2D fluctuation field, a spanwise periodic distortion of the mean flow, and the first harmonic of the 3D disturbance which is periodic in the streamwise and spanwise directions. Resonance with the 2D wave is not incorporated in the single-mode expansion. At third order, we obtain a Landau constant that accounts for those nonlinear effects on the growth rate of the 3D mode that directly originate from the 3D-3D interaction. The indirect effects of the modified mean flow on the TS amplitude growth, and through modification of the 2D wave field can be estimated a posteriori. It is not unexpected that the modifications of the planar field are especially strong in the neighborhood of the critical layer where the secondary modes exhibit maximum rms fluctuation. A first report on the formalism and results of this single-mode expansion has been given by Crouch & Herbert (1986).

A more complete model of combined 2D-3D and 3D-3D interaction is currently developed. In order to verify formulation and computer programs, we have recently implemented the symbolic manipulator Macsyma. The amplitude equations for this interaction model provide the essential coupling terms at second order. Although formally equivalent to the equations obtained from energy analysis, these amplitude equations provide more accurate information since they incorporate the change in the spatial structure of the flow field. In the a posteriori energy analysis, these changes cannot be taken into account.

Prior to the availability of detailed results on the nonlinear development, we have studied the three-dimensional flow field for subharmonic, fundamental, and combination modes. Velocity and vorticity distributions compare favorably with the scarce experimental data base. Since recent experimental work has emphasized the visualization of the 3D stage of transition, we have developed the tools for tracing path lines and for displaying the

temporal development of time lines on a high-resolution work station. The development due to subharmonic secondary instability has been recorded in a 8 mm movie. This movie shows for the first time in detail the formation of the often observed pattern of TS waves and the rapid evolution of the staggered structure of Λ vortices after the subharmonic disturbance has grown to sufficient amplitude. A second movie has been produced for visualization of other modes, especially those arising from combination resonance, and to demonstrate the dependence of the pictures on the location of the smoke wire.

For the analysis of three-dimensional equilibrium motions in plane Poiseuille flow, we have mapped the bifurcation points in terms of Reynolds number, wavenumber, and TS-amplitude. The nonlinear algebraic system representing the equations of motion for interacting two-dimensional and three-dimensional modes has been formulated and coded for the subharmonic and fundamental cases. The application of the programs has been held up, however, by the lack of convergence of the Newton method for solving the nonlinear equations. The suspicion of errors in the code turned out to be unjustified. The reason is the occurrence of a multiple (double) zero at the bifurcation point. Present work is directed toward overcoming this problem by use of improved starting solutions which may lead to local convergence at sufficient distance from the bifurcation point. Such improved solutions can be constructed by use of the perturbation method for 2D-3D interaction as soon as it has been verified and adapted to plane Poiseuille flow. As an alternative, we attempt to implement the extended Newton method that covers the case of double zeros.

3. Personnel

During the working period, the following personnel were partly supported under Contract F49620-84-K-0002:

Thorwald Herbert, Professor, Principal Investigator
Alan Haddow, Assistant Professor (visiting)
German Santos, Graduate Student (Ph.D. level)
Jeffrey Crouch, Graduate Student (Ph.D. level)
Joseph Croswell, Graduate Student (M.S. level)
Fabio Bertolotti, Graduate Student (M.S. level)
Charlotte R. Hawley, Research Specialist
Vineet Mehta, Undergraduate Student (hourly)

German Santos developed the concept of combination resonance for boundary layers and studied the application to plane shear flows. He also developed the numerical tools to study secondary instability in parallel flows in an infinite domain (mixing layer, wake). He will receive his degree in 1987.

Jeff Crouch developed formulation and computer programs for an innovative perturbation analysis of nonlinear secondary instability. He will receive his degree in 1987/88.

Joseph Croswell developed the formalism for the study of the energy balance and energy transfer between mean flow, primary and secondary disturbances. He applied this formalism to plane Poiseuille flow. He received the M.S. degree in Engineering Mechanics in July 1985.

Fabio Bertolotti was previously involved in research sponsored by the Office of Naval Research. He performed an analysis of spatially growing subharmonic modes in boundary layers with pressure gradients and studied the relation between secondary instability and separation. After receiving his M.S. in Engineering Science in June 1985, he designed and built the hardware and wrote a software system for computer animation of unstable boundary-layer flows on Apollo workstations. After a one-year work period in automobile aerodynamics with Pininfarina in Italy, he joined the Ph.D. program at VPI & SU in September 1986. He produced a movie on 'smoke-wire' visualizations of various routes to transition and works on a new concept for stability analysis of nonparallel flows.

4. Publications

The following publications, reports and communications acknowledge the support by AFOSR:

(1) "On the Early Stages of K-Breakdown in the Blasius Boundary Layer," by Th. Herbert, Bull. Amer. Phys. Soc. 29, p. 1540 (1984).

(2) "Secondary Instability of Plane Shear Flows - Theory and Application," by Th. Herbert, in: Laminar-Turbulent Transition, (Ed.) V. V. Kozlov, p. 9-21, Berlin - Heidelberg - New York: Springer-Verlag (1985).

(3) "Three-Dimensional Phenomena in the Transitional Flat-Plate Boundary Layer," by Th. Herbert, AIAA Paper No. 85-0489 (1985).

(4) "Aspects of Secondary Instability in Transition Management," by Th. Herbert, Abstract, AIAA Paper No. 85-0563 (1985).

(5) "On the Energetics of Primary and Secondary Instabilities in Plane Poiseuille Flow," by J. W. Croswell, M.S. Thesis, VPI & SU (1985).

(6) "The Subharmonic Route to Transition - An Animated Theory," by Th. Herbert and F. P. Bertolotti, 16 mm Movie, 8 min, VPI & SU (1985).

(7) "Floquet Analysis of Secondary Instability in Shear Flows," by Th. Herbert, F. P. Bertolotti, and G. R. Santos, in: Stability of Time Dependent and Spatially Varying Flows, (Eds.) D. L. Dwoyer and M. Y. Hussaini, pp. 43-57, Springer-Verlag (1985).

(8) "Vortical Mechanisms in Shear Flow Transition," Proc. Euromech 199 Colloquium "Direct and Large Eddy Simulation of Turbulent Flows," Munich, Germany, 1985. (Eds.) U. Schumann and R. Friedrich, Notes on Numerical Fluid Mechanics, Vol. 15, pp. 19-36, Braunschweig: Vieweg (1986).

(9) "Analysis of Secondary Instability in Boundary Layers," Proc. Tenth U. S. National Congress of Applied Mechanics, Austin, Texas (1986). (Ed.) J. Lamb, pp. 445-456 ASME (1986).

(10) "Combination Resonance in Boundary Layers," by G. R. Santos and Th. Herbert, Bull. Amer. Phys. Soc. *31*, p. 1718 (1986).

(11) "Perturbation Analysis of Nonlinear Secondary Instability in Boundary Layers," by J. D. Crouch and Th. Herbert, Bull. Amer. Phys. Soc. *31*, p. 1718 (1986).

(12) "Early Stages of Boundary-Layer Transition - An Animated Theory," by F. P. Bertolotti, G. R. Santos and Th. Herbert, 16 mm Movie, 8 min, Virginia Polytechnic Institute and State University, Blacksburg, Virginia (1986).

(13) "Instability Mechanisms in Shear Flow Transition," by B. J. Bayly, S. A. Orszag, and Th. Herbert, invited contribution to Ann. Rev. Fluid Mech. 20 (1988)

(14) "Secondary Instability of Boundary Layers," by Th. Herbert, invited contribution to Ann. Rev. Fluid Mech. 20 (1988)

The following papers reporting results obtained under the current support are in preparation:

(15) "Energetics of Secondary Instability in Plane Poiseuille Flow," by Th. Herbert and J. W. Croswell, to be submitted to J. Fluid Mech.

(16) "The Peak-Valley-Splitting Route to Transition in Boundary Layers," by Th. Herbert, to be submitted to AIAA Journal.

(17) "Vorticity Field and Energy Balance for Three-Dimensional Disturbances in Boundary Layers," by Th. Herbert, to be submitted to AIAA Journal.

(18) "Combination Resonance in Unstable Boundary Layers," by Th. Herbert, G. R. Santos and F. P. Bertolotti, to be submitted to AIAA Journal.

(19) "Weakly Nonlinear Analysis of Secondary Instability in the Blasius Boundary Layer," by Th. Herbert and J. D. Crouch, to be submitted to J. Fluid Mech.

(20) "A Study on Visualizations of Boundary-Layer Transition," by F. P. Bertolotti and Th. Herbert, to be submitted to Exp. Fluids.

5. Technical Presentations

The following papers were presented at meetings, conferences and seminars:

(1) "Three-Dimensional Phenomena in the Transitional Flat-Plate Boundary Layer," by Th. Herbert, AIAA 23rd Aerospace Sciences Meeting, Reno, Nevada (Jan. 1985).

(2) "Aspects of Secondary Instability in Transition Management," by Th. Herbert, AIAA Shear Flow Control Conference, Boulder, Colorado (March 1985).

(3) "Secondary Instability of Boundary Layers," by Th. Herbert, Department of Mechanical and Aerospace Engineering, Arizona State University, Tempe, Arizona (March 1985).

(4) "Three-Dimensional Instabilities of Boundary Layers," by Th. Herbert, School of Engineering, Georgia Institute of Technology, Atlanta, Georgia (May 1985).

(5) "Effect of Pressure Gradients on the Growth of Subharmonic Disturbances in Boundary Layers," by Th. Herbert and F. P. Bertolotti, Conference on Low Reynolds Number Aerodynamics, Notre Dame, Indiana (June 1985).

(6) "Three-Dimensional Phenomena in Boundary Layer Transition," by Th. Herbert, Department of Mechanical and Aerospace Engineering, Illinois Institute of Technology, Chicago, Illinois (June 1985).

(7) "Floquet Analysis of Secondary Instability in Shear Flows," by Th. Herbert, F. P. Bertolotti and G. R. Santos, ICASE/NASA Workshop on Stability of Time-Dependent and Spatially Varying Flows, Hampton, Virginia (Aug. 1985).

(8) "Vortical Mechanisms in Shear-Flow Transition," by Th. Herbert, Euromech Colloquium 199 on Direct and Large Eddy Simulation of Turbulent Flow, Munich,

Germany (Sept. 1985).

(9) "Three-Dimensional Instability of Boundary Layers," by Th. Herbert, University of Virginia, Charlottesville, Virginia (Oct. 1985).

(10) "Three-Dimensional Equilibrium States in Plane Channel Flow," by Th. Herbert, 22nd Annual Meeting of the Society of Engineering Science, University Park, Pennsylvania (Oct. 1985).

(11) "Puzzles in Nonlinear and Secondary Instability," by Th. Herbert, International Workshop on Stability and Transition in Bounded Shear Flows, Tucson, Arizona (Nov. 1985)

(12) "Stabilität ebener Scherströmungen," by Th. Herbert, Symposium on Laminar and Turbulent Boundary Layers - Dedicated in Memory of F. X. Wortmann, Universität Stuttgart, Germany (Dec. 1985).

(13) "Neue Wege zur Analyse sekundärer Instabilität," by Th. Herbert, Fakultät für Luft- und Raumfahrttechnik, Universität Stuttgart, Germany (Dec. 1985).

(14) "Three-Dimensional Instability of Boundary Layers," by Th. Herbert, Department of Applied Mathematics, Princeton University, Princeton, New Jersey (Feb. 1986).

(15) "Analysis of Secondary Instabilities in Boundary Layers," by Th. Herbert, Tenth U.S. National Congress of Applied Mechanics, Austin, Texas (June 1986).

(16) "Secondary Instability of the Blasius Boundary Layer," by Th. Herbert, Illinois Institute of Technology, Chicago, Illinois (July 1986).

(17) "Secondary Instability of the Hyperbolic Tangent Profile," by G. R. Santos and Th. Herbert, 23rd Annual Meeting of the Society of Engineering Science, Buffalo, New York (Aug. 1986).

(18) "Analysis of the Three-Dimensional Stage of Boundary-Layer Transition," by Th. Herbert, Florida State University, Tallahassee, Florida (Sept. 1986).

(19) "Analysis of the Three-Dimensional Stage of Boundary-Layer Transition," by Th. Herbert, Division of Engineering, Brown University, Providence, Rhode Island (Nov. 1986).

(20) "Nonlinear and Secondary Boundary-Layer Instabilities," by Th. Herbert, ICASE Workshop on Stability Theory, Hampton, Virginia (Nov. 1986).

(21) "Perturbation Analysis of Nonlinear Secondary Instability in Boundary Layers," by J. D. Crouch and Th. Herbert, 39th Annual Meeting of the Division of Fluid Dynamics, American Physical Society, Columbus, Ohio (Nov. 1986).

(22) "Combination Resonance in Boundary Layers," by G. R. Santos and Th. Herbert, 39th Annual Meeting of the Division of Fluid Dynamics, American Physical Society, Columbus, Ohio (Nov. 1986).

(23) "Three-Dimensional Instability of Boundary Layers," ICASE/NASA, Hampton, Virginia (Jan. 1987).

(24) "Three-Dimensional Instability of Boundary Layers," Department of Aerospace and Mechanical Engineering, University of Notre Dame South Bend, Indiana (Feb. 1987).

(25) "Three-Dimensional Instability of Boundary Layers," Department of Mechanical Engineering, Ohio State University, Columbus, Ohio (Feb. 1987).

6. References

K. C. Cornelius 1985 "Three dimensional wave development during boundary layer transition," Lockheed Georgia Research Report LG85RR0004.

J. W. Croswell 1985 "On the energetics of primary and secondary instabilities in plane Poiseuille flow," VPI & SU, M.S. thesis.

J. D. Crouch and Th. Herbert 1986 "Perturbation analysis of nonlinear secondary instability in boundary layers," *Bull. Am. Phys. Soc.*, vol. 31, p. 1718.

Th. Herbert 1980 "Nonlinear stability of parallel flows by high-order amplitude expansions," *AIAA J.*, vol. 18, pp. 243-247.

Th. Herbert 1981 "A secondary instability mechanism in plane Poiseuille flow," *Bull. Amer. Phys. Soc.*, vol. 26, p. 1257.

Th. Herbert 1983a "On perturbation methods in nonlinear stability theory," *J. Fluid Mech.*, vol. 126, pp. 167-186.

Th. Herbert 1983b "Secondary instability of plane channel flow to subharmonic three-dimensional disturbances," *Phys. Fluids*, vol. 26, pp. 871-874.

Th. Herbert 1983c "Subharmonic three-dimensional disturbances in unstable shear flows," AIAA Paper No. 83-1759.

Th. Herbert 1984 "Analysis of the subharmonic route to transition in boundary layers," AIAA Paper No. 84-0009.

Th. Herbert 1985 "Three-dimensional phenomena in the transitional flat-plate boundary layer," AIAA Paper No. 85-0489.

Th. Herbert 1986 "Vortical mechanisms in shear flow transition," in *Proc. Euromech 199 on Direct and Large Eddy Simulation of Turbulent Flow, Munich, Germany*, ed. U. Schumann and R. Friedrich, pp. 19-36, Vieweg-Verlag.

Th. Herbert and M. V. Morkovin 1980 "Dialogue on bridging some gaps in stability and transition research," in *Laminar-Turbulent Transition*, ed. R. Eppler and H. Fasel, pp. 47-72, Springer-Verlag.

Yu. S. Kachanov and V. Ya. Levchenko 1984 "The resonant interaction of disturbances at laminar-turbulent transition in a boundary layer," *J. Fluid Mech.*, vol. 138, pp. 209-247.

P. S. Klebanoff, K. D. Tidstrom, and L. M. Sargent 1962 "The three-dimensional nature of boundary-layer instability," *J. Fluid Mech.*, vol. 12, pp. 1-34.

A. H. Nayfeh 1985 "Three-dimensional spatial secondary instability in boundary-layer flows," AIAA Paper No. 85-1697.

M. Nishioka and M. Asai 1984 "Evolution of Tollmien-Schlichting waves into wall turbulence," in *Turbulence and Chaotic Phenomena in Fluids*, ed. T. Tatsumi, pp. 87-92, North-Holland.

S. A. Orszag and A. T. Patera 1981 "Subcritical transition to turbulence in plane shear flows," in *Transition and Turbulence*, ed. R. E. Meyer, pp. 127-146, Academic Press.

S. A. Orszag and A. T. Patera 1983 "Secondary instability of wall-bounded shear flows," *J. Fluid Mech.*, vol. 128, pp. 347-385.

Appendix A

Analysis of Secondary Instabilities in Boundary Layers

Proc. Tenth U. S. Natl. Cong. Appl. Mech., Austin, Texas, 1986
Ed. J. P. Lamb, pp. 445-456, ASME (1987)

ANALYSIS OF SECONDARY INSTABILITIES IN BOUNDARY LAYERS

T. Herbert
Department of Engineering Science and Mechanics
Virginia Polytechnic Institute and State University
Blacksburg, Virginia

Abstract

The practical need for prediction and ultimately control of laminar-turbulent transition requires deeper understanding of the transition mechanisms and tools for quantitative analysis of the transition process beyond the onset of primary instability with respect to TS waves. Motivated by this need, we have developed and applied a linear theory of secondary instability with respect to three-dimensional disturbances. This theory permits formal classification and quantitative study of the variety of observed three-dimensional phenomena that provide the link between TS waves and transition. The secondary instability originates from the dynamics of streamwise periodic vorticity concentrations subject to the surrounding shear flow. We give a survey on the key elements that guided the development of the theory and indicate the underlying mathematical concepts. Various classes of three-dimensional disturbances are identified. Some numerical results are given to characterize the parametric dependence of the secondary instability. A comparison with hot-wire data is made. The patterns of subharmonic modes in flow visualizations are reproduced by computer-animation of the theoretical data.

1. Introduction

Early experimental studies using hot-wire anemometers [1,2] or flow visualization techniques [3,4] have established a rather detailed picture of the phases of transition. In short, the sequence of events is as follows:

(1) Onset of instability with respect to essentially two-dimensional TS waves.

(2) Slow growth of the amplitude of the TS waves to a finite value, typically 1% in terms of the streamwise rms fluctuation.

(3) Onset of three-dimensionality on a spanwise scale similar to the TS wavelength. Formation of peaks and valleys, i.e. spanwise alternating regions of enhanced or reduced disturbance growth. Simultaneous occurrence of longitudinal vortices.

(4) Rapid growth of the three-dimensionality (peak-valley splitting). Formation of inflectional instantaneous velocity profiles with embedded high-shear layers at the peak positions.

(5) Occurrence of small-scale, high-frequency velocity fluctuations (spikes) in the neighborhood of the high-shear layers

(6) Onset of irregular motion, breakdown of the laminar flow.

Two remarks are in order on this picture of transition. First, this sequence of events relates only to the particular experimental procedure that raises the level of two-dimensional disturbances of given frequency above the noisy background by using a vibrating ribbon. Second, this picture is incomplete as will be discussed below. Nevertheless, this sequence of events is one possible route to transition and appears accessible to analysis. In fact, this picture has stimulated and guided various theoretical and computational work.

The first step of linear (primary) instability can be predicted using the Orr-Sommerfeld equation for parallel flows. Accounting for the streamwise growth of the boundary layer [5] slightly modifies the results at low Reynolds number and improves the agreement with the experimental data of Schubauer & Skramstad.[6] The characteristics of finite-amplitude TS waves in step 2 have been studied both with perturbation methods [7] and by numerically solving the Navier-Stokes equations.[8] At the low amplitudes of concern, however, there is little effect of nonlinearity on the disturbance growth or velocity distribution.

The true challenges are the qualitative changes from two-dimensional to three-dimensional motion in step 3 and from large to small scales in step 5. Originally, this latter phenomenon has been attributed to a secondary instability mechanism. In fact, stability analysis of the measured instantaneous velocity profiles indicates that the occurrence of higher-frequency disturbances can be understood as a vortical instability of the localized high-shear layers.[9, 10, 11]

The development of three-dimensionality in step 3 stimulated various theoretical analyses [12, 13, 14, 15, 16] using weakly nonlinear models. In some of these models, the spanwise wavelength of the peak-valley splitting appears as a parameter; other models are based on the concept of resonant wave interaction at specific spanwise wavelength. The development in this field continued with more complex models of resonant wave interactions [17] and non-resonant models involving waves and longitudinal vortices.[18] However, neither of these weakly nonlinear theories was able to provide satisfactory explanation and quantitative characterization of the experimental facts.

For a variety of reasons, the experiments of Nishioka and co-workers [19, 20, 21] on transition in plane channel flow are a milestone in transition research. First, this strictly parallel flow allows a rather clean mathematical treatment. Much pioneering work has been done on the nonlinear stability of this flow. This work, however, has been in conflict with the experimental fact of low subcritical transition. Nishioka et al. were the first to obtain laminar flow at supercritical Reynolds number and to verify the results of the linear stability analysis. At the same time, they verified the methods used and the results obtained in studies of nonlinear stability. Second, they found that transition in channel flow follows the same steps as in boundary layers, and hence established channel flow as a prototype for transition analysis in wall-bound shear flows. Third, they performed hot-wire measurements beyond the occurrence of spikes and breakdown [22, 23] and extended the above picture. They showed that at breakdown the flow exhibits all major characteristics of turbulent flow, including the formation of a viscous sublayer, and bursts (at the TS frequency).

The advance of computers and computational methods has been a creeping revolution that allowed simulations of transition, especially for channel flow [24, 25, 26] under controlled conditions. Similar work for boundary layers [27, 28] suffers somewhat from the lack of ideas to specify proper conditions for the outflow at the downstream end of the computational domain. Therefore, transition simulations for boundary layers usually consider the temporal development of the flow in a spatially periodic box. Surprisingly, computational and experimental results are strikingly similar up to the stage where numerical resolution becomes insufficient. The advantage of the numerical work is that the wealth of information concealed in the computer output can be extracted with relative ease which is not true of the data obtained in laboratory experiments.

Motivated by new results from the research group of the USSR Academy of Sciences in Novosibirsk, the exchange of ideas at the AGARD Meeting in Copenhagen, 1977, and the IUTAM Symposium on Laminar-Turbulent Transition in Stuttgart, 1979, a new generation of boundary-layer experiments was conducted. Hot-wire analysis [29, 30, 31, 32] and flow visualizations [33] led to a more detailed and extended picture of the transition process. Perhaps the most striking observation was the non-uniqueness of step 3 and the subsequent events. Depending on minute parameter changes (e.g. the level of ribbon vibration at otherwise fixed conditions), peak-valley splitting can change over into a subharmonic mode of three-dimensional development. This mode can be clearly identified by a relatively broad peak at half the TS frequency in power spectra of the streamwise velocity fluctuations.[34] Under controlled conditions,[30] clean subharmonic or combination resonance can be observed. The non-uniqueness also extends to the spanwise wavelength of the three-dimensional phenomena [33] which was earlier believed to be a repeatable characteristic of the transition process.[1, 35]

In parallel with the gathering of new observations, Blackwelder [36] and Herbert & Morkovin [18] suggested an essential modification of the transition picture. Earlier, the occurrence of three-dimensionality in step 3 had been attributed to spanwise differential amplification of TS waves, while the onset of spikes was considered as arising from secondary instability. The revised picture considers peak-valley splitting as the manifestation of a secondary instability. Herbert & Morkovin [18] suggested that three-dimensional disturbances originate from parametric excitation in the streamwise periodic flow created by the finite-amplitude TS wave. Simultaneously, Orszag & Patera [25] observed exponential growth of small three-dimensional disturbances in their transition simulations in a plane channel and attributed this fact to the activity of a new linear stability mechanism. Subsequent work [25, 37, 38, 39] led to the formulation of a theory of secondary instability for periodic equilibrium motions in a plane channel based on Floquet systems.

There are four main results of this work: (i) Three-dimensional secondary instability can lead to different types of disturbances. Primary resonance with the TS wave produces peak-valley splitting as the TS amplitude exceeds some threshold. Subharmonic resonance can occur at even smaller amplitudes. (ii) Calculated disturbance velocities and growth rates are consistent with experiments. Three-dimensional modes grow on a fast convective time scale, typically by a factor of 100 within 5 cycles of the TS wave. (iii) Secondary instability originates from the redistribution of spanwise vorticity into streamwise periodic lumps near the critical layer. Growth of three-dimensional modes arises from combined vortex tilting and stretching. (iv)

Analysis of the limit TS amplitude $A \rightarrow 0$ reveals the intricate connection between modes of primary and secondary instability. This provides for the first time a rational means for evaluating existing, and constructing new models of weakly nonlinear interactions.

Encouraged by the results for channel flow, and guided by the nature of the secondary instability mechanism, Herbert [40] introduced approximations which permit application of the theory to the full class of classical stability problems, especially boundary layers. Application of this Floquet theory of secondary instability to the Blasius boundary-layer flow [41, 42, 43] provided results consistent and mostly in quantitative agreement with the work of Klebanoff and co-workers [1] and Cornelius [44] on peak-valley splitting and with the results of Kachanov & Levchenko [29, 30] on subharmonic and combination resonance.

In this paper, we briefly describe the underlying concepts of the Floquet theory of secondary instability. From the general form of the disturbances we derive special classes of instability modes and relate their formal properties to the observations. Some numerical results are given in order to characterize the parametric dependence of the secondary growth rates. A comparison with hot-wire data on subharmonic instability and peak-valley splitting is made. The patterns of subharmonic modes in flow visualizations are reproduced by computer-animation based on the theoretical data.[45]

2. Formal Considerations

In our approach to secondary instability, we recognize in step 2 of the above described transition picture that the flow is no longer of the Blasius type but experiences a modulation by the finite-amplitude TS wave. In a coordinate system moving with the phase speed of this wave, the flow can be considered as almost steady and streamwise periodic. We follow the standard procedure of linear stability and decompose the velocity field $\mathbf{v}$ into a basic flow $\mathbf{v}_2$ and disturbances $\mathbf{v}_3$ that are sufficiently small for linearization. Substitution into the Navier-Stokes equations and subtracting the equations for the basic flow (which we assume to be identically satisfied) provides the linear stability equations

$$\left(\frac{1}{R}\nabla^2 - \frac{\partial}{\partial t}\right)\mathbf{v}_3 + (\mathbf{v}_2\cdot\nabla)\mathbf{v}_3 + (\mathbf{v}_3\cdot\nabla)\mathbf{v}_2 = -\nabla p_3 ,$$

$$\nabla \cdot \mathbf{v}_3 = 0 . \qquad (1)$$

In general, the basic flow and its derivatives determine the coefficients of the stability equations. In our case, we can write the basic flow in the form

$$\mathbf{v}_2(x',y,t) = \mathbf{v}_0(y) + A\,\mathbf{v}_1(x',y,t) , \qquad (2)$$

where $\mathbf{v}_0 = \mathbf{v}_0(y)$ represents the Blasius flow, A the amplitude of the periodic modulation, and $\mathbf{v}_1$ a solution of the Orr-Sommerfeld equation for a given set of parameters. We normalize $\mathbf{v}_1$ such that A is a direct measure for the maximum streamwise rms fluctuation (usually denoted as u'_m). All quantities are nondimensional using the outer velocity U_∞ and $\delta_r = (\nu L/U_\infty)^{1/2}$ for reference, where L is the distance from the leading edge. Consequently, $R = (U_\infty L/\nu)^{1/2}$. We change from the laboratory frame to a Galilean frame moving with the TS phase velocity c_r. In this frame, the basic flow satisfies

$$\mathbf{v}_2(x,y) = \mathbf{v}_2(x+\lambda_x,y) , \quad x = x' - c_r t , \qquad (3)$$

where $\lambda_x = 2\pi/\alpha_r$ is the wavelength of the TS wave.

Obviously, this choice of the basic flow involves some approximations that can be considered a generalization of the parallel-flow approximation. The parallel-flow assumption extends the local conditions at some streamwise position x_0 to the range $-\infty < x < \infty$. In our case, we neglect not only the small transverse velocity and the streamwise variation of the boundary layer profile, but moreover, the small (temporal or spatial) variation of the amplitude A, and the distortion of the TS velocity profile by nonlinear effects. Justification for these approximations will be given below.

A look at the linear disturbance equations (1) indicates a qualitative difference between the cases $A = 0$ and $A \neq 0$. In absence of the TS wave, equations (1) form the basis of the classical theory of primary instability. Due to the independence of the basic flow of t, x, and z, the normal mode concept can be applied with respect to these variables. After some rearrangement, this leads to the Orr-Sommerfeld equation for the velocity component v and to Squire's equation for the vorticity component η normal to the plate.

For $A \neq 0$, we are faced with a system of partial differential equations with x-periodic coefficients. The normal mode concept can still be applied with respect to z and t and three-dimensional disturbances can be written in the form

$$\mathbf{v}_3(x,y,z,t) = e^{\sigma t} e^{i\beta z}\,\mathbf{V}(x,y) . \qquad (4)$$

We consider the spanwise wave number $\beta = 2\pi/\lambda_z$ as real, whereas $\sigma = \sigma_r + i\sigma_i$ is in general complex. The key step in the development of the theory of secondary instability is the identification of classes and forms of $\mathbf{V}(x,y)$. In essence, insight into the streamwise structure of the disturbances can be gained from the Floquet theory of ordinary differential equations. Beyond the periodicity of the coefficients, we exploit the fact that the physical solution must be real, and therefore any complex solution $\mathbf{v}_3$ implies the existence of a complex conjugate solution $\mathbf{v}_3^\dagger$. Moreover, the system of equations can be written in a form with real coefficients. In this case, Floquet theory suggests solutions in the form

$$\mathbf{V}(x,y) = e^{\gamma x}\,\tilde{\mathbf{V}}(x,y) ,$$

$$\tilde{\mathbf{V}}(x+2\lambda_x,y) = \tilde{\mathbf{V}}(x,y) , \qquad (5)$$

where $\gamma = \gamma_r + i\gamma_i$ is a characteristic exponent, and

$\tilde{\mathbf{V}}$ is periodic in x with wavelength $2\lambda_x$. Hence, we can write $\mathbf{v}_3$ in the form

$$\mathbf{v}_3 = e^{\sigma t} e^{\gamma x} e^{i\beta z} \sum_{m=-\infty}^{\infty} \hat{\mathbf{v}}_m(y) e^{im\hat{\alpha}x}, \qquad (6)$$

where $\hat{\alpha} = \alpha_r/2$. The components of $\hat{\mathbf{v}}_m$ are governed by an infinite system of ordinary differential equations.

Since the basic flow $\mathbf{v}_2$ with wavenumber $\alpha_r = 2\hat{\alpha}$ provides coupling only between components $\hat{\mathbf{v}}_m$ and $\hat{\mathbf{v}}_{m\pm 2}$, this system splits into two separate systems for even and odd m that describe two classes of solutions

$$\mathbf{v}_f = e^{\sigma t} e^{\gamma x} e^{i\beta z} \tilde{\mathbf{v}}_f(x,y),$$

$$\tilde{\mathbf{v}}_f = \sum_{m\ even} \hat{\mathbf{v}}_m(y) e^{im\hat{\alpha}x}, \qquad (7)$$

$$\mathbf{v}_s = e^{\sigma t} e^{\gamma x} e^{i\beta z} \tilde{\mathbf{v}}_s(x,y),$$

$$\tilde{\mathbf{v}}_s = \sum_{m\ odd} \hat{\mathbf{v}}_m(y) e^{im\hat{\alpha}x}. \qquad (8)$$

The periodic functions $\tilde{\mathbf{v}}_f$ and $\tilde{\mathbf{v}}_s$ obviously satisfy

$$\tilde{\mathbf{v}}_f(x+\lambda_x, y) = \tilde{\mathbf{v}}_f(x,y),$$

$$\tilde{\mathbf{v}}_s(x+2\lambda_x, y) = \tilde{\mathbf{v}}_s(x,y). \qquad (9)$$

Therefore, we denote $\mathbf{v}_f$ as the fundamental mode, associated with primary resonance, and $\mathbf{v}_s$ as the subharmonic mode, originating from principal parametric resonance.

It is interesting to note that the two classes of modes are analytically connected, since no restriction is imposed on the value of γ_i. Replacing γ in (7) by $\gamma = \gamma' \pm i\hat{\alpha}$ and renumbering the terms in the Fourier series leads to an expression formally equivalent to (8). Nevertheless, it is convenient to distinguish the two classes for the analysis of special cases as well as in the numerical work. We also note that to within this renumbering modes with γ and $\gamma \pm i2k\hat{\alpha}$ are identical for any positive integer k. Therefore, it is sufficient to consider $|\gamma_i| \leq \hat{\alpha}$. It is convenient to introduce the following classification of modes:

- Fundamental modes: eq. (7) with $\gamma_i = 0$
- Subharmonic modes: eq. (8) with $\gamma_i = 0$
- Detuned fundamental modes: eq. (7) with $\gamma_i > 0$
- Detuned subharmonic modes: eq. (8) with $\gamma_i > 0$

The rational behind this choice of notation is the practical need for using truncated Fourier series that do not allow for renumbering, and the even or odd number of Fourier modes in symmetrically truncated series for subharmonic and fundamental modes, respectively, as will be discussed below.

The characteristics of the fundamental modes are formally consistent with observations. The modes are doubly periodic with wavelengths λ_x and λ_z as the ordered pattern in the flow visualizations of Saric & Thomas.[33] The aperiodic term $\mathbf{v}_0$ in (7) represents a spanwise periodic mean flow distortion (u_0) and a longitudinal vortex system (v_0, w_0). The fact that this vortex system is an integral part of the three-dimensional disturbance and grows simultaneously with the fluctuating components is consistent with the observations of peak-valley splitting. The aperiodic component is absent from the subharmonic modes (8). These modes are doubly periodic with $2\lambda_x$ and λ_z, and invariant under the translation $(x, z) \rightarrow (x + \lambda_x, z + \lambda_z/2)$, a characteristic of the staggered pattern in visualizations of subharmonic modes. In frequency spectra from a laboratory-fixed probe, linear subharmonic modes produce peaks at odd multiples of the subharmonic frequency but not at the fundamental frequency and its harmonics.

The occurrence of two complex quantities, σ and γ, in the eigenvalue problem for secondary disturbances leads to an ambiguity similar to that associated with the Orr-Sommerfeld equation. Only two of the four real quantities σ_r, σ_i, γ_r, γ_i can be determined; the other two must be chosen. We have already identified γ_i as the detuning parameter that controls the wavenumber content of the disturbed flow in the streamwise direction. In a similar way, σ_i is associated with the frequency content of the flow. The real parts σ_r and γ_r, on the other hand, govern the growth of the disturbance with respect to t or x, respectively, and are of prime interest in an analysis of secondary instability. It is important, however, to recognize that spatial growth of disturbances in the streamwise direction relates to the laboratory frame x', not to the moving frame x. In continuing the classification of modes of secondary instability, we distinguish

- Temporal (temporally growing) modes. In this case, we assume $\gamma_r = 0$ and consider σ as the eigenvalue. The temporal growth rate is given by σ_r, while σ_i can be interpreted as frequency shift with respect to the TS frequency. Modes with $\sigma_i = \gamma_i c_r$ travel synchronous with the basic flow, where γ_i is the given detuning with respect to the wave number.
- Spatial (spatially growing) modes. Since spatial growth is measured in the laboratory frame x', y, z, we rewrite

$$e^{\sigma t} e^{\gamma x} = e^{(\sigma - \gamma c_r)t} e^{\gamma x'}, \qquad (10)$$

and choose $\sigma_r = \gamma_r c_r$ in order to suppress temporal growth effects. Hence, γ_r provides the spatial growth rate in the laboratory frame while γ_i is the shift in the streamwise wavenumber. Detuning with respect to the frequency is given by the value of $\sigma_i - \gamma_i c_r$. Only in the case of tuned spatial modes can γ be considered the complex eigenvalue of the problem. Due to the occurrence of both σ_i and γ_i in the detuning parameter, the analysis of detuned spatial modes is a rather intricate task. It is of interest, though, since such modes have been observed by Kachanov & Levchenko.[29,30]

In general, detuned modes are associated with combination resonance. If we consider for simplicity the temporally growing modes, this can be immediately seen when forming the physical solution that must be real. Since $\gamma_i \neq 0$, the complex conjugate solution is detuned by $-\gamma_i$ and consequently the physical solution contains wavenumbers $m\alpha \pm \gamma_i$. The sum of suitable pairs of wave numbers matches the TS wave number.

3. Numerical Aspects

The derivation of the equations for the Fourier coefficients $\hat{\mathbf{v}}_m$ in (7), (8) is a straightforward but tedious matter. Simplifications of the equations arise for the temporal tuned modes with $\gamma = 0$. Moreover, the temporal eigenvalue σ appears linear in these equations.

Primary and secondary stability problems are numerically solved using a spectral collocation method with Chebyshev polynomials. This method converts the ordinary differential equations and boundary conditions into systems of algebraic equations. We prefer the direct treatment of the boundary value problem over shooting methods since we maintain access to spectra of eigenvalues for temporally growing modes. The spectrum is extremely helpful for reliably identifying the most relevant modes in different regions of the multi-dimensional parameter space and for untangling their analytical connections.

For boundary layers, we obtain a finite domain by an algebraic mapping $Y = y_0/(y + y_0)$ that transforms $y = 0, \infty$, into $Y = 1, 0$, respectively. The parameter y_0 controls the density of collocation points in the neighborhood of the wall. Only odd Chebyshev polynomials are applied such that the boundary conditions for $y \to \infty$ are automatically satisfied. Typically, $J = 30$ collocation points are used, and y_0 is chosen to place half of the points within the displacement thickness of the boundary layer. For every (real or complex) function $\hat{\mathbf{v}}_m(y)$ in (7), (8), $2J + 3$ (real or complex) unknowns have to be included into the homogeneous system of algebraic equations. In view of the size of the resulting systems, the truncation of the Fourier series is crucial for the numerical work.

For subharmonic modes, the lowest possible truncation is $|m| \leq 1$, which includes only $\hat{\mathbf{v}}_{-1}$ and $\hat{\mathbf{v}}_1$. The lowest approximation for fundamental modes is $|m| \leq 2$ and includes $\hat{\mathbf{v}}_{-2}$, $\hat{\mathbf{v}}_0$ and $\hat{\mathbf{v}}_2$. Detailed numerical studies [43] have shown that the Fourier series converge indeed rapidly, and the lowest truncation provides sufficient accuracy for any practical purpose.

The numerical work for tuned modes can be further simplified by exploiting that any complex solution $\mathbf{v}_3$ implies a second solution $\mathbf{v}_3^\dagger$. Moreover, only the square β^2 of the spanwise wavenumber appears in the equations such that the results for β and $-\beta$ are identical.

After proper rearrangement, the coefficient functions are governed by systems of equations with real coefficients.[46] The solution however is only real for real σ. The case of real $\sigma = \sigma_r$ is of particular interest since synchronization between basic flow and disturbances offers an optimum chance for energy transfer, and the principal modes of subharmonic and fundamental instability at larger amplitudes are indeed associated with a real solution. Since the amplitude A appears linear in the stability equations, real $\sigma(A)$ enables an inverse eigenvalue search for $A(\sigma)$, i.e. the search for the value of the amplitude that produces a given amplification rate. Similar conclusions can be drawn for spatially growing modes.

Concerning the choice between temporal and spatial growth concept, the situation is analogue to the primary stability analysis. The temporal eigenvalue σ appears linear in the equations. Therefore, spectra and single eigenvalues can be obtained by standard procedures of linear algebra. In the spatial formulation, the eigenvalue γ appears up to the fourth power. Although methods exist to obtain spectra in this case, the required computations are rather demanding. Therefore, we have exploited the fact that neutral behavior is independent of the chosen growth concept. Parameter combinations for neutral behavior, $\sigma_r = 0$, have been identified using the temporal concept. Starting from these points, the principal eigenvalue can be traced using the spatial concept. The local procedure for spatial eigenvalues γ rests on Newton iteration. Although this procedure is more costly than tracing temporal eigenvalues, it is more convenient for following the downstream development of disturbances of fixed dimensional frequency and spanwise wavelength, as it occurs in experiments.

4. Results

In the following, we use the frequency parameter $F = 10^6 \cdot \alpha_r c_r / R$, and $b = 10^3 \cdot \beta / R$ in order to specify three-dimensional disturbances of fixed dimensional frequency and spanwise wavelength as they travel downstream. The key experiments provide details on different aspects of secondary instability at different frequencies:

- $F = 58.8$: hot-wire data on peak-valley splitting, Klebanoff et al.[1]
- $F = 64.4$: hot-wire data on peak-valley splitting, Cornelius [44]
- $F = 83$: flow-visualizations of various modes, Saric & Thomas [33]
- $F = 124$: hot-wire data on subharmonic and combination resonance, Kachanov & Levchenko [29, 30]

Figure 1 relates the location of the vibrating ribbon (or wire) and the range of Reynolds numbers studied in these experiments to the stability diagram for Blasius flow. There is yet no set of hot-wire data available

that would allow for a comparison of subharmonic and fundamental modes at fixed frequency.

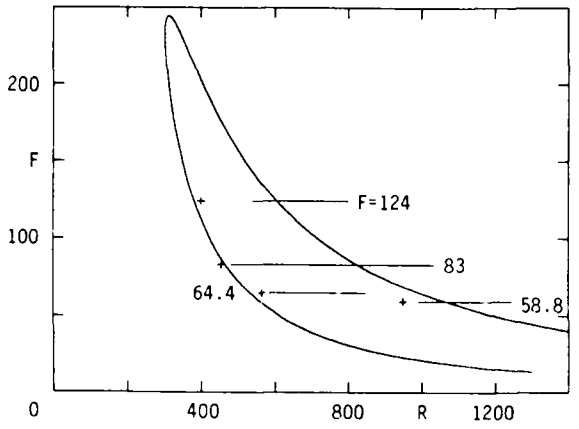

Figure 1. Stability diagram for the Blasius boundary layer. The horizontal lines indicate the frequency and Reynolds number range in the experiments.

Preference for lower frequencies in studies on peak-valley splitting is likely due to the need for stronger TS growth and larger amplitudes. The amplitude growth curves for TS waves at frequencies $F = 124$ and 64.4 are given in figure 2, and show the essentially larger amplitude ratio for the lower frequency. The growth rate of secondary modes, however, depends on the absolute amplitude, and therefore the curves in figure 2 become significant only for given initial amplitude A_0, or given disturbance background for that matter.

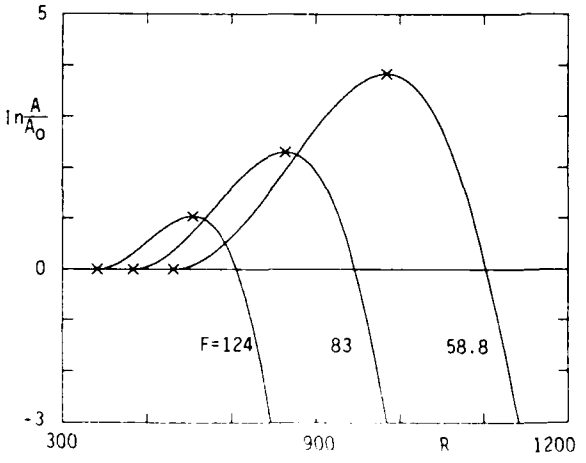

Figure 2. Amplitude growth curves for TS waves.

A systematic discussion of the parametrical dependencies exceeds the scope of this paper. For relevant amplitudes, $A \gtrsim 0.005$ say, the properties of the principal, i.e. most amplified modes of temporal subharmonic or fundamental instability can be summarized as follows:

- The eigenvalue σ is real, i.e. secondary mode and TS wave are phase-locked and travel at the same phase speed.
- The growth rate σ_r is large in comparison with the maximum growth rate of TS waves. Typically, secondary modes grow by two orders of magnitude within a few TS cycles.
- Instability, $\sigma_r > 0$, occurs in a broad band of spanwise wave numbers.
- The growth rate σ_r increases with increasing TS amplitude A at otherwise fixed parameters.
- The growth rate σ_r increases with increasing Reynolds number at otherwise fixed parameters.
- The growth characteristics of subharmonic and fundamental modes are similar with the subharmonic being the most dangerous mode at low TS amplitude levels.

The latter fact is due to a characteristic difference between subharmonic and fundamental modes: fundamental instability, i.e. peak-valley splitting is a threshold phenomenon and occurs only at sufficiently large TS amplitudes. Subharmonic instability, in contrast, can occur at arbitrarily small TS amplitudes due to resonance of Craik's[15] wave triad. We note, however, that growth of secondary modes is only observable and leads only to transition if

- The initial amplitude of the three-dimensional disturbance is sufficiently large.
- The conditions for growth persist for a sufficiently long time or streamwise distance.

The role of the fetch for occurrence of subharmonic instability has been discussed by Saric & Thomas.[33] It also seems that the frequent observation of peak-valley splitting is due to favorization of longitudinal vorticity disturbances in wind tunnels with usually large contraction ratios. Computer simulations of boundary-layer transition by Spalart & Yang [47] show that even at large TS amplitudes pure peak-valley splitting cannot be obtained from a uniform or random disturbance background.

4.1 Mechanism of Secondary Instability

The dramatic growth of three-dimensional disturbances at small TS amplitudes can be explained by the parametric nature of the excitation. Guided by earlier work on plane Poiseuille flow,[25] the rapid development of secondary modes and the underlying physical mechanism can also be understood from a close look at the periodic basic flow.

Figure 3 shows the streamlines of the flow (2) for $F = 124$, $R = 606$, and $A = 0.02$ in the wave-fixed coordinate system. The center of the cat's eye indicates an extremum of the streamfunction located just

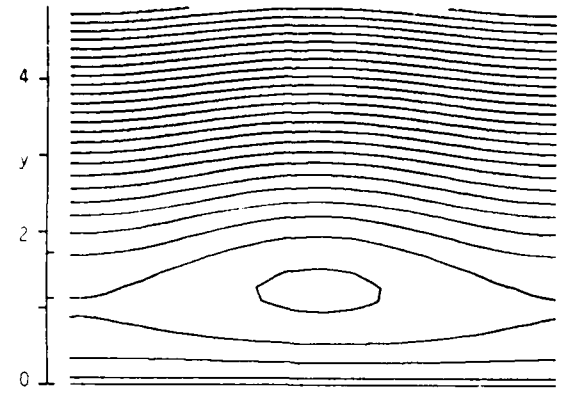

Figure 3. Streamlines of the periodic basic flow at $F = 124$, $R = 606$, and $A = 0.02$. The marks at $y = 1.12$ and $y = 1.72$ indicate the position of the critical layer and the displacement thickness, respectively.

outside the critical layer at y_c. The associated vorticity contours are given in figure 4. Remarkable are the high levels of vorticity near the wall that diffuse into the flow. The viscous effects, however, extend only to the neighborhood of the critical layer. For $y > y_c$, streamlines and isolines of vorticity are nearly parallel, indicating essentially inviscid flow.[37] A weak extremum of vorticity occurs near the center of the cat's eye. Therefore, the flow in this neighborhood resembles a distributed, clockwise rotating vortex at the edge of the viscous layer near the wall. As the amplitude increases, this vortex strengthens and moves further into the inviscid region.

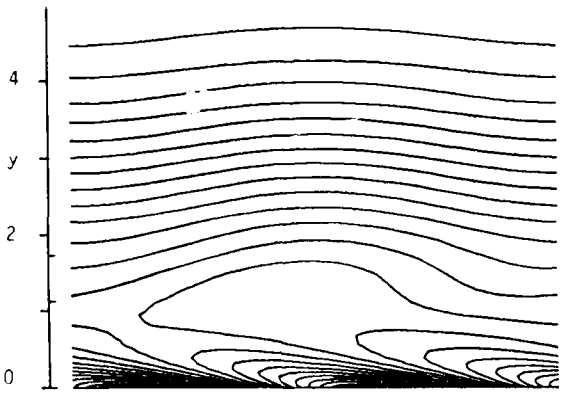

Figure 4. Isolines of vorticity for the periodic basic flow in figure 3.

The study of simplified theoretical models of a single vortex in a viscous shear layer[48, 10] provided some of the features of peak-valley splitting. In more physical terms, the dynamics of such models has been discussed in context with flow visualizations by Hama[49] and Wortmann.[50] Wortmann considers the distributed vortex tube in a two-dimensional flow as a salient feature only in the presence of a spanwise, three-dimensional disturbance. Owing to the surrounding shear, any deformation of the tube initiates transport processes which in turn enhance the deformation. He concludes: "We have to expect a strong, exponential growth of any three-dimensional perturbation once the Reynolds number and wave amplitude of the Tollmien wave establish a local vorticity peak of sufficient strength near the critical layer." His arguments clearly indicate the necessity of combined vortex stretching and retrograde rotation of a bent vortex tube for the exponential growth of three-dimensionality. This model of peak-valley splitting has been verified by the formal and numerical analysis of the vorticity dynamics by Orszag & Patera.[37] For a deeper understanding of the various types of three-dimensional secondary instability, however, it is crucial to recognize the streamwise periodic nature of the flow and to consider a vortex array instead of a single vortex. The TS wavelength λ_z introduces a new characteristic length scale into the problem.

The vortical nature of the secondary instability mechanism and the strong disturbance growth on a convective time scale ultimately justify the approximations implied in the periodic basic flow (2). While nonlinear effects may change primary stability characteristics through modification of the Reynolds stress, the modification of the vorticity distribution at the amplitudes of concern is indeed negligible. Computations of Fasel & Hama (personal communication) show that the two-dimensional field essentially maintains the u'-profile of a linear TS wave even at amplitudes of $A \approx 0.1$. The weak nonparallelism of the boundary layer and the developing TS wave blurs some detail at the onset of secondary instability but can be neglected in the situation of practical interest where strong growth of the three-dimensional modes occurs.

4.2 Peak-Valley Splitting

In order to verify the theory of secondary instability, a detailed analysis of fundamental modes has been performed[42] for the experimental conditions of Klebanoff.[1] This analysis revealed two discrepancies. First, the streamwise growth of the TS wave in the experiment is not in agreement with the predictions of linear stability theory. Dr. Klebanoff expressed that at the time of this experiment emphasis was on a description of the nonlinear and three-dimensional phenomena in transition, and no special effort was made to reproduce the linear TS characteristics that were already verified in the work of Schubauer & Skramstad.[6] Second, our results indicate that subharmonic instability should have prevailed in this experiment if the background amplitudes for fundamental and subhar-

monic modes were equal. In fact, the experiments were conducted in a similar region with respect to the stability diagram in figure 1 as later studies [30] on subharmonic resonance. The experimental arrangement, however, especially the spanwise spacers on the plate surface beneath the ribbon enhanced spanwise periodic mean-flow variations and disturbances of the longitudinal vortex type that directly participate in the resonant mechanism of peak-valley splitting. Our theoretical predictions are consistent with the results of recent computer simulations of transition in a temporally growing boundary layer by Spalart & Yang.[47]

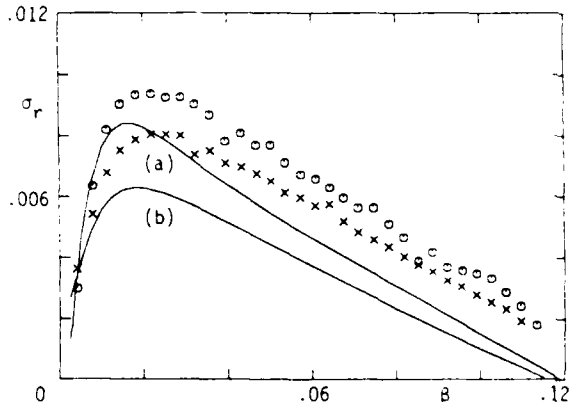

Figure 5. Growth rate of three-dimensional disturbances as a function of the spanwise wavenumber β for $F = 58.8$, $R = 950$, and $A = 0.014$. Theory: (a) subharmonic, (b) peak-valley splitting. Computation: (o) subharmonic, (x) peak-valley splitting.

The dependence of the temporal fundamental and subharmonic growth rates σ_r on the spanwise wave number β is shown in figure 5. The parameters are chosen to match the experimental conditions.[1] Theoretical and computational results are very similar and both show the stronger amplification of the subharmonic mode. The systematic quantitative differences can be attributed to approximations contained in the theoretical and computational work.

Conversion of the temporal growth rates σ_r into spatial growth rates $\gamma_r = \sigma_r/c_r$ and integration in the streamwise direction provides

$$\ln\frac{B(R)}{B_0} = 2\int_{R_0}^{R}\frac{\sigma_r}{\gamma_r}dR \qquad (11)$$

for the amplitude ratio B/B_0 of the three dimensional disturbances, where $B_0 = B(R_0)$ and R_0 is the Reynolds number at the onset of secondary instability for a given value of A_0. Comparison of the amplitude ratios for fundamental and subharmonic modes indicates that the initial amplitudes B_0 for peak-valley splitting in the experiments [1] must have exceeded those for subharmonic instability by more than an order of magnitude. Disregarding this bias, the streamwise variation of the u'-values at peak and valley is in good qualitative agreement with the observation.

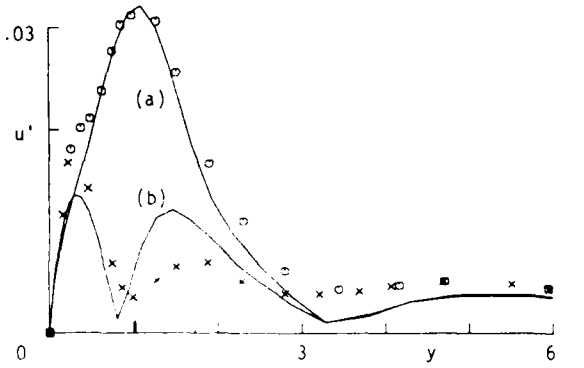

Figure 6. Distribution of u' across the boundary layer for $F = 58.8$, $b = 0.243$, and $R = 960$. Experiment: (o) peak, (x) valley. Theory: (a) peak, (b) valley.

Once the amplitudes A and B at a given streamwise position are established, one can analyze the distribution of the disturbance velocities in the spanwise direction and normal to the plate. Figure 6 shows the u'-distributions across the boundary layer at peak and valley for conditions close to station B in the experiments. A similar comparison at station C indicates that nonlinear three-dimensional effects become significant somewhere between stations B and C, i.e. at maximum peak amplitudes of $u' \approx 5\%$. Essential agreement between theoretical and experimental results is also found for the spanwise component w_0 of the mean longitudinal vortex system, as shown in figure 7, and for the mean flow at peak and valley.

A new set of experimental data on peak-valley splitting has been recently obtained by Cornelius.[44] Not only are the theoretical characteristics of the TS wave reproduced but data are given for different spanwise wavenumbers. We currently perform a theoretical analysis for the conditions of this experiment. The results will be published elsewhere.

4.3 Subharmonic Instability

Detailed hot-wire data on the subharmonic route to transition have been reported by Kachanov & Levchenko.[29,30] Their theoretical explanation of the observations is closely tied to the studies of Craik's model by Volodin & Zelman [51] although the measured wave angle is way off the triad resonance conditions. A detailed analysis of their experimental conditions based on the Floquet theory of secondary instability [41] has shown that their results can be well understood in the light of the broad-band nature of secondary instability.

Figure 8 shows the variation of the subharmonic growth rate σ_r with the wavenumber parameter b for

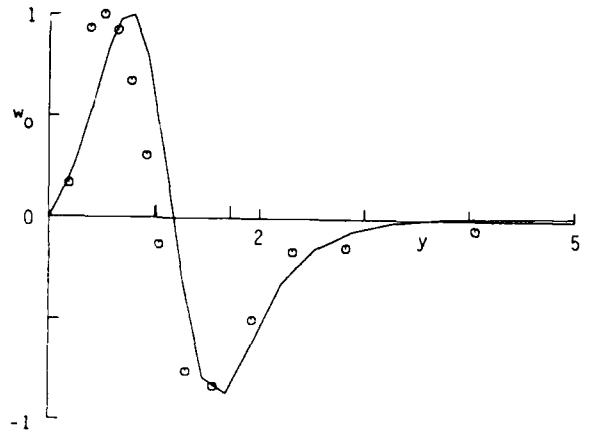

Figure 7. Normalized distribution of the spanwise component of the mean-flow disturbance across the boundary layer at $F = 58.8$, $b = 0.243$, and $R = 980$. (———) Theory, (o) experiment at station C.

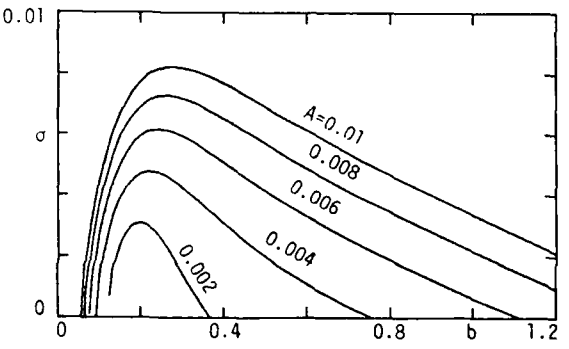

Figure 8. Subharmonic growth rate σ_r as a function of the wavenumber b for $F = 124$, $R_{II} = 606$.

different TS amplitude levels at branch II for $F = 124$. At small amplitudes, considerable growth rates are obtained in a narrow band of wave numbers that centers around the wave number $b = 0.18$ for Craik resonance. Instability at this rather small wavenumber is responsible for the selection of subharmonic disturbances with large spanwise wavelength in experiments at low TS amplitude levels.[33] As the amplitude increases, the band of dangerous wavenumbers extends to larger values of b, and the maximum of σ_r shifts to $b = 0.28$ at $A = 0.01$. The observed value $b = 0.33$ is well within the range of strong instability. The sharp cutoff of the instability at low wavenumbers indicates that subharmonic instability in the Blasius flow always leads to three-dimensionality. The two-dimensional mode of vortex pairing [52, 53] in inflectional mean flows occurs only at very large amplitudes of the periodic modulation.

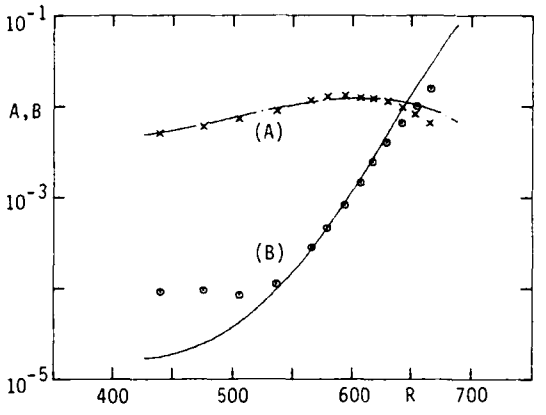

Figure 9. Amplitude growth with the Reynolds number R for (A) TS wave with $A_0 = 0.0044$, (B) subharmonic mode with $B_0 = 1.86 \times 10^{-5}$, $b = 0.33$. (———) Theory, (o) experiment.

Simultaneous integration of the spatial growth rates of TS wave and subharmonic mode with initial amplitudes matching the experimental conditions provides the data shown in figure 9 together with the measurements. Except for the region of transient behavior downstream of the ribbon in the experiment, the streamwise variation of the subharmonic amplitude is well predicted by the theory. Earlier results using the temporal growth concept and the transformation (11) led to very similar results. A detailed comparison of spatial growth rates and transformed temporal rates [54] indicates that the restrictions of Gaster's transformation do not apply to secondary instability. In fact, the close relation between temporal and spatial growth of secondary disturbances could explain the successful modeling of experiments on transition by temporal computer simulations.

Beyond the growth rates, the theory also reproduces the spatial structure of the subharmonic disturbances. At fixed distance from the plate, the spanwise variation of the subharmonic rms fluctuation u'_3 is proportional to $|\cos\beta z|$ with 180° phase jumps at the positions where $\cos\beta z = 0$. The distribution of u'_3 across the boundary layer is compared with experimental data in figure 10. Similar agreement is obtained for the phase of the disturbance velocity. Qualitative agreement also extends to the small higher Fourier components of the subharmonic disturbance as shown in figure 11. The deviation near $y = 0$ is likely to originate from using the hot-wire probe very close to the wall.

The experiments [30] with a natural, i.e. uncontrolled background of three-dimensional disturbances exhibit no pure subharmonic resonance but a broad peak of spectral components in the neighborhood of the subharmonic frequency. The band width of this reso-

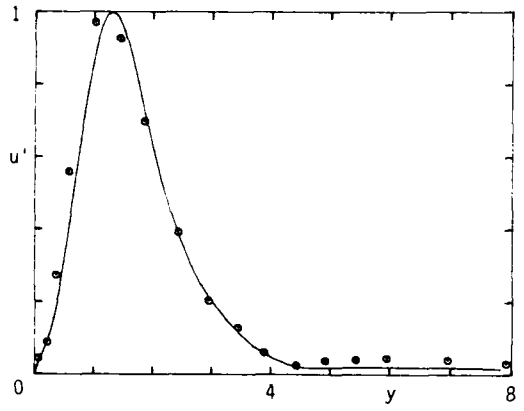

Figure 10. Normalized u'-distribution of the subharmonic mode at $F = 124$, $R = 608$, $A = 0.0122$, and $b = 0.38$. (———) Theory, (o) experiment.

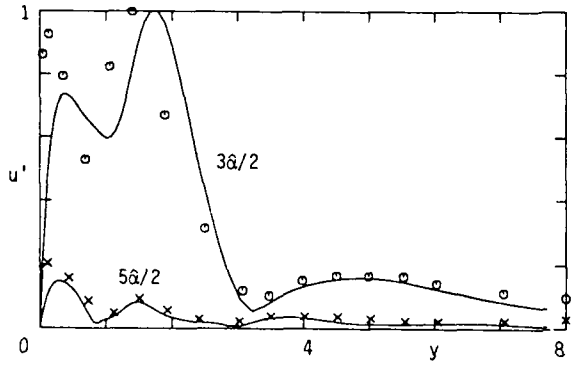

Figure 11. Normalized u'-distributions of the subharmonic components with $3\hat{\alpha}/2$ and $5\hat{\alpha}/2$ at $F = 124$, $R = 606$, $A = 0.01$, $b = 0.33$. (———) Theory, (o,x) experiment.

nance was studied by exciting with the vibrating ribbon a second frequency which differed by up to 50% from the subharmonic frequency. All cases produced strong combination resonance. This fact is consistent with the results of our temporal analysis of detuned modes. The eigenvalues σ are shown in figure 12 for modes with wavenumbers between $\hat{\alpha}$ and $2\hat{\alpha} = \alpha_r$.

The growth rate σ_r exhibits a broad maximum near $\hat{\alpha}$, such that detuned modes with $\hat{\alpha} + \gamma_i$, $\gamma_i \neq 0$ experience almost the same growth as the subharmonic mode. Reality of the physical solution requires the presence of the complex conjugate mode with wavenumber $\hat{\alpha} - \gamma_i$ and equal amplitude. In the experiments, this fact is reflected by the appearance of two sharp spectral components of the same amplitude to both sides of the subharmonic frequency. The growth rate of the fundamental mode is relatively small for these parameters. However, the relation between subharmonic and fundamental growth rate may drasti-

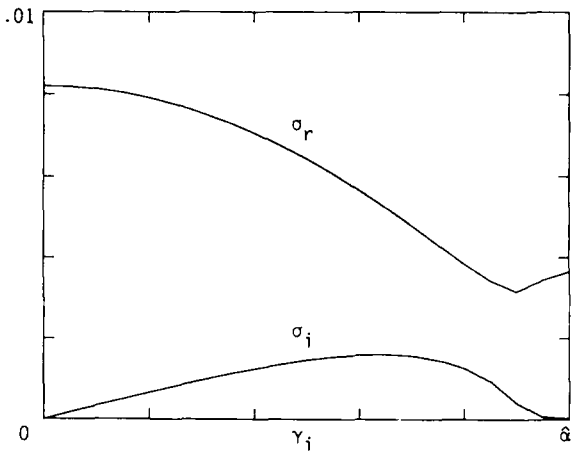

Figure 12. Growth rate σ_r and frequency shift σ_i for detuned modes at $F = 124$, $R = 606$, $A = 0.01$, $B = 0.33$. Subharmonic and fundamental modes correspond to $\gamma_i = 0$ and $\gamma_i = \hat{\alpha}$, respectively.

cally change if the parameters are varied. Figure 12 also shows that only the tuned modes travel synchronously with the TS wave, $\sigma_i = 0$. Detuned modes are always associated with a low-frequency modulation of the disturbance field. This result may be related to observations of low-frequency components and a slow spanwise meandering of the disturbed flow in experiments with a natural disturbance background.

5. Conclusions

The Floquet theory of secondary instability reveals that three-dimensional disturbances in the early stages of transition originate from parametric instability of a basic flow that is periodic in space and time. The [illegible] shortcomings of weakly nonlinear models and methods are circumvented and moreover means are provided for identifying relevant interactions for constructing new models.

The two distinct classes of subharmonic and fundamental modes are found to be special cases of a generalized class of secondary disturbances. The disturbances may grow in space or time. Comparison with experimental data verifies the capability of the theory to predict growth rates and spatial disturbance field up to the stages immediately preceding breakdown and transition.

The mechanism of secondary instability involves combined tilting and stretching of an array of distributed vortices in a surrounding shear flow. By its vortical nature, the stage of three-dimensioinal evolution bridges the gap between the slow viscous time scale of the TS instability and the fast convective scale of the transition process.

Acknowledgment

I am grateful to Fabio P. Bertolotti, Joseph W. Croswell, and German R. Santos who contributed valuable ideas and results to this study. This work is supported by the Office of Naval Research under Contract N00014-84-K-0093 and by the Air Force Office of Scientific Research under Contract F49620-84-K-0002.

References

1. P. S. Klebanoff, K. D. Tidstrom, and L. M. Sargent 1962 "The three-dimensional nature of boundary-layer instability," *J. Fluid Mech.*, vol. 12, pp. 1-34.
2. L. S. G. Kovasznay, H. Komoda, and B. R. Vasudeva 1962 "Detailed flow field in transition," in *Proc. 1962 Heat Transfer and Fluid Mech. Inst.*, pp. 1-26, Stanford Univ. Press.
3. F. R. Hama 1959 "Some transition patterns in axisymmetric boundary layers," *Phys. Fluids*, vol. 2, p. 664.
4. C. F. Knapp and P. J. Roache 1968 "A combined visual and hot-wire anemometer investigation of boundary-layer transition," *AIAA J.*, vol. 6, pp. 29-36.
5. W. S. Saric and A. H. Nayfeh 1977 "Nonparallel stability of boundary layers with pressure gradients and suction," in *Laminar-Turbulent Transition*, pp. 6/1-21, AGARD CP-224.
6. G. B. Schubauer and H. K. Skramstad 1947 "Laminar boundary-layer oscillations and transition on a flat plate," *J. Res. Nat. Bur. Stand*, vol. 38, pp. 251-292.
7. Th. Herbert 1975 "On finite amplitudes of periodic disturbances of the boundary layer along a flat plate," in *Proc. 4th Int. Conf. Numer. Meth. Fluid Dyn., Boulder, Colorado*, Lecture Notes in Physics, vol. 35, p. 212, Springer-Verlag.
8. H. Fasel 1976 "Investigation of the stability of boundary layers by a finite-difference model of the Navier-Stokes equations," *J. Fluid Mech.*, vol. 78, pp. 355-383.
9. H. P. Greenspan and D. J. Benney 1963 "On shear layer instability, breakdown and transition," *J. Fluid Mech.*, vol. 15, pp. 133-153.
10. J. T. Stuart 1965 "The production of intense shear layers by vortex stretching and convection," AGARD Report 514.
11. M. T. Landahl 1972 "Wave mechanics of breakdown," *J. Fluid Mech.*, vol. 56, pp. 775-802.
12. G. S. Raetz 1959 "A new theory of the cause of transition in fluid flows," NORAIR Report NOR-59-383, Hawthorne, CA.
13. G. S. Raetz 1964 "Current status of resonance theory of transition," NORAIR Report NOR-64-111, Hawthorne, CA..
14. D. J. Benney and C. C. Lin 1960 "On the secondary motion induced by oscillations in a shear flow," *Phys. Fluids*, vol. 3, pp. 656-657.
15. A. D. D. Craik 1971 "Nonlinear resonant instability in boundary layers," *J. Fluid Mech.*, vol. 50, pp. 393-413.
16. C. Nakaya 1980 "Three-dimensional waves in a boundary layer," in *Laminar-Turbulent Transition*, ed. R. Eppler and H. Fasel, pp. 239-242, Springer-Verlag.
17. A. H. Nayfeh and A. N. Bozatli 1979 "Secondary instability in boundary-layer flows," *Phys. Fluids*, vol. 22, pp. 805-813.
18. Th. Herbert and M. V. Morkovin 1980 "Dialogue on bridging some gaps in stability and transition research," in *Laminar-Turbulent Transition*, ed. R. Eppler and H. Fasel, pp. 47-72, Springer-Verlag.
19. M. Nishioka, S. Iida, and J. Ichikawa 1975 "An experimental investigation on the stability of plane Poiseuille flow," *J. Fluid Mech.*, vol. 72, pp. 731-751.
20. M. Nishioka, M. Asai, and S. Iida 1980 "An experimental investigation of secondary instability," in *Laminar-Turbulent Transition*, ed. R. Eppler and H. Fasel, pp. 37-46, Springer-Verlag.
21. M. Nishioka, M. Asai, and S. Iida 1981 "Wall phenomena in the final stage of transition to turbulence," in *Transition and Turbulence*, ed. R. E. Meyer, pp. 113-126, Academic Press.
22. M. Asai and M. Nishioka 1982 "Development of wall turbulence (3-dimensional structures, 2nd report)," in *Proc. 14th Turbulence Symposium*, pp. 191-196, Tokyo. (In Japanese)
23. M. Nishioka and M. Asai 1984 "Evolution of Tollmien-Schlichting waves into wall turbulence," in *Turbulence and Chaotic Phenomena in Fluids*, ed. T. Tatsumi, pp. 87-92, North-Holland.
24. S. A. Orszag and L. C. Kells 1980 "Transition to turbulence in plane Poiseuille flow and plane Couette flow," *J. Fluid Mech.*, vol. 96, pp. 159-206.
25. S. A. Orszag and A. T. Patera 1981 "Subcritical transition to turbulence in plane shear flows," in *Transition and Turbulence*, ed. R. E. Meyer, pp. 127-146, Academic Press.
26. L. Kleiser 1982 "Spectral simulations of laminar-turbulent transition in plane Poiseuille flow and comparison with experiments," in *Proc. 8th Int. Conf. Numer. Meth. Fluid Dyn., Aachen, Germany*, ed. E. Krause, Lecture Notes in Physics, vol. 170, pp. 280-287, Springer-Verlag.

27. J. W. Murdock 1977 "A numerical study of nonlinear effects on boundary-layer stability," AIAA Paper No. 77-127, pp. 1-9.

28. A. A. Wray and M. Y. Hussaini 1980 "Numerical experiments in boundary-layer stability," AIAA Paper No. 80-0275, pp. 1-9.

29. Yu. S. Kachanov and V. Ya. Levchenko 1982 "Resonant interactions of disturbances in transition to turbulence in a boundary layer," Preprint No. 10-82, I.T.A.M., USSR Acad. Sci., Novosibirsk. (In Russian)

30. Yu. S. Kachanov and V. Ya. Levchenko 1984 "The resonant interaction of disturbances at laminar-turbulent transition in a boundary layer," *J. Fluid Mech.*, vol. 138, pp. 209-247.

31. Yu. S. Kachanov, V. V. Kozlov, V. Ya. Levchenko, and M. P. Ramazanov 1985 "On nature of K-breakdown of a laminar boundary layer. New experimental data," in *Laminar-Turbulent Transition*, ed. V. V. Kozlov, pp. 61-73, Springer-Verlag.

32. W. S. Saric, V. V. Kozlov, and V. Ya. Levchenko 1984 "Forced and unforced subharmonic resonance in boundary layer transition," AIAA Paper No. 84-0007.

33. W. S. Saric and A. S. W. Thomas 1984 "Experiments on the subharmonic route to turbulence in boundary layers," in *Turbulence and Chaotic Phenomena in Fluids*, ed. T. Tatsumi, pp. 117-122, North-Holland.

34. Yu. S. Kachanov, V. V. Kozlov, and V. Ya. Levchenko 1977 "Nonlinear development of a wave in a boundary layer," *Izv. AN USSR, Mekh. Zhidk. i Gaza*, vol. 3, pp. 49-53. (In Russian)

35. J. B. Anders and R. F. Blackwelder 1980 "Longitudinal vortices in a transitioning boundary layer," in *Laminar-Turbulent Transition*, ed. R. Eppler and H. Fasel, pp. 110-119, Springer-Verlag.

36. R. F. Blackwelder 1979 "Boundary-layer transition," *Phys. Fluids*, vol. 22, pp. 583-584.

37. S. A. Orszag and A. T. Patera 1983 "Secondary instability of wall-bounded shear flows," *J. Fluid Mech.*, vol. 128, pp. 347-385.

38. Th. Herbert 1981 "A secondary instability mechanism in plane Poiseuille flow," *Bull. Amer. Phys. Soc.*, vol. 26, p. 1257.

39. Th. Herbert 1983 "Secondary instability of plane channel flow to subharmonic three-dimensional disturbances," *Phys. Fluids*, vol. 26, pp. 871-874.

40. Th. Herbert 1983 "Subharmonic three-dimensional disturbances in unstable shear flows," AIAA Paper No. 83-1759.

41. Th. Herbert 1984 "Analysis of the subharmonic route to transition in boundary layers," AIAA Paper No. 84-0009.

42. Th. Herbert 1985 "Three-dimensional phenomena in the transitional flat-plate boundary layer," AIAA Paper No. 85-0489.

43. Th. Herbert, F. P. Bertolotti, and G. R. Santos 1986 "Floquet analysis of secondary instability in shear flows," in *Proc. ICASE/NASA Workshop on Stability of Time-Dependent and Spatially Varying Flows*, Springer-Verlag. To appear.

44. K. C. Cornelius 1985 "Three dimensional wave development during boundary layer transition," Lockheed Georgia Research Report LG85RR0004.

45. Th. Herbert and F. P. Bertolotti 1985 "The subharmonic route to transition - an animated theory," 16 mm Movie, Virginia Polytechnic Institute and State University.

46. Th. Herbert 1984 "Secondary Instability of Shear Flows," in *Special Course on Stability and Transition of Laminar Flow*, AGARD Report No. 709.

47. P. R. Spalart and Kyung-Soo Yang 1986 "Numerical simulation of boundary layers: Part 2. Ribbon-induced transition in Blasius flow," NASA Technical Memorandum 88221, pp. 1-24.

48. F. R. Hama 1963 "Progressive deformation of a perturbed line vortex filament," *Phys. Fluids*, vol. 6, pp. 526-534.

49. F. R. Hama 1960 "Boundary-layer transition induced by a vibrating ribbon on a flat plate," in *Proc. 1960 Heat Transfer and Fluid Mechanics Institute*, pp. 92-105, Stanford Univ. Press.

50. F. X. Wortmann 1981 "Boundary-layer waves and transition," in *Advances in Fluid Mechanics*, ed. E. Krause, Lecture Notes in Physics, vol. 148, pp. 268-279, Springer-Verlag.

51. A. G. Volodin and M. B. Zelman 1978 "Three-wave resonance interaction of disturbances in a boundary layer," *Izv. AN USSR, Mekh. Zhidk. i Gaza*, vol. 5, pp. 78-84. (In Russian)

52. R. T. Pierrehumbert and S. E. Widnall 1982 "The two- and three-dimensional instabilities of a spatially periodic shear layer," *J. Fluid Mech.*, vol. 114, pp. 59-82.

53. Th. Herbert and F. P. Bertolotti 1985 "Effect of pressure gradients on the growth of subharmonic disturbances in boundary layers," in *Proc. Conf. on Low Reynolds Number Airfoil Aerodynamics*, ed. T. J. Mueller, Univ. of Notre Dame.

54. F. P. Bertolotti 1985 "Temporal and spatial growth of subharmonic disturbances in Falkner-Skan flows," VPI & SU, M.S. thesis.

reprinted from

Proceedings of the Tenth U.S. National Congress of Applied Mechanics
Editor: J. P. Lamb
(Book No. H00338)

published by

THE AMERICAN SOCIETY OF MECHANICAL ENGINEERS
345 East 47th Street, New York, N.Y. 10017
Printed in U.S.A.

Appendix B

Secondary Instability of Boundary Layers

To appear: Ann. Rev. Fluid Mech., Vol. 20 (1988)

SECONDARY INSTABILITY OF BOUNDARY LAYERS

Thorwald Herbert

Department of Engineering Science and Mechanics, Virginia Polytechnic Institute and State University, Blacksburg, Virginia 24061

1. INTRODUCTION

The problem of transition from laminar to turbulent flow in viscous boundary layers is of great practical interest. The low skin friction coefficient of laminar boundary layer flow is very attractive to those who lay out the engines or pay the fuel for high-speed vehicles such as airplanes. However, the low mixing of fluid properties such as chemical species, heat, or momentum may be intolerable for others who design these engines or cope with the danger of separation in adverse pressure gradients; they may clearly prefer a turbulent state of the flow. Therefore, it would be highly desirable to at least predict, if not to control, whether the flow under consideration is laminar or turbulent. The tremendous efforts of decades of intense research, however, have been to little avail (Reshotko 1976). The empirical e^n-criterion is still the standard tool in engineering practice, although it is known to ignore essential ingredients of the physics of transition and therefore may dangerously mislead if used beyond the supporting data base. Numerical transition simulations have gained reliability in reproducing the transition process in sufficient detail to extract information unobtainable from laboratory experiments. However, the inherent assumptions of streamwise periodicity and temporal growth of the boundary layer, in addition to the uncertainty of initial conditions prevent predicting transition in practice. Hence, theory still holds an important place in identifying inherent mechanisms and structures of the transition process and in explaining otherwise unintelligible observations. The past decade saw some important progress of stability theory, slow or fast, depending on the reader's judgement.

Because of the multitude of identified and concealed effects on the response of the boundary layer to external forcing, the development of a general theory of transition is yet an utopia. In noisy environments, e. g. in turbomachinery,

turbulent boundary-layer flow develops virtually 'out of the blue'; the intermediate unsteady but still laminar motions accessible to stability analysis are bypassed (Morkovin 1969). For large areas of practical interest such as vehicles moving through the ocean or atmosphere, however, the environment is relatively 'quiet', i. e. the external disturbances produce only small spectral components that match the scale of natural oscillations in the boundary layer. The detailed mechanism of how the boundary layer ingests external acoustic waves or turbulent fluctuations in a given geometry with inadvertent roughness and vibrations of the solid boundary is denoted as receptivity. The study of this receptivity issue has recently seen major progress (Goldstein 1985; Tam 1986) but will not be addressed here. We concentrate on the situation after receptivity has established a low level of disturbances inside the boundary layer. Initially, the amplitudes of all spectral components are assumed sufficiently small for neglecting nonlinear modifications to the mean flow. In this case, the initial response of the boundary layer to disturbances is governed by linear equations and can be studied for isolated spectral components. We further restrict our attention to the simplest and best understood case of two-dimensional boundary layers along essentially flat surfaces. The issues of centrifugal instability with respect to Görtler vortices, cross-flow instability in three-dimensional boundary layers, and the wealth of interactions between the various modes of instability will be briefly reviewed in section 3.3.

TS WAVES The initial stage of linear instability, henceforth denoted as *primary instability*, can be roughly predicted using the Orr-Sommerfeld equation for temporally growing disturbances in a *locally parallel flow*. Earlier doubts about validity and relevance of Tollmien's (1929) theoretical results for two-dimensional traveling waves and the calculations of growth rates by Schlichting (1933) were swept away by the convincing experiments of Liepmann (1943) and Schubauer & Skramstad (1943/1947). The disturbance background in the latter experiments was kept extremely low and small two-dimensional oscillations were introduced by a vibrating ribbon. It has become custom to use such a biased, or *controlled* background in experiment and computation. We should remain aware that these studies are launched from a simplified model of the *natural*, i. e. uncontrolled and unknown noise that causes instability and transition in real life. Although Squire's (1933) transformation highlights the stronger instability of two-dimensional waves, oblique waves or streamwise vortices cannot be considered irrelevant. The natural background must be viewed as an irregular pattern of three-dimensional wave packets with nonuniform spectral content. Moreover, the study of isolated spectral components is only a valid concept as long as nonlinear coupling can be ignored. With this in mind, we will adopt for the following the controlled background and primary instability with respect to two-dimensional traveling TS waves as the starting point for the theoretical analysis of the subsequent steps toward transition.

The quantitative prediction of growth rates and velocity distributions for TS

waves can be improved by considering spatially growing waves (Gaster 1962) and accounting for the streamwise variation of the boundary layer (Bouthier 1973; Gaster 1974; Saric & Nayfeh 1977). The distinction between temporal and spatial concept slightly changes the total streamwise growth but provides a common neutral curve. This curve (see Figure 8 below) outlines the region of instability in the frequency-Reynolds number plane. Since the Reynolds number depends on the distance from the leading edge, the neutral curve marks for each suitable frequency the region of growth by two streamwise positions, branch I and branch II. The nonparallelism moderately enlarges this region and enhances the growth, which improves the agreement with experimental data.

The characteristics of finite-amplitude TS waves have been studied both with perturbation methods (Itoh 1974; Herbert 1975) and by numerically solving the Navier-Stokes equations (Fasel 1976). At the low amplitudes of concern, however, there is no remarkable effect of nonlinearity on disturbance growth or velocity distribution.

From a qualitative point of view, the most significant effect of TS waves is the breakup of the uniform flow in streamwise direction characterized by the redistribution of spanwise vorticity into periodic concentrations near the critical layer where wave speed and mean velocity coincide. Downstream of branch I, the waves grow on a slow viscous scale and decay once they pass branch II of the neutral curve. The challenge then is to find out how these harmless two-dimensional waves of large wavelength are related to the violent three-dimensional, small-scale, and high-frequency motion that is commonly denoted as turbulence. A partial answer to this question will occupy the main part of this review.

One more remark seems to be in place. Research on transition has historically been full of contradictions and sudden changes in views and trends that often hampered progress (see the section "Some Lessons from History", Morkovin 1969). Different reviews on shear flow stability may have little in common and a zero-overlap of cited literature (e. g. Maslowe 1986). This curious fact illustrates the many facets of the overall problem, the multitude of views, concepts and methods, and the need to remain open-minded. It also grants me the right to present my own view supported by a selection of references that I know is far from complete.

A critical evaluation and interpretation of the 1983 state-of-the-art has been given by Morkovin (1983, 1985). The latter reference contains an extensive list of related literature.

2. EARLY WORK AND RECENT PROGRESS

In retrospect, the tortuous route to our current perception is astonishing. For twenty years, conflicting yet correct experimental views of the early stages of transition were never clearly discerned nor reconciliated. Research by different groups and with different techniques applied to the same problem were virtually

considered separate issues. Most theoretical work was guided by one single study: the detailed hot-wire data of Klebanoff et al (1962) on "the three-dimensional nature of boundary-layer instability". This paper is in fact very appealing to the theoretician.

2.1 Early Observations

VISUALIZATION One of the first clear observations of the fate of growing (axisymmetric) TS waves is the smoke photograph of the flow over an axisymmetric body shown in Figure 1. This photograph was taken by F. N. M. Brown at Notre Dame as early as 1957 but barely published in the open literature (Mueller 1987, to appear). Later work in Brown's facility (Knapp & Roache 1968) revealed two clearly distinguished arrangements of the Λ-shaped smoke accumulations (termed "trusses") which were characterized as *staggered* or *aligned in rows*. In natural transition at zero pressure gradient, the staggered arrangement dominated, while adverse pressure gradients, and even more forcing by sound, favored the alignment in rows. Knapp & Roache concluded "that any condition which causes the two-dimensional waves to amplify more slowly" will enhance the tendency toward the staggered arrangement. The qualitative difference of the staggered pattern from the observations of Klebanoff et al (1962) was not recognized. The trusses were attributed to concentrated vorticity and their development and breakdown discussed in some detail. The qualitative changes in the Λ pattern by an adverse pressure gradient are like those recently observed in the decelerating boundary layer on a flat plate (Gad-el-Hak et al 1984). More recent visualizations of staggered and aligned Λ's are shown in Figures 2 and 3, respectively.

The Λ-shaped structures were also observed by Hama et al (1957) in the flow of water over a flat plate. A trip wire was used to create initial two-dimensionality. Besides the flow photographs, the discussion of the dynamics of vortex filaments in a shear flow is intriguing. In later work, Hama & Nutant (1963) used hydrogen bubbles in water to visualize what they denoted as Λ vortices. The observations were supported by an analysis of the dynamics of a vortex line under three-dimensional disturbances (Hama 1963). The Λ's were aligned in all cases.

Using techniques similar to those of Hama & Nutant, a detailed phenomenological description of single trusses or Λ vortices was given in the movie "Tollmien-Schlichting Waves and Beyond" by Wortmann (1977), although the narrow water tunnel prevented identification of their arrangement. Similar to Hama, Wortmann (1981) modeled the generation of Λ vortices in terms of combined tilting and stretching of a disturbed vortex line in a surrounding shear flow. The perception of the Λ's as vortices was strongly supported by the tendency of the lighter-than-water bubbles to concentrate on the axis of a swirling flow. Although the relation between the Λ-shaped accumulations of fluid markers and the vorticity field has been a matter of controversy, the name Λ-*vortices* sustains

(see section 3.2) .

HOT-WIRE DATA Klebanoff & Tidstrom (1959) and Klebanoff et al (1962) performed detailed hot-wire surveys of the three-dimensional stage of transition. The earlier experiments adopted the vibrating ribbon technique but suffered from the unrest of the three-dimensional phenomena. Spanwise modulations occurred with a specific wavelength λ_z while the phase changed erratically with respect to a fixed hot wire. In the later work, the spanwise phase was controlled by strips of scotch tape underneath the ribbon spaced according to the wavelength found in the earlier experiments. The repeatability of the signals and careful selection of what to measure in order to prove or disprove existing theories and concepts led to a treasure of data that has been exploited uncounted times. However, the experiments were focused on the qualitative rather than quantitative features of the nonlinear development. No effort was made to tune the facility to reproduce the quantitative characteristics of TS waves as predicted by theory.

At sufficiently low amplitude, TS waves of frequency f and wavelength λ_z grow and harmlessly decay in the downstream direction. At larger amplitude, however, a three-dimensional structure evolves whenever the TS amplitude A exceeds a threshold value of typically 1% of the free-stream velocity U_∞ (A denotes the nondimensional maximum streamwise rms fluctuation, $A = u'_m / U_\infty$). This structure is characterized by spanwise alternating *peaks* and *valleys*, i. e. regions of enhanced and reduced amplitude. A system of streamwise vortices develops simultaneously with the peaks and valleys. The growth rate of the wave at the peak positions is much larger than the original TS growth and leads rapidly to the formation of localized high-shear layers at the peak positions. The periodicity of the flow is consistent with the visualizations of aligned Λ vortices. The highly inflectional instantaneous velocity profiles become unstable with respect to high-frequency disturbances that cause *spikes* in the hot-wire signals. The onset of spikes initiates the ultimate breakdown of the laminar flow into turbulence. The development of three-dimensionality up to the appearance of spikes occupies about five TS wavelengths, while onset of spikes and breakdown occur within one wavelength. The virulent disturbance growth in the three-dimensional stage is in remarkable contrast to the slow TS growth on a viscous time scale.

Other experiments with controlled TS frequency and spanwise wavelength were carried out by Kovasznay et al (1962) with various configurations of multiple hot wires. The details of the development were not as clearly revealed as in the study by Klebanoff et al. There evolved, however, a general consensus on the various stages of boundary layer transition (Tani 1969) which stimulated and guided theoretical work for almost two decades. The equi-shear contours recorded by Kovasznay et al are still a benchmark for the verification of computer simulations of transition.

THE THREE-DIMENSIONAL STAGE The sequence of events from onset of

primary instability to turbulence has often been reviewed. Many of the descriptions need revision in today's perspective for the findings of Knapp & Roache (1968). In addition, one needs to recall the peculiar conditions of the supporting controlled experiments. Here, we focus on the stages that succeed the onset of TS waves and their slow growth to amplitudes of the order of 0.5% to 1%. At this level, three-dimensionality occurs with a spanwise scale similar to the TS wavelength, $\lambda_z \sim \lambda_x$, but in a nonunique manner. At lower amplitudes, three-dimensionality produces staggered patterns of Λ vortices that at larger amplitude are replaced by a virtually mixed type and at even larger values by an aligned pattern of Λ vortices. This aligned pattern is consistent with peak-valley splitting.

The three-dimensional disturbances grow dramatically. Nonlinear deformation of the flow field produces embedded high-shear layers associated with inflectional instantaneous velocity profiles. Small-scale, high-frequency velocity fluctuations (spikes) appear owing to wrinkling of the high-shear layers and herald the onset of irregular motion or breakdown of the laminar flow.

2.2 Early Theoretical Work

WEAKLY NONLINEAR MODELS Numerous attempts have been made to explain the observations of Klebanoff et al (1962) by low-order perturbation analysis of wave interactions. The interactions were modeled by a composite of Orr-Sommerfeld modes with different wave vectors (α_k, β_k) in the plane spanned by streamwise and spanwise direction. Two groups of models can be distinguished. Nonresonant models consider the observed wavelength as a given parameter and study the superposition of a TS wave $(\alpha, 0)$ with two oblique waves $(\alpha, \pm\beta)$ (Benney & Lin 1960; Nakaya 1980) or with a longitudinal vortex mode $(0, \beta)$ (Herbert & Morkovin 1980). Stuart (1962) criticized the Benney-Lin model because the different wave speeds should cause a slow phase change between the waves, which would contradict the observations. Itoh (1980) has shown that nonlinear synchronization of the waves may occur in plane Poiseuille flow. In boundary layers, however, the calculation of the mean flow distortion and longitudinal vortex components inherent to both models suffers from the nonparallelism of the basic flow (Herbert & Morkovin 1980). Neither the TS interaction with oblique waves nor with longitudinal vortices has been capable of fully reproducing the characteristics of peak-valley splitting.

The second group of models (Raetz 1959; Craik 1971) exploits resonance between Orr-Sommerfeld modes for selected spanwise wave numbers $\pm\beta^*$. The prototype of these models is Craik's resonant triad. This triad consists of the TS wave $(\alpha, 0)$ and two subharmonic oblique waves $(\alpha/2, \pm\beta^*)$ with twice the wavelength λ_z of the TS wave. Craik found resonance for the experimental conditions of Klebanoff et al (1962) at a frequency of 145 Hz, but his results became subject to criticism since peak-valley splitting is not associated with subharmonic waves. The discovery of subharmonic signals in boundary layer transition

(Kachanov et al 1977) revived the interest in Craik's model. Nayfeh & Bozatli (1979) found subharmonic resonance at amplitudes of 29% which by far exceed the observed values and may strain the validity of a low-order perturbation analysis.

The weakly nonlinear theory suffers from two shortcomings, the first of which is common to all perturbation methods when applied at a finite value of the perturbation parameter. Low order of truncation compromises the judgement whether this finite value is 'sufficiently small' for rapid convergence of the perturbation series and accurate results. The second problem is the lack of reliable methods for constructing the model of a vaguely known physical phenomenon, i. e. to find the right pieces to assemble the puzzle. Intuition alone cannot secure the relevance and completeness of the modes chosen to interact.

AN OUTSIDER Beginning in 1968, L. M. Maseev published a series of reports of the Engineering Institute for Railway Transportation in Moscow. The first report (Maseev 1968a) was entitled "Secondary Instability of Boundary Layers" - like this article. Two pages in English translation (Maseev 1968b) sketched lengthy equations derived with Kantorovich's method. A suspicious solution procedure provided reasonable thresholds for the occurrence of longitudinal vortices (Figure 4) in the experiments of Klebanoff et al (1962) and near the critical Reynolds number. L. M. Maseev never answered my letters, nor could I find him in Moscow. He must have been the first to realize that peak-valley splitting, not the spikes as thought by Klebanoff et al, are produced by *secondary instability* and that this instability originates from parametric excitation in a periodic flow, not from spanwise differential amplification of the TS wave.

2.3 Recent Progress

EXPERIMENTS The experiments of Nishioka and co-workers (1975, 1980, 1981) on stability and transition in plane channel flow are a milestone in transition research. Much pioneering theoretical work has been done on the nonlinear stability of this strictly parallel flow that allows a clean mathematical treatment. For a long time, this theoretical work had been overshadowed by the experimental fact of low subcritical transition. Nishioka et al were the first to obtain laminar channel flow at supercritical Reynolds number and to verify the basic results of linear and nonlinear stability analyses. In this way, they also verified the methods used for nonlinear studies. Moreover, they found that transition in channel flow follows the same steps as in boundary layers, and hence established channel flow as a sensible prototype for transition analysis in wall-bound shear flows.

The exchange of ideas at the AGARD Meeting 1977 in Copenhagen and the IUTAM Symposium on Laminar-Turbulent Transition 1979 in Stuttgart spawned a new generation of boundary-layer experiments. A survey of these efforts has been given by Thomas (1986). Kachanov et al (1977) were the first to observe a

broad peak of near-subharmonic signals in spectra of hot-wire data. More detailed measurements with lower-than-before ribbon excitation (Kachanov & Levchenko 1982, 1984; Kachanov et al 1985; Saric et al 1984) and flow visualizations (Saric & Thomas 1984) soon led to a more precise and extended picture of the transition process.

Most notable, perhaps, was the rediscovery and apprehension of the non-uniqueness of the early three-dimensional stage of transition. Depending on minute changes of the level of ribbon vibration at otherwise fixed conditions, the aligned arrangement of Λ vortices was observed to change into the staggered arrangement, accompanied by changes in the spanwise wavelength. The spanwise wavelength of the three-dimensional phenomena was earlier believed to be a repeatable characteristic of the transition process (Klebanoff et al 1962; Anders & Blackwelder 1980). For the first time, Thomas & Saric (1981) associated the *staggered* arrangement of Λ vortices with *subharmonic* hot-wire signals: the stationary hot wire records the same conditions for every other wave.

Kachanov & Levchenko (1984) provided controlled conditions by stimulating the (two-dimensional) ribbon with the TS frequency f_1 and a superposed lower frequency $f = f_1/2 + \Delta f$. For $\Delta f = 0$, they substantiated the phase synchronization between TS wave and subharmonic wave as required for Craik's resonant triad. However, the wave angle $\theta = \tan^{-1}(\lambda_z/\lambda_x)$ was different from the prediction for triad resonance. For $\Delta f \neq 0$, two peaks at frequencies $f_1/2 \pm \Delta f$ of nearly equal strength appeared in the spectra.

COMPUTER SIMULATIONS Advances in computers and computational methods enabled rapid progress in transition simulations for boundary layers (Murdock 1977; Wray & Hussaini 1980) and channel flow (Orszag & Kells 1980; Orszag & Patera 1981; Kleiser 1982) under controlled conditions. The wealth of information concealed in the computer output can be extracted with relative ease which is not true of the data obtained in laboratory experiments. The work on boundary layers suffers from the inability to specify proper conditions for the outflow at the nonphysical downstream boundary of the computational domain. Therefore, transition simulations for boundary layers consider the temporal development of the flow in a spatially periodic box. Surprisingly, computational results are strikingly similar to the experimental data up to the stage where numerical and experimental resolution becomes insufficient. The artificial temporal growth, however, prevents prediction of the transition location - disappointing some euphoric hopes.

REVISED CONCEPTS In parallel with the gathering of new observations, Blackwelder (1979) and Herbert & Morkovin (1980) questioned the traditional transition picture. Earlier (Klebanoff et al 1962), the occurrence of three-dimensionality had been attributed to spanwise differential amplification of TS waves, while the onset of spikes was considered to arise from secondary instability. This latter view had often been reiterated and gained trust from theoretical

work (Landahl 1972). The revised picture considered the onset of three-dimensionality as manifestation of secondary instability. Herbert & Morkovin (1980) suggested that three-dimensional disturbances originate from parametric excitation in the streamwise periodic flow created by the finite-amplitude TS wave.

PARAMETRIC INSTABILITY Orszag & Patera (1980, 1981) attributed the exponential growth of small three-dimensional disturbances in their simulations of peak-valley splitting in a plane channel to a linear stability mechanism and analyzed the instability of large-amplitude stable equilibrium states in a plane channel based on a Floquet system. At the same time, Herbert (1981) studied the instability of (two-dimensionally unstable) equilibrium motions at lower amplitudes in the experimentally relevant range of $0 \leq A \leq 0.05$. Besides peak-valley-splitting modes of opposite symmetry, Herbert (1983a) found subharmonic modes, although Craik's triad is inactive in plane channel flow owing to adverse symmetry of the wave motion. The universality of secondary instability for various shear flows was shown by Orszag & Patera (1983).

The main results of this work are as follows: (i) Three-dimensional secondary instability can lead to different types of disturbances. Primary resonance with the TS wave produces peak-valley splitting as the TS amplitude exceeds some threshold. Subharmonic resonance can occur at even smaller amplitudes. (ii) Calculated disturbance velocities and growth rates are consistent with experiments. (iii) Secondary instability originates from the redistribution of spanwise vorticity into streamwise periodic lumps near the critical layer. Growth of three-dimensional modes arises from combined vortex tilting and stretching. (iv) The limit $A \rightarrow 0$ reveals the intricate connection between modes of primary and secondary instability. This connection provides for the first time a rational means for evaluating existing and constructing new models of wave interaction.

APPLICATION TO BOUNDARY LAYERS Guided by the nature of the secondary instability mechanism, Herbert (1983b) introduced approximations which permit application of the theory to the variety of classical stability problems, especially to boundary layers. Application of this Floquet theory of secondary instability to the Blasius boundary-layer flow (Herbert 1984, 1985; Herbert et al 1986) provides results consistent and in good agreement with the work of Klebanoff et al (1962) and Cornelius (1985) on peak-valley splitting and with the results of Kachanov & Levchenko (1984) on subharmonic and combination resonance.

UNBIASED COOPERATION The progress during the past decade has been achieved by individual efforts. This progress had not been possible, however, without the open discussions between those involved to the extent that priority questions are at times difficult to reconcile. Cooperation spanned experimental, theoretical, and computational work performed by researchers from USA, USSR,

Europe, and Japan. Studies of plane Poiseuille flow by Nishioka et al (1984), May & Kleiser (1985), and Singer, Reed & Ferziger (1986) supported the development of the theory for boundary layers. Boundary-layer experiments directed by V. Ya. Levchenko, V. V. Kozlov, W. S. Saric, A. S. W. Thomas, K. C. Cornelius and T. C. Corke (1987, to appear), computations by P. R. Spalart, and the development of the theory by Th. Herbert (see the text for references) were performed in a fruitful atmosphere of open exchange.

3. FLOQUET ANALYSIS

Key to the successful analysis of secondary instability is the observation that at the onset of three-dimensionality the flow is no longer of the Blasius type but has experienced a modulation by the finite-amplitude TS wave. In a coordinate system moving with the phase speed of this wave, the flow can be considered as approximately *steady* and *periodic* in the streamwise direction. Analysis of the linear stability of this modulated flow with respect to three-dimensional disturbances, therefore, leads to a *Floquet system* of linear differential equations with periodic coefficients. Well-known mathematical properties of such systems (Coddington & Levinson 1955) are exploited to identify form and classes of solutions. Numerical methods provide quantitative detail. This straightforward approach is obviously very similar to the classical theory of primary instability. The effort involved in the elaborate formulation and demanding numerical work is rewarded by a rich variety of solutions with interesting properties.

HISTORICAL REMARK Floquet theory has been widely applied to analyze the stability of time-periodic flows (Davis 1976). In comparison with the often dramatic resonances in other mechanical systems, the effect of time-periodicity, e.g. in plane channel flow is rather mild. The reason is the uniformity of the vorticity distribution as in steady flow. Clever & Busse (1974) solved a Floquet system for the instability of steady, spatially periodic convection rolls. In this case, the effect of periodicity is mild due to the absence of shearing motion. Strong resonance is caused by the combination of redistributed vorticity with the surrounding shear flow. It seems that Kelly (1967) was the first to apply the Floquet concept in shear flows; he studied vortex pairing in an inviscid shear layer. Soon thereafter appeared the long overlooked work of Maseev (1968a, b). A separate branch of analysis developed for flows with the periodic direction normal to the mean flow direction (Gotoh & Yamada 1986).

Floquet theory was frequently applied in studies on gravity waves as an alternative to the weakly nonlinear theory of resonant wave interactions. In principle, both approaches should give identical conditions for resonance, provided the model of wave interaction contains all the waves involved in the physics and the wave amplitudes are small. Floquet theory appears as the more general and more

powerful method not only for gravity waves but also for boundary layers.

3.1 Formal Background

DISTURBANCE EQUATIONS The standard procedure of linear stability decomposes the velocity field $\mathbf{v}$ (and pressure p) into a basic flow $\mathbf{v}_2$ and a disturbance $\mathbf{v}_3$ that is sufficiently small for linearization. Substitution into the Navier-Stokes equations and subtracting the equations for the basic flow (which we assume to be identically satisfied) provides the linear stability equations

$$(\frac{1}{R}\nabla^2 - \frac{\partial}{\partial t})\mathbf{v}_3 - (\mathbf{v}_2\cdot\nabla)\mathbf{v}_3 - (\mathbf{v}_3\cdot\nabla)\mathbf{v}_2 = \nabla p_3 ,$$

$$\nabla \cdot \mathbf{v}_3 = 0 . \qquad (1)$$

The basic flow and its derivatives determine the coefficients of the stability equations. For the analysis of secondary instability, we write the basic flow in the form

$$\mathbf{v}_2(x',y,t) = \mathbf{v}_0(y) + A\,\mathbf{v}_1(x',y,t) . \qquad (2)$$

where $\mathbf{v}_0 = \mathbf{v}_0(y)$ represents the boundary layer flow, A the amplitude of the periodic modulation, and $\mathbf{v}_1$ a TS wave for a given set of parameters. We denote with x', y, z the streamwise, normal, and spanwise direction, respectively, with associated velocity components u, v, w. We normalize $\mathbf{v}_1$ such that A is a direct measure for the maximum streamwise rms fluctuation u'_m. All quantities are nondimensional using the outer velocity U_∞ and $\delta_r = (\nu L/U_\infty)^{1/2}$ for reference, where L is the distance from the leading edge. Consequently, $R = (U_\infty L/\nu)^{1/2}$. We change from the laboratory frame x' to a Galilean frame x moving with the TS phase velocity c_r. In this frame, the basic flow is independent of time and satisfies

$$\mathbf{v}_2(x,y) = \mathbf{v}_2(x+\lambda_x,y), \quad x = x' - c_r t , \qquad (3)$$

where λ_x is the wavelength of the TS wave.

The choice of the basic flow (2) involves three *approximations*, the first of which is well-established in the primary stability theory: the assumption of a locally parallel flow $\mathbf{v}_0$. The second approximation is the assumption of a locally constant amplitude A of the TS wave, i. e. the amplitude is assumed to vary slowly in comparison with the disturbances. This *quasi-steady approach* blurs the onset of secondary instability but is well justified in the interesting region of strong convective growth of the three-dimensional disturbances. The last approximation is the *shape assumption*, i. e. the neglect of the non-linear distortion of the velocity distribution $\mathbf{v}_1(y)$ at finite amplitude A. This step is justified by the weak nonlinear distortion of the u' distribution even at amplitudes of 10% (Hama, personal communication), and by the vortical nature of the secondary instability mechanism (Bayly et al 1988). Nonlinearity mainly affects the phase

of $\mathbf{v}_1$ but has little influence on the vorticity distribution.

NATURE OF THE SOLUTIONS The linear disturbance equations (1) with $\mathbf{v}_2$ given by (2) are qualitatively different for $A = 0$ and $A \neq 0$. In absence of the TS wave, equations (1) form the basis of the classical theory of primary instability. Since the basic flow is independent of t, x, and z, the normal mode concept can be applied with respect to these variables. After some rearrangement, this leads to the Orr-Sommerfeld equation for the velocity component v and to Squire's equation for the vorticity component η (Squire 1933) normal to the plate.

For $A \neq 0$, equations (1) represent a system of partial differential equations with x-periodic coefficients. The normal mode concept can still be applied with respect to z and t and three-dimensional disturbances can be written in the form

$$\mathbf{v}_3(x,y,z,t) = e^{\sigma t}\, e^{i\beta z}\, \mathbf{V}(x,y)\,. \tag{4}$$

Due to the spanwise homogeneity of the basic flow, we consider the spanwise wave number $\beta = 2\pi/\lambda_z$ as real, whereas $\sigma = \sigma_r + i\sigma_i$ is in general complex. An important step in developing the theory of secondary instability is the identification of classes and form of $\mathbf{V}(x,y)$. Insight into the streamwise structure of the disturbances is given by the Floquet theory of differential equations with periodic coefficients: the function $\mathbf{V}$ has the general form

$$\mathbf{V}(x,y) = e^{\gamma x}\,\tilde{\mathbf{V}}(x,y)\,,\quad \tilde{\mathbf{V}}(x+\lambda_x,y) = \tilde{\mathbf{V}}(x,y)\,, \tag{5}$$

where $\gamma = \gamma_r + i\gamma_i$ is a characteristic exponent, and $\tilde{\mathbf{V}}$ is periodic in x with wavelength λ_x. Hence, we can express $\tilde{\mathbf{V}}$ in terms of a Fourier series and obtain the *general form of three-dimensional disturbances*:

$$\mathbf{v}_3 = e^{\sigma t}\, e^{\gamma x}\, e^{i\beta z} \sum_{m=-\infty}^{\infty} \hat{\mathbf{v}}_m(y)\, e^{im\alpha x}\,, \tag{6}$$

where $\alpha = 2\pi/\lambda_x$. The Fourier coefficients $\hat{\mathbf{v}}_m(y)$ are governed by an infinite system of ordinary differential equations. Since the physical solution must be real, any complex solution $\mathbf{v}_3$ implies the existence of a complex conjugate solution $\mathbf{v}_3^{\dagger}$. Consequently, the system of equations can be written in a form with real coefficients.

CLASSIFICATION OF MODES The occurrence of two complex quantities, σ and γ, in the eigenvalue problem for secondary disturbances leads to an ambiguity similar to that associated with the Orr-Sommerfeld equation. Only two of the four real quantities σ_r, σ_i, γ_r, γ_i are determined by the eigenvalue problem for $\mathbf{v}_3$; the other two must be chosen.

We first note that γ and $\gamma \pm ik\alpha$ yield identical modes for any positive integer k to within renumbering the Fourier coefficients. Therefore, it is sufficient to consider $-\alpha/2 < \gamma_i \leq \alpha/2$. For convenience, we replace α by $\hat{\alpha} = \alpha/2$ and introduce $\epsilon = \gamma_i/\hat{\alpha}$. Distinguishing the three cases $\epsilon = 0$, $\epsilon = 1$,

and $0 < |\epsilon| < 1$ provides the following classification of modes:

Fundamental modes, $\epsilon = 0$:

$$\mathbf{v}_f = e^{\sigma t} e^{\gamma_r z} e^{i\beta z} \tilde{\mathbf{v}}_f(x,y), \quad \tilde{\mathbf{v}}_f = \sum_{m \text{ even}} \hat{\mathbf{v}}_m(y) e^{im\hat{\alpha}z} \tag{7}$$

Subharmonic modes, $\epsilon = 1$:

$$\mathbf{v}_s = e^{\sigma t} e^{\gamma_r z} e^{i\beta z} \tilde{\mathbf{v}}_s(x,y), \quad \tilde{\mathbf{v}}_s = \sum_{m \text{ odd}} \hat{\mathbf{v}}_m(y) e^{im\hat{\alpha}z}. \tag{8}$$

Detuned modes, $0 < |\epsilon| < 1$:

$$\mathbf{v}_d = e^{\sigma t} e^{\gamma_r z} e^{i\beta z} \sum_{m \text{ even}} \hat{\mathbf{v}}_m(y) e^{i(m+\epsilon)\hat{\alpha}z}. \tag{9}$$

The periodic functions $\tilde{\mathbf{v}}_f$ in (7) and $\tilde{\mathbf{v}}_s$ in (8) satisfy

$$\tilde{\mathbf{v}}_f(x + \lambda_x, y) = \tilde{\mathbf{v}}_f(x,y), \quad \tilde{\mathbf{v}}_s(x + 2\lambda_x, y) = \tilde{\mathbf{v}}_s(x,y). \tag{10}$$

The fundamental modes $\mathbf{v}_f$ are associated with primary resonance in the Floquet system, while subharmonic modes $\mathbf{v}_s$ originate from principal parametric resonance. Detuned modes are related to combination resonance. It is obvious from equation (9) that the construction of a physical solution requires two complex conjugate modes with opposite detuning $\pm\epsilon$. Consequently, the real disturbance contains wave numbers $m\hat{\alpha} \pm \gamma_i$, and the sum of such wave-number pairs matches the TS wave number. We denote the real disturbance as *combination mode*. Owing to the complex conjugate components, opposite detuning $\pm\gamma_i$ in wave number is conjoint with opposite detuning $\pm\Delta f$ in frequency.

GROWTH CONCEPTS The real parts σ_r and γ_r govern the growth of the disturbance with respect to t or x, respectively, and are of prime interest in the analysis of secondary instability. Similar to Gaster (1962) for primary instability, we distinguish temporally growing and spatially growing modes of secondary instability. It is important to recognize that spatial growth of disturbances in the streamwise direction is measured in the laboratory frame x' and $e^{\sigma t} e^{\gamma z} = e^{(\sigma - \gamma c_r)t} e^{\gamma x'}$.

Temporal growth requires $\gamma_r = 0$. The temporal growth rate is given by σ_r, while σ_i can be interpreted as frequency shift with respect to the TS frequency. Modes with $\sigma_i = 0$ travel synchronous with the modulated basic flow. The detuning γ_i of the wave number is a given quantity.

Spatial growth in the laboratory frame requires $\sigma_r = \gamma_r c_r$ for suppression of temporal growth effects. Hence, γ_r provides the spatial growth rate while γ_i is the shift in the streamwise wave number. The detuning of the frequency is given by the value of $\sigma_i - \gamma_i c_r$.

FORMAL PROPERTIES Without solving for the modes, we can identify various characteristics that are consistent with observations. The fundamental modes are doubly periodic with wavelengths λ_x and λ_z like the ordered or aligned pattern in the flow visualizations of Saric & Thomas (1984) and the flow field during peak-valley splitting (Klebanoff et al 1962). The aperiodic term $\mathbf{v}_0$ in (7) represents a spanwise periodic mean flow distortion (u_0) and a longitudinal vortex system (v_0, w_0). This vortex system is an integral part of the three-dimensional disturbance; it grows simultaneously with the fluctuating components and at the same rate. This result is consistent with the observations of peak-valley splitting, but different from the prediction of the weakly nonlinear models proposed by Benney & Lin (1960) and Herbert & Morkovin (1980).

Subharmonic modes are doubly periodic with $2\lambda_x$ and λ_z, and invariant under the translation $(x, z) \rightarrow (x + \lambda_x, z + \lambda_z/2)$, which is characteristic of the staggered pattern in flow visualizations. In frequency spectra from a laboratory-fixed probe, linear subharmonic modes produce peaks only at odd multiples of the subharmonic frequency, not at the fundamental frequency and its harmonics. Subharmonic modes are not associated with an aperiodic component. The spanwise variation of the subharmonic disturbance $\sim |\cos\beta z|$ and the 180^o phase jumps at the positions where $\cos\beta z = 0$ is consistent with measurements of Kachanov & Levchenko (1984, fig. 20).

Nearly equal amplitude of the two detuned modes that form a combination mode has been observed in controlled experiments (Kachanov & Levchenko 1984, fig. 19). Equal difference in wave number (or frequency) for different values of m is consistent with the experiment. It is interesting to note that combination resonance is governed by a *linear* Floquet system. Occurrence of spectral peaks near odd multiples of $f/2$ in the experiments is not caused by nonlinearity.

In all cases, the three-dimensional disturbance grows and travels as a whole. All Fourier components have the same phase speed, as in the experiments of Kachanov & Levchenko (1984, fig. 21, curves 2, 6, 7). At finite amplitude A, modes of secondary instability and oblique TS waves are qualitatively different; they are 'two kinds of animals'.

NUMERICAL ASPECTS The numerical effort increases from subharmonic through fundamental to detuned modes provided real systems are used for the former two. The temporal problem is less demanding since the temporal eigenvalue σ appears linearly in the equations. Primary and secondary stability problem can be treated with similar numerical methods. Most of the work yet done utilized spectral collocation methods with Chebyshev polynomials in y-direction. This method converts the ordinary differential equations and boundary conditions into algebraic equations. Direct treatment of the boundary value problem is preferred over shooting methods since it maintains access to the spectra of eigenvalues. Spectra are helpful for reliably identifying the most relevant modes in different regions of the multi-dimensional parameter space and for untangling

their analytical connections. Such help is appreciated when dealing with problems without prior guidance.

The truncation of the Fourier series involved is crucial for the numerical work. For subharmonic modes, the lowest possible truncation is $| m | \leq 1$, which includes only $\hat{\mathbf{v}}_{-1}$ and $\hat{\mathbf{v}}_1$. The lowest approximation for fundamental modes is $| m | \leq 2$ and includes $\hat{\mathbf{v}}_{-2}$, $\hat{\mathbf{v}}_0$ and $\hat{\mathbf{v}}_2$. Detailed numerical studies (Herbert et al 1986) have shown that the Fourier series converge rapidly, and the lowest truncation provides sufficient accuracy for practical purpose.

3.2 Portrait of Secondary Instability

Numerical results from Floquet analysis and computer simulations in conjunction with the few sets of experimental data have developed a consistent picture of secondary instability. Most of these data are for the Blasius boundary layer. Studies of other cases (Herbert & Bertolotti 1985) and the physical mechanism of secondary instability (Bayly et al 1988) promise, however, that this picture is generic for two-dimensional boundary layers in absence of strong concave curvature (Görtler instability). In the following, we use the frequency parameter $F = 10^6 \cdot \alpha_r c_r / R$, and wave number $b = 10^3 \cdot \beta / R$ to specify three-dimensional disturbances of fixed dimensional frequency and spanwise wavelength as they travel downstream. The amplitude of secondary modes is denoted by B. For convenience, we distinguish three ranges of the TS amplitude: small, $A < 0.5\%$, medium, $0.5\% \leq A \leq 2\%$, and large, $A > 2\%$. Except if stated otherwise, the results are for temporally growing modes in the Blasius boundary layer.

EIGENVALUE SPECTRA For medium and large amplitudes, the principal, i. e. most amplified modes of temporal subharmonic or fundamental instability are associated with a real eigenvalue σ. Secondary mode and TS wave are phase-locked and travel at the same phase speed, in agreement with the observations of Klebanoff et al (1962) and Kachanov & Levchenko (1984). Synchronization provides an optimum chance for the transfer of energy into the three-dimensional disturbance. As in plane Poiseuille flow, a second mode with smaller growth rate may become unstable. This 'complex mode' is not phase-locked and will be disregarded since no evidence for its role in transition has been found.

SUBHARMONIC GROWTH The variation of the growth rate $\sigma = \sigma_r$ for the principal subharmonic mode as a function of the spanwise wave number b is shown in Figure 5. At very small amplitudes, instability ($\sigma_r > 0$) is restricted to a narrow band near $b = 0.18$. As A increases, instability occurs in a broadening band of spanwise wave numbers. The range of maximum growth shifts toward larger values of b, and σ_r decreases nearly linear as b increases. The instability is sharply cut off at lower wave numbers. Hence, the two-dimensional mode of pairing instability is suppressed. Vortex pairing has been found only in

inflectional boundary layers at large amplitudes of the periodic modulation. (Herbert & Bertolotti 1985). The maximum growth rates are large in comparison with the maximum growth rate of TS waves, justifying the quasi-steady approximation At $A = 1\%$, the secondary mode grows by two orders of magnitude within less than 6 TS cycles. With the other parameters fixed, the growth rate σ_r increases with increasing TS amplitude A as in the experiments of Gaster (1984, fig. 8) and Kachanov & Levchenko (1984, fig. 2). Unfortunately, the spanwise wavelength is unknown in both experiments.

The effect of the downstream increasing Reynolds number R on σ_r is twofold. The growth rate σ_r increases with increasing R at otherwise fixed parameters. In addition, the amplitude A increases with R between branches I and II and thus further enhances the secondary instability. Figure 5 partially explains the observation of different wavelength by Saric & Thomas (1984). At amplitudes of $A \leq 0.3\%$, subharmonic resonance is restricted to the neighborhood of $b \approx 0.18$ and results in $\lambda_z \approx 1.5\lambda_z$. The wider band at higher amplitude levels permits amplification for larger wavenumbers. The selection of $b \approx 0.4$ and $\lambda_z \approx 0.68\lambda_z$ with $A \leq 0.4\%$, however, can only be understood in the light of a nonuniform disturbance background. A similar spanwise wavelength was found for the fundamental instability at higher $A \leq 0.7\%$. The value of $b = 0.33$ observed by Kachanov & Levchenko at medium amplitudes is well within the range of maximum amplification.

The important role of the initial amplitude B_0 of the three-dimensional disturbance is clearly shown by the experiments of Kachanov & Levchenko (1984, fig. 15c) and Saric et al (1984) with simultaneous ribbon excitation by the TS frequency and its subharmonic. A linear variation of the phase ϕ between the two signals results in an amplitude $B \sim |\cos\phi|$ of the amplified subharmonic, proportional to the initial amplitude of the phase-locked component of the ribbon excitation. The subharmonic mode can lock on in two different phases with jumps of 180^o when $\cos\phi = 0$.

Simultaneous integration of the spatial growth rates of TS wave and subharmonic mode with initial amplitudes matching the experimental conditions provides the data shown in Figure 6 together with the measurements. Except for the first few points, the streamwise variation of the subharmonic amplitude is well predicted by the theory. The experimental data for $R < 500$ were taken in the region of transient behavior immediately downstream of the ribbon. The important role of the wave fetch in the formation of the subharmonic disturbance field has been demonstrated by Thomas (1986). Results similar to Figure 6 were earlier (Herbert 1984) obtained using the temporal growth concept and the transformation $\gamma_r = \sigma_r / c_r$. Detailed comparison of spatial growth rates and transformed temporal rates as in Figure 7 (Herbert & Bertolotti 1985) verifies that the restriction of Gaster's transformation to small growth rates does not apply to secondary instability. The wave propagation properties of secondary modes are quite different from those of primary modes. Principal subharmonic

and fundamental modes travel at a speed independent of the spanwise wavelength; they are swept along with the TS wave. Bertolotti (1985) has shown that c_r is indeed the leading term in the temporal-spatial transformation, with small corrections by dispersive terms. The surprisingly simple relation between spatial and temporal growth helps to explain the success of temporal computer simulations in reproducing the characteristics of spatially developing transition.

K-, H-, C-, AND OTHER TYPES To emphasize the distinctive features of the route to breakdown described by Klebanoff et al, Herbert & Morkovin (1980) suggested that it be called K-breakdown. The attribute 'K-type' found widespread acceptance. Saric & Thomas (1984) then extended the catalogue by introducing the attributes 'C-type' for Craik and 'H-type' for Herbert to distinguish two different mechanisms of subharmonic development. Resonance of Craik's triad causes the narrow peak of amplification at small amplitudes in Figure 5, while this peak is absent under other conditions. For these parameters, $F = 124$, $R = 606$, oblique waves with $b = 0.18$ are unstable owing to primary instability even at $A = 0$. Other modes participate in the wave interaction to minor extent. At different wave numbers b, however, subharmonic resonance occurs owing to these other modes and Craik's triad plays a minor role. Study of Craik's model (Maslennikova & Zelman 1985) reveals some aspects of the observations but fails to provide a full quantitative picture. Craik's triad is a valid but incomplete model of subharmonic wave interaction. The shortcoming is most clearly shown by the broad-band subharmonic instability of plane Poiseuille flow (Herbert 1983a) where Craik's triad is inoperative. There, subharmonic instability originates from Squire modes that were 'forgotten' in weakly nonlinear modeling since they are always stable. Meanwhile, Nayfeh (1985) found that Squire modes can strongly interact with TS waves. H-type is the more general type of subharmonic instability that may occur in various flows and for a broad band of spanwise wave numbers. At other parameters, where the sharp peak of C-type resonance disappears, subharmonic instability becomes a threshold phenomenon. Since Floquet analysis is more general, it reveals Craik's triad when appropriate. In short, C-type is a sensitive mechanism with many 'ifs and whens', H-type is a robust subharmonic instability that needs nothing but periodically concentrated vorticity in a shear flow, no matter what wavelength, the stronger the better.

Often one is confused by the use of the same name (e. g. haipin vortex) for different phenomena. Here, we are fortunate to have many names for just two phenomena. Staggered, subharmonic, C-type and H-type are synonyms for principal parametric resonance in the boundary layer. Aligned, fundamental, peak-valley splitting, and K-type are synonyms for primary resonance.

Two questions remain open. The first is how to name the combination modes that are most likely to dominate in nature. K for Kachanov would be confusing; L for Levchenko would honor his contributions over the past decade and the first description of these modes; S could stand for Santos who developed the theory to incorporate these modes; or simply E since these modes embrace, embody, enclose

every other type as a special case. The second question is why subharmonic instability remained concealed for so long.

PEAK-VALLEY SPLITTING Growth of secondary modes is only observable and leads to transition if the initial amplitude of the three-dimensional disturbance is sufficiently large and the conditions for growth persist for a sufficiently long time or streamwise distance. Theory predicts that growth characteristics of subharmonic and fundamental modes are similar, with the subharmonic being the most dangerous mode at small and medium TS amplitudes. The key experiments provide details on different aspects of secondary instability at different frequencies:

$F = 58.8$: hot-wire data on peak-valley splitting, Klebanoff et al (1962),
$F = 64.4$: hot-wire data on peak-valley splitting, Cornelius (1986),
$F = 83$: flow-visualizations of various modes, Saric & Thomas (1984),
$F = 124$: hot-wire data on subharmonic and combination resonance, Kachanov & Levchenko (1984).

None of the available sets of hot-wire data allows comparison of subharmonic and fundamental modes at fixed frequency. Figure 8 relates the location of the vibrating ribbon (or wire) and the range of Reynolds numbers studied in these experiments to the stability diagram for Blasius flow. According to Floquet analysis, peak-valley splitting is likely to occur at lower frequencies since it needs stronger TS growth to produce larger amplitudes. (By the way, the Strutt diagram for the Mathieu equation with damping shows the same qualitative features.) An analysis of fundamental modes has been performed by Herbert (1985) for the experimental conditions of Klebanoff et al. This analysis revealed two discrepancies. First, the streamwise growth of the TS wave in the experiment is not in agreement with the predictions of linear stability theory. Dr. Klebanoff explained to me that, at the time of this experiment, emphasis was on a description of the nonlinear and three-dimensional phenomena in transition; the characteristics of linear TS waves were already verified in the work of Schubauer & Skramstad. Second, the calculations indicate that subharmonic instability should have prevailed in this experiment if the background amplitudes for fundamental and subharmonic modes were equal. The experiments were conducted in a similar region of the stability diagram as the studies of Kachanov & Levchenko on subharmonic resonance. The experimental arrangement of Klebanoff & Tidstrom (1959), however, and especially the spanwise spacers on the plate surface beneath the ribbon in the later work enhanced spanwise periodic mean-flow variations and disturbances of the longitudinal vortex type. In Poiseuille flow, longitudinal vortices and pure spanwise modulations of the mean flow (degenerate Squire modes) are the ingredients for the resonant mechanism of peak-valley splitting. In boundary layers, such modes are concealed in the continuous spectrum but pop out to contribute to the formation of fundamental modes. K-type three-dimensionality, therefore, seems to develop only under specific circumstances.

A comparison of subharmonic and fundamental growth rates is given in

Figure 9. The lines represent theoretical data while the symbols were obtained from computer simulations of transition in a temporally growing boundary layer by Spalart & Yang (1986). The systematic deviation reflects approximations in both theory and computation. The common conclusion is that subharmonic modes are more unstable than fundamental modes, at least for wave numbers near maximum amplification. The computer simulations show that even at large TS amplitudes pure peak-valley splitting cannot be obtained from a uniform or random disturbance background.

Herbert (1983b) has blamed the biased conditions in wind and water tunnels for the distorted perception of transition in channel flow. Measures to calm down the noisy flow in tunnels commonly involve a settling chamber and strong contraction. The large contraction ratio converts most of the residual disturbances into streamwise vorticity. This vorticity, on the other hand, favors the fundamental mode of secondary instability. Clear evidence for this preference are the computer simulations of Singer at al. (1986) for Poiseuille flow. By introducing small longitudinal vortices in the initial conditions, the otherwise subharmonic development was suppressed and peak-valley splitting occurred, H-type switched into K-type. To provide data for quantitative verification of theoretical results, Cornelius (1985) studied peak-valley splitting at a frequency close to that of Klebanoff et al but further upstream of branch II (see Figure 8). By placing spanwise spacers at different distance, Cornelius documented the three-dimensional development for $\beta = 0.24$ and $\beta = 0.48$ and hence experimentally verified for the first time the broad-band nature of fundamental instability. The accuracy of these data does not permit the parallel-flow approximation in theoretical work and detailed comparison awaits its turn.

LOSS OF SELECTIVITY The theoretician who relies on the rigid basis of classical mathematics, and in his numerical work, on increases in raw speed and memory of computers, recognizes stunning progress in experimental techniques. More sophisticated flow control in wind tunnels, computer-controlled data acquisition and data reduction have reduced the irritating bias of earlier experiments. What appeared repeatedly as a selectivity of the transition mechanisms has been a selectivity of the experimental apparatus. The attempt of Anders & Blackwelder (1980) to vary the characteristic spanwise spacing of the K-type field was unsuccessful owing to a concealed source of streamwise vortices with a preferred spanwise scale.

The portrait of secondary instability would be incomplete without a glance at combination modes. These modes travel in general with a speed different from the TS wave speed and, as a team, lead to a beating hot-wire signal as it has been seen by Kachanov & Levchenko and Thomas & Saric. For small amplitudes, Santos & Herbert (1986) found a broad peak of amplification for detuned modes in the neighborhood of the subharmonic mode, $\epsilon \approx 1$. This nearly even amplification of modes in a whole range of streamwise wave numbers or frequencies is consistent with the observation of a broad peak centered at the

subharmonic frequency in the various experiments (Thomas 1986). The width of this peak varies with the amplitude A and flattens out into a plateau of almost uniform amplification at larger amplitudes, as shown in Figure 10.

From the parametric dependence of the growth rates which appear to be well predicted by the Floquet theory, we may draw the following conclusions for an environment with controlled TS frequency but random three-dimensionality: At extremely small initial TS amplitude at branch I, TS waves grow and decay according to primary stability characteristics. At small A, C-type instability occurs near branch II with a specific spanwise wavelength typically larger than the TS wavelength. As the branch I amplitude further increases, amplification broadens in a range of near-subharmonic frequencies with a tendency toward larger spanwise wave numbers. Ultimately, at large amplitudes the 'black box' of secondary instability amplifies whatever the background provides, no matter whether subharmonic, fundamental or detuned, in an extended range of spanwise wavelengths of order $O(\lambda_x)$.

Within a linear framework, the phenomena arising from a mixture of different TS frequencies are a superposition of the above with proper account for the downstream shift of branch I. In a low-noise natural environment, then, the preference of primary instability for two-dimensional waves may still support secondary instability on a modified planform of oblique and bent vorticity concentrations with less regular spacing accumulated in wave packets. In noisy environments, however, the TS mechanism is no longer needed and may be bypassed; preexisting vorticity concentrations of irregular spacing and orientation combined with the mean shear directly activate the processes of vortex tilting and stretching (Bayly et al 1988) that lead to transition. Verification of these latter conclusions may be a challenging target for computer simulations. Most of the present boundary-layer codes are restricted to a computational domain one or two λ_x long and λ_z wide and therefore do not allow for studies on the selection and interaction of waves. The wider domain in Spalart's code (Spalart & Yang 1986) is an exception. Small domains, however, permit great detail in resolving breakdown (Krist & Zang 1987).

VELOCITY PROFILES Returning from speculation to the factual results of the Floquet analysis, it is revealing to closely examine the distribution of the streamwise velocity normal to the wall shown in Figure 11 for the various modes. All modes show maximum activity slightly above the critical layer for the TS wave, the center of Kelvin's cats eyes in the moving coordinate frame, and rapid decay toward the edge of the boundary layer. The detailed power spectra Gaster (1984) obtained at the edge of the boundary layer severely underestimate the strength of combination resonance at lower distance from the wall. The distinct frequency allows direct measurements for subharmonic (and combination) modes. The comparison between results of Kachanov & Levchenko and theory is shown in Figure 12. The fundamental mode is usually observed in superposition with the TS wave and discerned by comparison at spanwise positions $\lambda_z/2$ apart, as in Figure

13. Besides the streamwise fluctuations, mean-flow distortion, the longitudinal vortex system, and spanwise fluctuations are consistent with available hot-wire data.

COMPUTER VISUALIZATION Knowledge of the velocity field in the various stages of transition permits constructing data for conclusive evaluation of hazy or controversial concepts or connections. One of the first applications is the reproduction of the patterns of various modes in flow visualizations by computer-animation based on the theoretical data (Bertolotti et al 1986). The motion pictures show the development of particle lines released from a 'smoke wire' at different times and locations. Obviously, the staggered subharmonic pattern and the aligned fundamental pattern can be reproduced, and for the conditions of the experiments, the first indication of spanwise structure leads within about five TS cycles to a dramatic stretching of the particle lines which to describe is beyond the power of a linear analysis. The pictures vary sensitively with the distance of the smoke wire from the wall, especially when passing through the critical layer. The appearance of the Λ vortices changes with the different history of the particle field when the smoke wire is moved downstream (Bertolotti & Herbert 1987, in preparation). Two instantaneous pictures of a strongly detuned combination mode ($\epsilon = \pm 0.5$) are shown in Figure 14. The pattern resembles the staggered or the aligned mode depending on the phase relation to the TS wave. Many of the observed 'mixed' patterns are likely to involve competing combination modes of different spanwise wavelength.

Λ VORTICES The second application of velocity fields is borrowed from the world of computing: are the Λ's really vortices? Reconstruction of the flow field from hot-wire data by Williams et al (1984) supports the vortex concept. Analysis of numerical data by Kleiser & Laurien (1985) shows only a dislocation of vortex lines along the legs of the Λ while Zang & Hussaini (1985) agree with the general features depicted by Williams et al. Recent all out efforts of Krist & Zang (1987) aim specifically at the origin of the Λ's, there called 'hairpin vortices'. High-resolution runs for K-type and H-type transition at different Reynolds numbers produce similar vortices; the streamwise and spanwise vorticity distributions conform with the measurements of Williams et al (1984). The Λ's are vortices, as shown in Figure 15.

3.3 Görtler Vortices and Cross-Flow Vortices

The success of the Floquet theory in explaining the secondary instability excited by TS waves suggests to search for other applications. If one limits this search to boundary layers, counter-rotating Görtler vortices in the flow over concave surfaces and co-rotating cross-flow vortices in three-dimensional boundary layers are the two prime candidates. Primary and secondary instability and the relation to transition for these two cases have been reviewed by Saric & Reed (1987, to

appear) with the conclusion that many questions remain to be solved.

GÖRTLER VORTICES The Görtler instability is of centrifugal nature and governed by the streamline curvature of the flow with stabilization by viscosity. Nayfeh (1981) found by a weakly nonlinear method strong double-exponential growth of oblique TS waves in presence of finite-amplitude Görtler vortices. Srivastava (1985) obtained with similar methods significant but less dramatic amplification while computer simulations by Malik (1986) were unable to reproduce Nayfeh's result.

In the light of the Floquet theory, the disturbances can be written as

$$\mathbf{v}_3(x',y,z,t) = e^{\sigma t}\, e^{\gamma z}\, e^{\alpha x'}\, \tilde{\mathbf{V}}(y,z) \tag{11}$$

where spanwise homogeneity requires $\gamma_r = 0$, and $\sigma_r = 0$ for the streamwise growing disturbances. Special solutions are traveling waves $\sim\exp(i\,\alpha_i\, x + i\,\sigma_i\, t)$. The streamwise amplification rate α_r is expected to be small owing to the uniform vorticity in the mean-shear direction. An inviscid model of the instability mechanism rests on the tilting of the vortices and their images which is governed by Biot-Savart's law. Some vortex stretching will occur and the shear flow will fold and sweep away the bows, enhancing the longitudinal vorticity. The strong stretching effect that reorients preexisting vortex filaments, however, is missing. Since interaction happens between neighboring vortices of opposite sense, the break of symmetry is governed by two fundamental modes of different spanwise phase, $\lambda_z/4$ apart. In both cases each single vortex meanders downstream. All vortices wind synchronously in one case, out of phase with their neighbors in the other. The former motion is similar to wavy Taylor vortices and is more likely to appear than the latter which involves deformation besides bending. The occurrence of subharmonic modes seems to be largely precluded by topological reasons. The generation of small scales and high frequencies for breakdown is likely to be associated with localized high-shear layers that develop from the uplift of low-momentum fluid between vortices (Hall 1986).

Floquet analysis of the secondary instability of Görtler vortices with the assumptions introduced in section 3.1 will be of qualitative character. Not only has Hall (1983) shown that the streamwise variation of the boundary layer prevents application of the normal-mode concept, but the growth of the vortex amplitude (Malik 1986) cannot be considered small in comparison with the growth rate of secondary modes.

CROSS-FLOW VORTICES The catalogue of mean flows with important cross-flow instability ranges from the boundary-layer flow over a rotating disk through flows over spinning axisymmetric bodies to the flow over swept wings. These cases are distinguished by decreasing angle θ between the vortex axes (in ζ direction) and the x direction of the potential flow. Observation and physical intuition suggest that x is the proper direction for the growth of primary and secondary instabilities and development toward transition - x means downstream.

Since cross-flow instability may cause transition in swept-wing flows before the competing TS instability develops, this flow of practical interest has been chosen to study secondary instability of basic flows with cross-flow vortices. In this flow, the angle θ is small, say 3^o. Reed (1985) applied the method of multiple scales to analyze the interaction with oblique waves. Reed (1984) and Fischer & Dallmann (1987) used Floquet analysis to find temporal growth rates of secondary modes. The two more recent studies agree about the tendency toward a rising second harmonic in the Floquet direction ξ normal to ς. Fischer & Dallmann found growth rates of subharmonic, combination, and fundamental modes with different wave numbers in ς lower than the (neglected) growth rate of the cross-flow vortices even at amplitudes of 6.9%. A strong instability has not yet been discovered.

The cross-flow instability over swept wings is caused by a small inflectional velocity distribution normal to the potential flow. The primary disturbances draw their energy from this weak component. Stretching of the x-vorticity component by non-parallel effects may have a first order effect on the primary growth (Morkovin 1983). As for Görtler vortices, the orientation of the disturbance vorticity in the mean flow direction may prevent strong instability from occurring. Along which path the main body of the flow feeds enough energy into the disturbances to cause transition remains an open question.

4. SECONDARY INSTABILITY AND TRANSITION

Floquet analysis of linear secondary instability supported by computer simulations has certainly increased our insight into the transition mechanism and the capability of predicting the quantitative characteristics of the early three-dimensional stages of transition. However, it has not yet improved the capability of predicting transition in practice. Two ingredients are missing for such prediction. The first ingredient is the frequency and amplitude composition of the noisy background which is hardly measurable. Reasonable assumptions, empirical data, and receptivity studies may alleviate this lack. The second missing element is a quantitative criterion for the conditions that lead to *self-sustained growth* of three-dimensional disturbances. Linear theory is unable to provide this ingredient.

In a linear framework, secondary instability leads a parasitic existence on the TS waves. Secondary modes may grow but will harmlessly decay as the vital vorticity concentrations fade away. This decay is clearly shown in Figure 16 reproduced from Kachanov & Levchenko (1984) at low levels of the amplitude A. At higher amplitude levels, however, the stronger growth leads to three-dimensional amplitudes B large enough to affect the two-dimensional wave development. Nonlinear interaction prevents the decay of the signal at the TS frequency. Primary and secondary disturbances join in a rapid evolution toward breakdown. Similar curves were obtained from transition simulations (Spalart &

Yang 1986).

4.1 Energy Balance

Investigation of the energy balance is a first step into exploring the nonlinear interaction between the components of the flow field. The main path of energy transfer which leads directly from the mean flow into secondary modes was identified earlier by Orszag & Patera (1983); the TS wave plays only a catalyst role. Croswell (1985) used solutions from Floquet analysis and studied the energy transfer between mean flow $\mathbf{v}_0$, two-dimensional wave $A\,\mathbf{v}_1$, and three-dimensional disturbances $B\,\mathbf{v}_3$ in plane Poiseuille flow at a fixed time, i. e. for fixed amplitudes A^* and B^*. Herbert (1986) reports some results of this study which show an interesting spatial distribution of the energy transfer and give a first lead toward insight into the feedback loop of self-sustained growth.

SPATIAL DISTRIBUTION For unstable TS waves, the distribution of the power in the x , y plane shows shallow extrema near the critical layer, spreads far away from the wall, and is periodic in x with wavelength $\lambda_x/2$. Averaging in the streamwise direction provides a sharp peak at the critical layer. Integration normal to the wall yields the small positive growth rate (multiplied with twice the energy of the TS wave). For fundamental and subharmonic secondary modes, the picture changes drastically. The spanwise averaged power has sharp oval peaks near the center of the cat's eyes, a clear indicator for the close association between vorticity redistribution and secondary instability. Though less obvious, a similar concentration of the streamwise averaged power can be seen in the y , z plane normal to the mean flow direction. A more detailed scan reveals that the energy transfer into secondary modes is confined to shallow ellipsoids centered above the critical layer and at the positions where the deflection of the distributed spanwise vortices is strongest.

The observation of this highly *localized energy transfer* stimulates some abstraction. The tie to the critical layer stems from creating the distributed vortex array by a TS wave. Such an array created in another way at a different distance from the wall and convected with the local mean velocity will behave similar to within changes in shear and viscous effects. Because of the broad-band nature of the secondary instability, spanwise periodicity of the three-dimensional disturbance will not be necessary. A single twist or kink may be enough to give birth to a patch of Λ vortices. Small curvature, small variation in strength, and finite spanwise extent of the vortices like the crests of a wave packet will barely cause dramatic changes. The spanwise and streamwise periodicity is essential for the pattern formation and distinction of various modes. The streamwise wavelength determines the spanwise scale of the pattern. However, the pattern is not vital to transition. Should not a single vortex convected with the local mean velocity and exposed to a single kink reveal the dynamics of the early stages of transition? Stuart (1965) studied peridic disturbances of a single vortex and

found scales similar to those in the experiments of Klebanoff et al (1962). More understanding of this subject might reveal the secret of 'bypasses'.

A FEEDBACK LOOP The global energy balance was studied by Croswell (1985) at amplitudes in the range of 1% and with the shape assumption for the basic flow. His findings are summarized in Figure 17. (1) For unstable TS waves, the transfer of energy from the mean flow to the two-dimensional wave is weak owing to the viscous mechanism; a considerable part of the gained energy is dissipated. (2) At sufficiently large amplitude A, the two-dimensional wave leads to parametric excitation of three-dimensional modes. (3) This excitation causes strong energy transfer from the mean flow into the three-dimensional wave. One part of this energy is dissipated, a second part increases the amplitude B of the three-dimensional wave. Steps two and three agree with results of Orszag & Patera (1983) for the instability of large-amplitude periodic motions. (4) A third part of the gained energy is transferred into the two-dimensional wave. This component draws off a minor amount of the three-dimensional growth but boosts the modest energy budget of the two-dimensional wave; the gain in growth rate is proportional to B^2/A. (5) Once B has attained a sufficiently large value, the energy of the two-dimensional wave can increase even if the TS mechanism fails to support this growth. This result is consistent with computational results of Spalart & Yang (1986). (6) Provided the gain in energy maintains the vital catalytic effect of the earlier steps, it enhances the parametric excitation. (7) Parametric excitation of three-dimensional disturbances by the two-dimensional field they create would establish a positive feedback loop and lead to self-sustained simultaneous growth of two-dimensional and three-dimensional waves. Existence of such a loop is supported by experience, experiment, and computation.

4.2 Threshold Conditions for Self-Sustained Growth

The energy analysis of Croswell involves approximations and neglects nonlinear effects such as the distortion of the velocity profiles and the generation of harmonics. Crouch & Herbert (1986) study a model of the nonlinear interaction based on an expansion about the periodic basic flow of a given amplitude A^*. The interaction model consists of two modes of secondary instability the first of which is two-dimensional. This mode describes the instability of the basic flow in a strictly two-dimensional framework. The other mode is either a subharmonic or fundamental mode of three-dimensional instability. Similar to the energy analysis, the expansion yields up to second order the amplitude equations

$$\frac{d\hat{A}}{dt} = a_0\hat{A} + a_1\hat{A}^2 + a_2B^2, \quad \frac{dB}{dt} = b_0B + b_1\hat{A}B \tag{12}$$

where $\hat{A} = A - A^*$, and a_0 and b_0 are the linear growth rates of the secondary modes. The parametric effect of A on the three-dimensional growth rate is

represented by $b_1 > 0$. The unusual self-interaction of the two-dimensional mode at second order is caused by the periodic character of the basic flow, and a_1 is of minor importance. Of prime interest is the coefficient a_2 which incorporates the effect of the three-dimensional disturbance on the two-dimensional mode. In accordance with the energy analysis, this effect is proportional to B^2, and a_2 is expected to be positive and large in comparison with $|a_1|$ whenever A^* is sufficiently large. Hence, the two-dimensional mode will always grow if $a_0\hat{A} + a_1\hat{A}^2 > 0$. Otherwise, it will grow only if B exceeds the threshold value B_t, where $B_t{}^2 = -(a_0\hat{A} + a_1\hat{A}^2)/a_2$. Numerical results of this study will be reported by Herbert (1987).

5. Concluding Remarks

The past decade has seen important progress in the exploration of the three-dimensional aspects of transition in boundary layers. Experiment, theory, and computation have contributed their share and taken their profit. Perhaps, the most significant progress is the consistency of the current picture of transition as it evolves from the ribbon-controlled background. Much work remains to be done to relax this and other restrictions that made the methods successful. The downstream changing conditions in boundary layers demand wider application of the spatial growth concept in theory and computation, especially when dealing with resonant interactions. The Floquet theory of secondary instability has revealed great potential in coping with the periodic flows that frequently evolve from primary instability. However, the assumptions inherent to this theory are not always easy to satisfy. Finding the key to transition caused by Görtler vortices or cross-flow vortices is still a challenge. Exploration of the nonlinear level of secondary instability is in an infant stage. When looking at tertiary instability, wave packets, and other localized phenomena, our tools seem not as powerful as we would like them to be. We have learned a lot, however, and this review is not the final report on transition in boundary layers.

Acknowledgment

I am grateful to my graduate students Fabio P. Bertolotti, Joseph W. Croswell, German R. Santos, and Jeffrey D. Crouch, who contributed valuable ideas and results. I benefited from discussions with many of those who wrote the cited papers. Mark V. Morkovin generously let me share his treasure of insight which guided and encouraged my steps. Charlotte R. Hawley improved my writing and prepared the manuscript and references. Through the years, the work on the Floquet theory of secondary instability has been supported by the National Science Foundation, the Office of Naval Research, and the Air Force Office of Scientific Research. While writing this review, I enjoyed support by the Air

Force Office of Scientific Research under Contract F49620-87-K-0005.

Literature Cited

Anders, J. B. and Blackwelder, R. F. 1980 "Longitudinal vortices in a transitioning boundary layer," in *Laminar-Turbulent Transition*, Ed. R. Eppler and H. Fasel, 110-119, Springer-Verlag.

Bayly, B. J., Orszag, S. A., and Herbert, Th. 1988 "Instability mechanisms in shear flow transition," *Ann. Rev. Fluid Mech.*, 20. This volume.

Benney, D. J. and Lin, C. C. 1960 "On the secondary motion induced by oscillations in a shear flow," *Phys. Fluids*, 3:656-657.

Bertolotti, F. P. 1985 "Temporal and spatial growth of subharmonic disturbances in Falkner-Skan flows," VPI & SU, M.S. thesis.

Bertolotti, F. P., Santos, G. R., and Herbert, Th. 1986 "Early stages of boundary-layer transition - an animated theory," 16 mm movie, VPI & SU.

Blackwelder, R. F. 1979 "Boundary-layer transition," *Phys. Fluids*, 22:583-584.

Bouthier, M. 1973 "Stabilité linéair des écoulements presque parallèles. Part II. La couche limite de Blasius," *J. de Mécanique*, 12:75-95.

Clever, R. M. and Busse, F. H. 1974 "Transition to time-dependent convection," *J. Fluid Mech.*, 65:625-645.

Coddington, E. A. and Levinson, N. 1955 *Theory of Ordinary Differential Equations*, McGraw-Hill.

Cornelius, K. C. 1985 "Three dimensional wave development during boundary layer transition," Lockheed Georgia Research Report LG85RR0004.

Craik, A. D. D. 1971 "Nonlinear resonant instability in boundary layers," *J. Fluid Mech.*, 50:393-413.

Croswell, J. W. 1985 "On the energetics of primary and secondary instabilities in plane Poiseuille flow," VPI & SU, M.S. thesis.

Crouch, J. D. and Herbert, Th. 1986 "Perturbation analysis of nonlinear secondary instability in boundary layers," *Bull. Am. Phys. Soc.*, 31:1718.

Davis, S. H. 1976 "The stability of time-periodic flows," *Ann. Rev. Fluid Mech.*, 8:57-74.

Fasel, H. 1976 "Investigation of the stability of boundary layers by a finite-difference model of the Navier-Stokes equations," *J. Fluid Mech.*, 78:355-383.

Fischer, T. M. and Dallmann, U. 1987 "Theoretical investigation of secondary instability of three-dimensional boundary-layer flows," AIAA Paper No. 87-1338.

Gad-el-Hak, M., Davis, S. H., McMurray, J. T., and Orszag, S. A. 1984 "On the stability of the decelerating laminar boundary layer," *J. Fluid Mech.*, 138:297-323.

Gaster, M. 1962 "A note on the relation between temporally-increasing and spatially-increasing disturbances in hydrodynamic stability," *J. Fluid Mech.*, 14:222-224.

Gaster, M. 1974 "On the effects of boundary-layer growth on flow stability," *J. Fluid Mech.*, 66:465-480.

Gaster, M. 1984 "On transition to turbulence in boundary layers," in *Turbulence and Chaotic Phenomena in Fluids*, Ed. T. Tatsumi, 99-106, North-Holland.

Goldstein, M. E. 1985 "Scattering of acoustic waves into Tollmien-Schlichting waves by small streamwise variations in surface geometry," *J. Fluid Mech.*, 154:509-529.

Gotoh, K. and Yamada, M. 1986 "Stability of spatially periodic flows," in *Encyclopedia of Fluid Mechanics*, 589-610, Gulf Publ. Co., Houston.

Hall, P. 1983 "The linear development of Görtler vortices in growing boundary layers," *J. Fluid Mech.*, 130:41-58.

Hall, P. 1986 "The nonlinear development

of Görtler vortices in growing boundary layers," ICASE Report No. 86-83. Submitted to J. Fluid Mech.

Hama, F. R. 1963 "Progressive deformation of a perturbed line vortex filament," *Phys. Fluids*, 6:526-534.

Hama, F. R., Long, J. D., and Hegarty, J. C. 1957 "On transition from laminar to turbulent flow," *J. Appl. Phys.*, 27:388-394.

Hama, F. R. and Nutant, J. 1963 "Detailed flow-field observations in the transition process in a thick boundary layer," in *Proc. 1961 Heat Transfer and Fluid Mechanics Inst.*, 77-93, Stanford Univ. Press.

Herbert, Th. 1975 "On finite amplitudes of periodic disturbances of the boundary layer along a flat plate," in *Proc. 4th Int. Conf. Numer. Meth. Fluid Dyn., Boulder, CO*, Lecture Notes in Physics, 35, :212-217, Springer-Verlag.

Herbert, Th. 1981 "A secondary instability mechanism in plane Poiseuille flow," *Bull. Amer. Phys. Soc.*, 26:1257.

Herbert, Th. 1983a "Secondary instability of plane channel flow to subharmonic three-dimensional disturbances," *Phys. Fluids*, 26:871-874.

Herbert, Th. 1983b "Subharmonic three-dimensional disturbances in unstable shear flows," AIAA Paper No. 83-1759.

Herbert, Th. 1984 "Analysis of the subharmonic route to transition in boundary layers," AIAA Paper No. 84-0009.

Herbert, Th. 1985 "Three-dimensional phenomena in the transitional flat-plate boundary layer," AIAA Paper No. 85-0489.

Herbert, Th. 1986 "Vortical mechanisms in shear flow transition," in *Direct and Large Eddy Simulation of Turbulence*, Ed. U. Schumann and R. Friedrich, 19-36, Vieweg-Verlag.

Herbert, Th. 1987 "On the mechanism of transition in boundary layers," AIAA Paper No. 87-1201.

Herbert, Th. and Bertolotti, F. P. 1985 "Effect of pressure gradients on the growth of subharmonic disturbances in boundary layers," in *Proc. Conf. on Low Reynolds Number Airfoil Aerodynamics*, Ed. T. J. Mueller, Univ. of Notre Dame.

Herbert, Th., Bertolotti, F. P., and Santos, G. R. 1986 "Floquet analysis of secondary instability in shear flows," in *Stability of Time-Dependent and Spatially Varying Flows*, Ed. D. L. Dwoyer and M. Y. Hussaini, 43-57, Springer-Verlag.

Herbert, Th. and Morkovin, M. V. 1980 "Dialogue on bridging some gaps in stability and transition research," in *Laminar-Turbulent Transition*, Ed. R. Eppler and H. Fasel, 47-72, Springer-Verlag.

Itoh, N. 1974 "Spatial growth of finite wave disturbances in parallel and nearly parallel flows, Part 1.," *Trans. Japan Soc. Aeron. Space Sci.*, 17:160-174.

Itoh, N. 1980 "Three-dimensional growth of finite wave disturbances in plane Poiseuille flow," *Trans. Japan Soc. Aeron. Space Sci.*, 23:91-103.

Kachanov, Yu. S., Kozlov, V. V., and Levchenko, V. Ya. 1977 "Nonlinear development of a wave in a boundary layer," *Izv. AN USSR, Mekh. Zhidk. i Gaza*, 3:49-53. (In Russian)

Kachanov, Yu. S., Kozlov, V. V., Levchenko, V. Ya., and Ramazanov, M. P. 1985 "On nature of K-breakdown of a laminar boundary layer. New experimental data," *in Laminar-Turbulent Transition*, Ed. V. V. Kozlov, 61-73, Springer-Verlag.

Kachanov, Yu. S. and Levchenko, V. Ya. 1982 "Resonant interactions of disturbances in transition to turbulence in a boundary layer," Preprint No. 10-82, I.T.A.M., USSR Acad. Sci., Novosibirsk. (In Russian)

Kachanov, Yu. S. and Levchenko, V. Ya. 1984 "The resonant interaction of disturbances at laminar-turbulent transition in a boundary layer," *J. Fluid Mech.*, 138:209-247.

Kelly, R. E. 1967 "On the stability of an inviscid shear layer which is periodic in space and time," *J. Fluid Mech.*, 27:657-689.

Klebanoff, P. S. and Tidstrom, K. D. 1959 "Evaluation of amplified waves leading to transition in a boundary layer with zero pressure gradient," NASA TN D-195.

Klebanoff, P. S., Tidstrom, K. D., and Sargent, L. M. 1962 "The three-dimensional

nature of boundary-layer instability," *J. Fluid Mech.*, 12:1-34.

Kleiser, L. 1982 "Spectral simulations of laminar-turbulent transition in plane Poiseuille flow and comparison with experiments," in *Proc. 8th Int. Conf. Numer. Meth. Fluid Dyn., Aachen, Germany*, Ed. E. Krause, Lecture Notes in Physics, 170, :280-287, Springer-Verlag.

Kleiser, L. and Laurien, E. 1985 "Three-dimensional numerical simulation of laminar-turbulent transition and its control by periodic disturbances," in *Laminar-Turbulent Transition*, Ed. V. V. Kozlov, 29-37, Springer-Verlag, Berlin, Heidelberg.

Knapp, C. F. and Roache, P. J. 1968 "A combined visual and hot-wire anemometer investigation of boundary-layer transition," *AIAA J.*, 6:29-36.

Kovasznay, L. S. G., Komoda, H., and Vasudeva, B. R. 1962 "Detailed flow field in transition," in *Proc. 1962 Heat Transfer and Fluid Mech. Inst.*, 1-26, Stanford Univ. Press.

Krist, S. E. and Zang, T. A. 1987 "Numerical simulation of channel flow transition," NASA Techn. Paper 2667.

Landahl, M. T. 1972 "Wave mechanics of breakdown," *J. Fluid Mech.*, 56:775-802.

Liepmann, H. W. 1943 "Investigations on laminar boundary-layer stability and transition on curved boundaries," NACA Adv. Conf. Rep. 3H30.

Malik, M. R. 1986 "Wave interaction in three-dimensional boundary layers," AIAA Paper No. 86-1129.

Maseev, L. M. 1968b "Occurrence of three-dimensional perturbations in a boundary layer," *Fluid Dyn.*, 3:23-24.

Maseev, L. M. 1968a "Secondary instability of boundary layers," Tr. MIITa No. 222. (In Russian).

Maslennikova, I. I. and Zelman, M. B. 1985 "On subharmonic-type laminar-turbulent transition in boundary layer," in *Laminar-Turbulent Transition*, Ed. V. V. Kozlov, 21-28, Springer-Verlag.

Maslowe, S. A. 1986 "Critical layers in shear flows," *Ann. Rev. Fluid Mech.*, 18:405-432.

May, C. L. and Kleiser, L. 1985 "Numerical simulation of subharmonic transition in plane Poiseuille flow," *Bull. Amer. Phys. Soc.*, 30:1748.

Morkovin, M. V. 1969 "On the many faces of transition," in *Viscous Drag Reduction*, Ed. C. S. Wells, 1-31, Plenum Press.

Morkovin, M. V. 1983 "Understanding transition to turbulence in shear layers - 1983," AFOSR Final Report AD-A134796.

Morkovin, M. V. 1985 "Guide to experiments on instability and laminar-turbulent transition in shear layers.," AIAA Professional Study Series: Instabilities and Transition to Turbulence, Cincinnati, OH. Course Notes.

Murdock, J. W. 1977 "A numerical study of nonlinear effects on boundary-layer stability," AIAA Paper No. 77-127.

Nakaya, C. 1980 "Three-dimensional waves in a boundary layer," in *Laminar-Turbulent Transition*, Ed. R. Eppler and H. Fasel, 239-242, Springer-Verlag.

Nayfeh, A. H. 1981 "Effect of streamwise vortices on Tollmien-Schlichting waves," *J. Fluid Mech.*, 107:441-453.

Nayfeh, A. H. 1985 "Three-dimensional spatial secondary instability in boundary-layer flows," AIAA Paper No. 85-1697.

Nayfeh, A. H. and Bozatli, A. N. 1979 "Secondary instability in boundary-layer flows," *Phys. Fluids*, 22:805-813.

Nishioka, M. and Asai, M. 1984 "Evolution of Tollmien-Schlichting waves into wall turbulence," in *Turbulence and Chaotic Phenomena in Fluids*, Ed. T. Tatsumi, 87-92, North-Holland.

Nishioka, M., Asai, M., and Iida, S. 1980 "An experimental investigation of secondary instability," in *Laminar-Turbulent Transition*, Ed. R. Eppler and H. Fasel, 37-46, Springer-Verlag.

Nishioka, M., Asai, M., and Iida, S. 1981 "Wall phenomena in the final stage of transition to turbulence," in *Transition and Turbulence*, Ed. R. E. Meyer, 113-126, Academic Press.

Nishioka, M., Iida, S., and Ichikawa, J. 1975 "An experimental investigation on the stability of plane Poiseuille flow," *J. Fluid Mech.*, 72:731-751.

Orszag, S. A. and Kells, L. C. 1980 "Transition to turbulence in plane Poiseuille flow

and plane Couette flow," *J. Fluid Mech.*, 96:159-206.

Orszag, S. A. and Patera, A. T. 1980 "Subcritical transition to turbulence in plane channel flows," *Phys. Rev. Lett.*, 45:989-993.

Orszag, S. A. and Patera, A. T. 1981 "Subcritical transition to turbulence in plane shear flows," in *Transition and Turbulence*, Ed. R. E. Meyer, 127-146, Academic Press.

Orszag, S. A. and Patera, A. T. 1983 "Secondary instability of wall-bounded shear flows," *J. Fluid Mech.*, 128:347-385.

Raetz, G. S. 1959 "A new theory of the cause of transition in fluid flows," NORAIR Report NOR-59-383, Hawthorne, CA.

Reed, H. 1984 "Wave-interactions in swept-wing flows," AIAA Paper No. 84-1678.

Reed, H. 1985 "Disturbance-wave interactions in flows with crossflow," AIAA Paper No. 85-0494.

Reshotko, E. 1976 "Boundary-layer stability and transition," *Ann. Rev. Fluid Mech.*, 8:311-349.

Santos, G. R. and Herbert, Th. 1986 "Combination resonance in boundary layers," *Bull. Am. Phys. Soc.*, 31:1718.

Saric, W. S., Kozlov, V. V., and Levchenko, V. Ya. 1984 "Forced and unforced subharmonic resonance in boundary layer transition," AIAA Paper No. 84-0007.

Saric, W. S. and Nayfeh, A. H. 1977 "Nonparallel stability of boundary layers with pressure gradients and suction," in *Laminar-Turbulent Transition*, 6/1-21, AGARD CP-224.

Saric, W. S. and Thomas, A. S. W. 1984 "Experiments on the subharmonic route to turbulence in boundary layers," in *Turbulence and Chaotic Phenomena in Fluids*, Ed. T. Tatsumi, 117-122, North-Holland.

Schlichting, H. 1933 "Zur Entstehung der Turbulenz bei der Plattenströmung," *Nachr. Ges. Wiss. Göttingen, Math.-Phys. Kl.*, 181-208.

Schubauer, G. B. and Skramstad, H. K. 1947 "Laminar boundary-layer oscillations and transition on a flat plate," *J. Res. Nat. Bur. Stand.*, 38:251-292. Reprint of NACA Adv. Conf. Rep. (1943).

Singer, B., Reed, H. L., and Ferziger, J. H. 1986 "Investigation of the effects of initial disturbances on plane channel transition," AIAA Paper No. 86-0433.

Spalart, P. R. and Yang, K. S. 1986 "Numerical simulation of boundary layers: Part 2. Ribbon-induced transition in Blasius flow," NASA Technical Memorandum 88221, 1-24.

Squire, H. B. 1933 "On the stability for three-dimensional disturbances of viscous fluid flow between parallel walls," *Proc. Roy. Soc. A.*, 142:621-628.

Srivastava, K. M. 1985 "Effect of streamwise vortices on Tollmien-Schlichting waves in growing boundary layers," Internal Report IB 221-85 A 07, DFVLR-AVA, Göttingen.

Stuart, J. T. 1962 "On three-dimensional non-linear effects in the stability of parallel flows," *Adv. Aero. Sci.*, 3:121-142.

Stuart, J. T. 1965 "The production of intense shear layers by vortex stretching and convection," AGARD Report 514.

Tam, C. K. W. 1986 "Excitation of instability waves by sound - a physical interpretation," *J. Sound Vibr.*, 105:169-172.

Tani, I. 1969 "Boundary layer transition," *Ann. Rev. Fluid Mech.*, 1:169-196.

Thomas, A. S. W. 1987 "Experiments on secondary instabilities in boundary layers," in *Proc. Tenth U.S. National Congress of Applied Mechanics, Austin, TX*, ASME.

Thomas, A. S. W. and Saric, W. S. 1981 "Harmonic and subharmonic waves during boundary-layer transition," *Bull. Amer. Phys. Soc.*, 26:1252.

Tollmien, W. 1929 "Über die Entstehung der Turbulenz," *Nachr. Ges. Wiss. Göttingen, Math.-Phys. Kl.*, 21-44.

Williams, D. R., Fasel, H., and Hama, F. R. 1984 "Experimental determination of the three-dimensional vorticity field in the boundary layer transition process," *J. Fluid Mech.*, 149:179-203.

Wortmann, F. X. 1977 "The incompressible fluid motion downstream of two-dimensional Tollmien-Schlichting waves," in *Laminar-Turbulent Transition*, 12-1-8,

AGARD CP-224.

Wortmann, F. X. 1981 "Boundary-layer waves and transition," in *Advances in Fluid Mechanics*, Ed. E. Krause, Lecture Notes in Physics, 148, :268-279, Springer-Verlag.

Wray, A. A. and Hussaini, M. Y. 1980 "Numerical experiments in boundary-layer stability," AIAA Paper No. 80-0275.

Zang, T. A. and Hussaini, M. Y. 1985 "Numerical experiments on subcritical transition mechanism," AIAA Paper No. 85-0296.

Literature Cited - To appear

Bertolotti, F. P. and Herbert, Th. 1987 "A study on visualizations of boundary-layer transition," ***Exp. Fluids.*** In preparation.

Corke, T. C. and Mangano, R. A. 1987 "Transition of a boundary layer: controlled fundamental-subharmonic interactions," in *Proc. IUTAM Symposium on Turbulence Management and Relaminarization*, Ed. H. W. Liepmann and R. Narasimha, Bangalore, India. To appear.

Mueller, T. J. 1987 "Laminar to turbulent transition using smoke visualization and hot-wire anemometry," in *Recent Advances in Turbulence*, Ed. R. E. A. Arndt and W. K. George, Hemisphere. To appear.

Saric, W. S. and Reed, H. L. 1987 "Three-dimensional stability of boundary layers," in *Proc. Perspectives in Turbulence Symp.*, Göttingen. To appear.

Figure Captions

Figure 1 Smoke-flow visualization of transition in the boundary layer over an axisymmetric body. Photograph by F. N. M. Brown. (Courtesy of the University of Notre Dame).

Figure 2 Staggered pattern of Λ vortices. (Courtesy of J. T. Kegelman).

Figure 3 Aligned pattern of Λ vortices. (Courtesy of W. S. Saric).

Figure 4 Threshold amplitudes A for the onset of three-dimensionality with spanwise wavenumber σ in the boundary layer. Curve 1: $R = 1203$, $\alpha = 0.43$, curve 2: $R = 519$, $\alpha = 0.27$. (Maseev 1968b).

Figure 5 Subharmonic growth rate σ_r as a function of the wavenumber b for $F = 124$, $R_{II} = 606$. (Herbert 1984).

Figure 6 Amplitude growth with the Reynolds number R at $F = 124$. (A) TS wave with $A_0 = 0.0044$, (B) subharmonic mode with $B_0 = 1.26 \cdot 10^{-5}$, $b = 0.33$. Comparison of the theory (——) with experiments (x, o) of Kachanov & Levchenko. (Herbert et al 1986)

Figure 7 Spatial growth rate γ_r vs. spanwise wave number β for the principal subharmonic mode. Results of (a) direct calculation and (b) transformation of temporal data. $R = 826$, $F = 83$, $A = 0.02$. (Herbert & Bertolotti 1985).

Figure 8 Stability diagram for the Blasius boundary layer and ribbon positions (+). The horizontal lines indicate frequency and Reynolds number range in the experiments.

Figure 9 Growth rate of three-dimensional disturbances as a function of the spanwise wavenumber β for $F = 58.8$, $R = 950$, and $A = 0.014$. Theory: (a) subharmonic, (b) fundamental. Computation by Spalart (1986): (o) subharmonic, (x) fundamental.

Figure 10 Growth rate σ_r for detuned modes at $F = 124$, $R = 606$, $A = 0.01$, $b = 0.33$. Subharmonic and fundamental modes correspond to $\hat{\alpha} = \alpha/2$ and α, respectively.

Figure 11 Normalized streamwise velocity components. Subharmonic mode, $\epsilon = 1$ (left), detuned mode $\epsilon = 0.5$ (middle), fundamental mode $\epsilon = 0$ (right). $R = 606$, $\hat{\alpha} = 0.1017$, $A = 0.01$, $\beta = 0.2$.

Figure 12 Normalized u'-distribution of the subharmonic mode at $F = 124$, $R = 608$, $A = 0.0122$, and $b = 0.38$. Theory (——) and experiment (o) of Kachanov & Levchenko.

Figure 13 Distribution of u' across the boundary layer for $F = 58.8$, $b = 0.243$, and $R = 960$. Theory: (a) peak, (b) valley. Experiment of Klebanoff et al: (o) peak, (x) valley.

Figure 14 Computer visualization of combination resonance at two different phases with respect to the TS wave.

Figure 15 Λ vortices in plane Poiseuille flow shown by the streamwise vorticity component at $R = 1500$. K-type (left) and H-type (right). (Krist & Zang 1987).

Figure 16 Amplitude growth curves for disturbances at different levels of the TS amplitude. (o) fundamental frequency f, $A_0 = 0.00163$, (+) subharmonic frequency $f/2$, $A_0 = 0.00163$, (Δ) f, $A_0 = 0.00654$, (x) $f/2$, $A_0 = 0.00645$. After Kachanov & Levchenko (1984).

Figure 17 Schematic of the energy transfer between mean flow $\mathbf{v}_0$, two-dimensional wave $\mathbf{v}_1$, and three-dimensional disturbances $\mathbf{v}_3$ (——), and catalytic effect of $\mathbf{v}_1$ (- - - -). The numbers refer to the text.

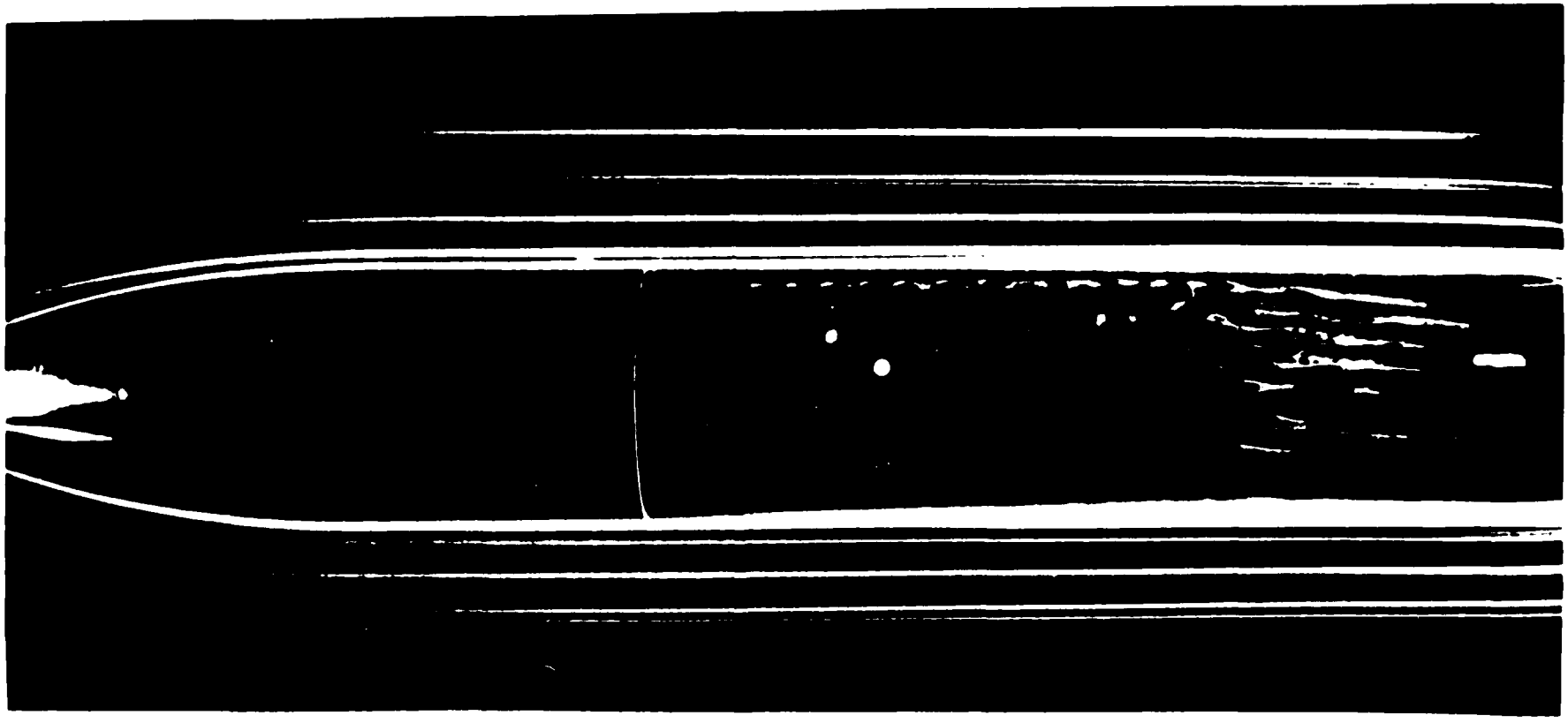

Figure 1 Smoke-flow visualization of transition in the boundary layer over an axisymmetric body. Photograph by F. N. M. Brown. (Courtesy of the University of Notre Dame).

Figure 2 Staggered pattern of Λ vortices. (Courtesy of J. T. Kegelman).

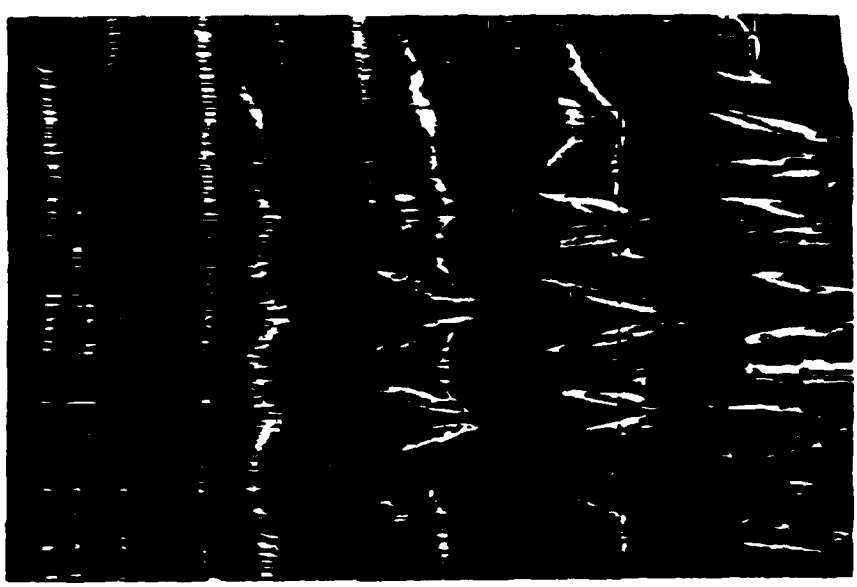

Figure 3 Aligned pattern of Λ vortices. (Courtesy of W. S. Saric).

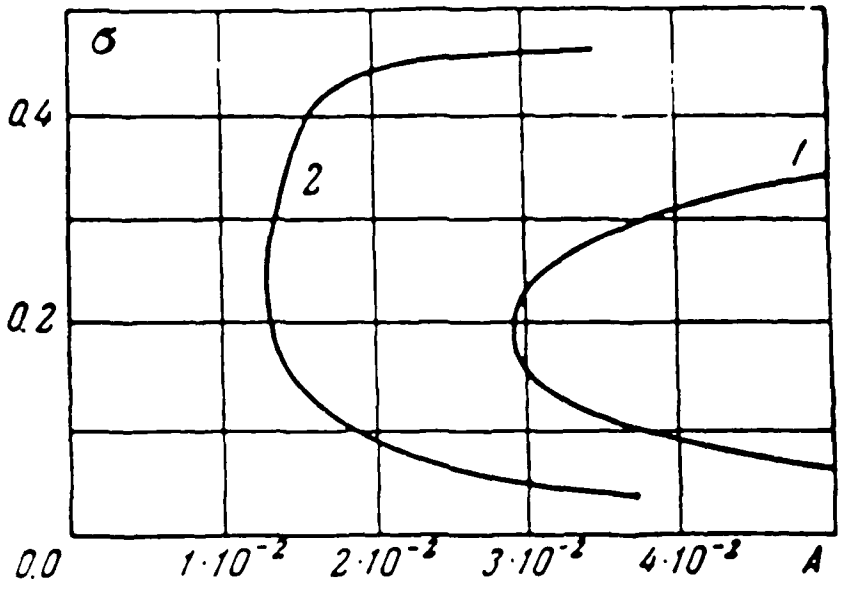

Figure 4 Threshold amplitudes A for the onset of three-dimensionality with spanwise wavenumber σ in the boundary layer. Curve 1: $R = 1203$, $\alpha = 0.43$, curve 2: $R = 519$, $\alpha = 0.27$. (Maseev 1968b).

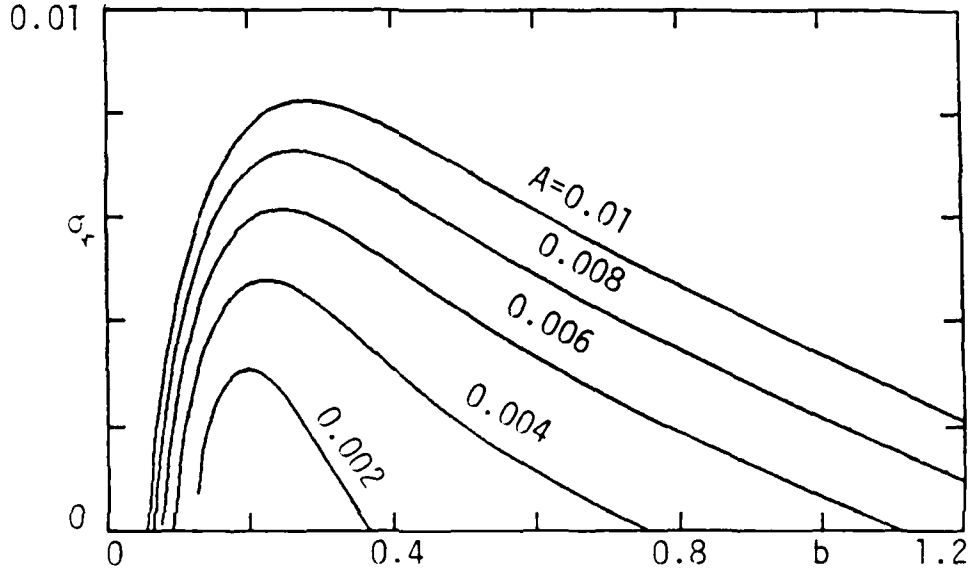

Figure 5 Subharmonic growth rate σ_r as a function of the wavenumber b for $F = 124$, $R_{II} = 606$. (Herbert 1984).

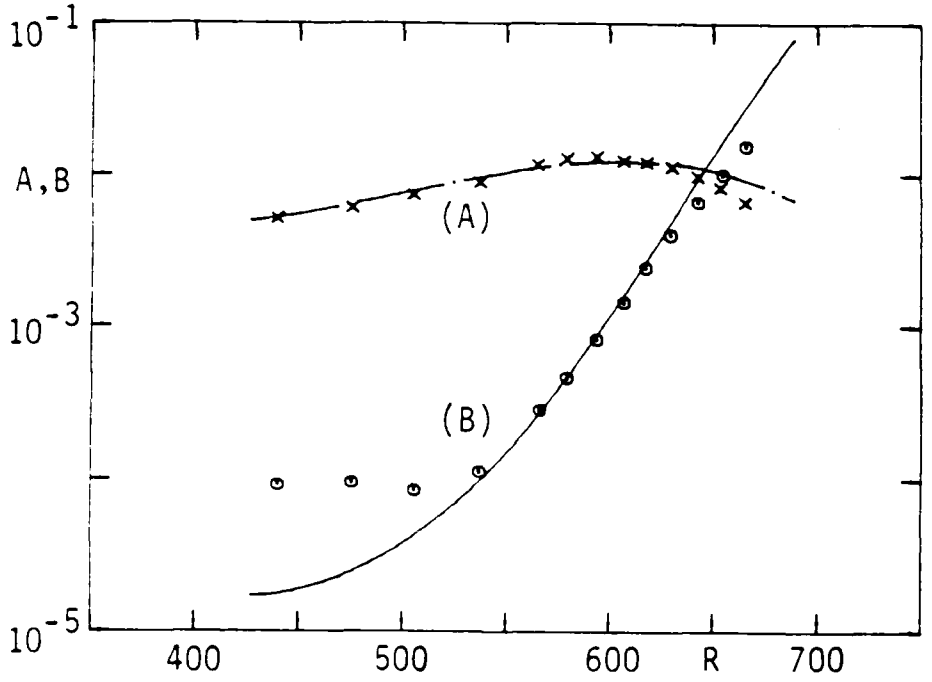

Figure 6 Amplitude growth with the Reynolds number R at $F = 124$. (A) TS wave with $A_0 = 0.0044$. (B) subharmonic mode with $B_0 = 1.26 \cdot 10^{-5}$, $b = 0.33$. Comparison of the theory (——) with experiments (x, o) of Kachanov & Levchenko. (Herbert et al 1986)

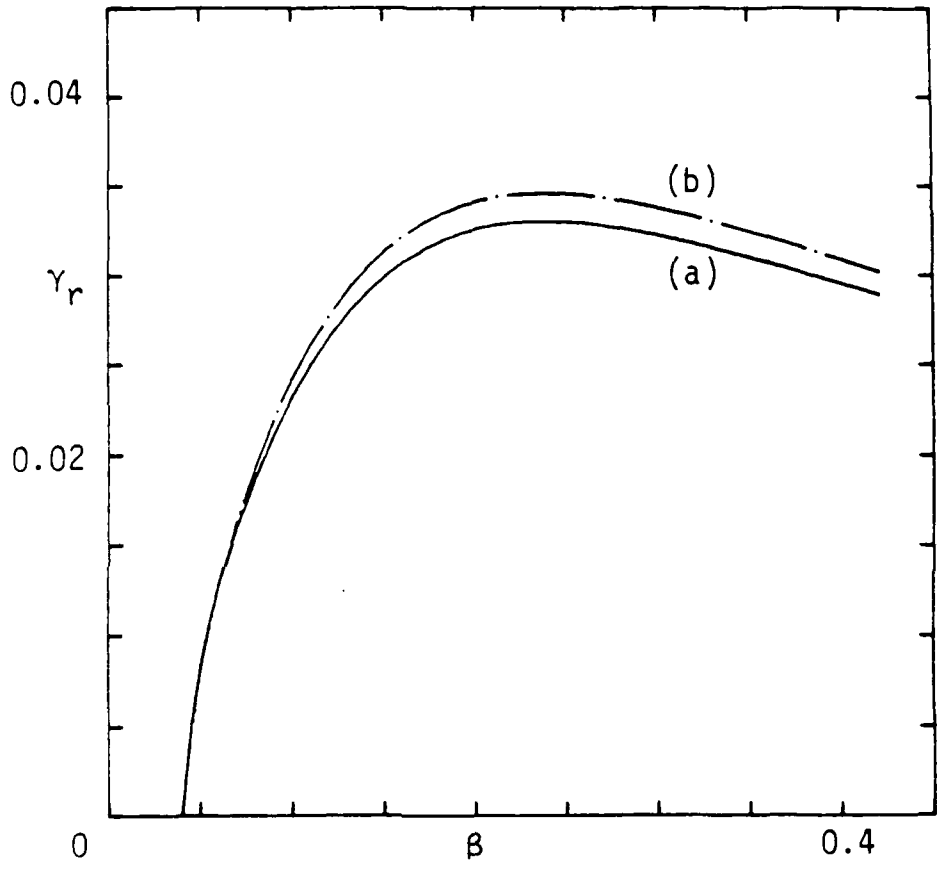

Figure 7 Spatial growth rate γ_r vs. spanwise wave number β for the principal subharmonic mode. Results of (a) direct calculation and (b) transformation of temporal data. $Re = 826$, $F = 83$, $A = 0.02$. (Herbert & Bertolotti 1985).

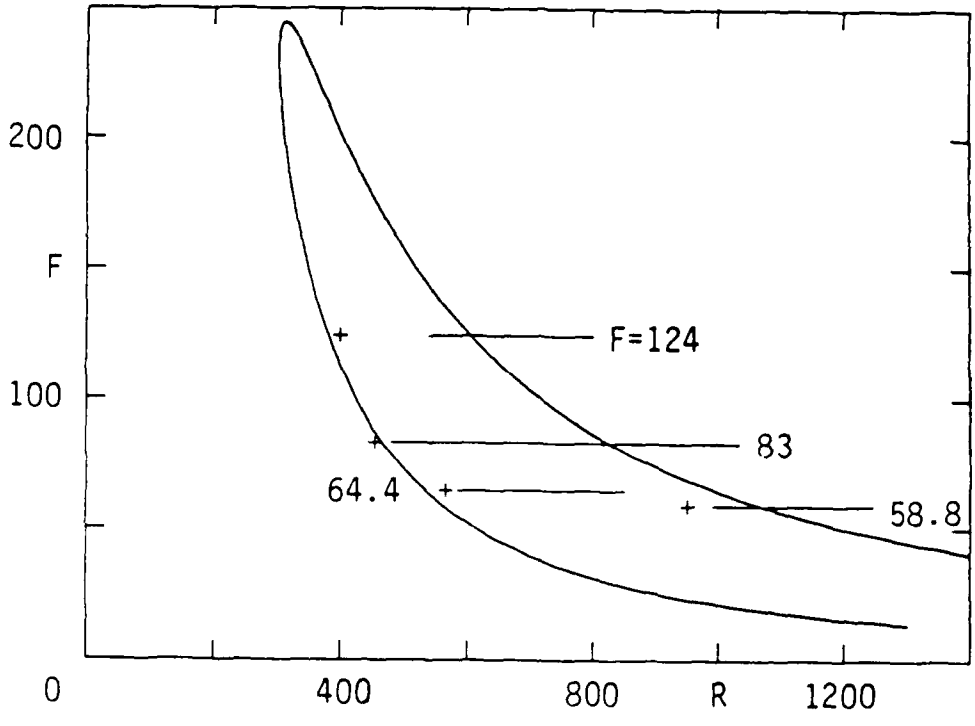

Figure 8 Stability diagram for the Blasius boundary layer and ribbon positions (+). The horizontal lines indicate frequency and Reynolds number range in the experiments.

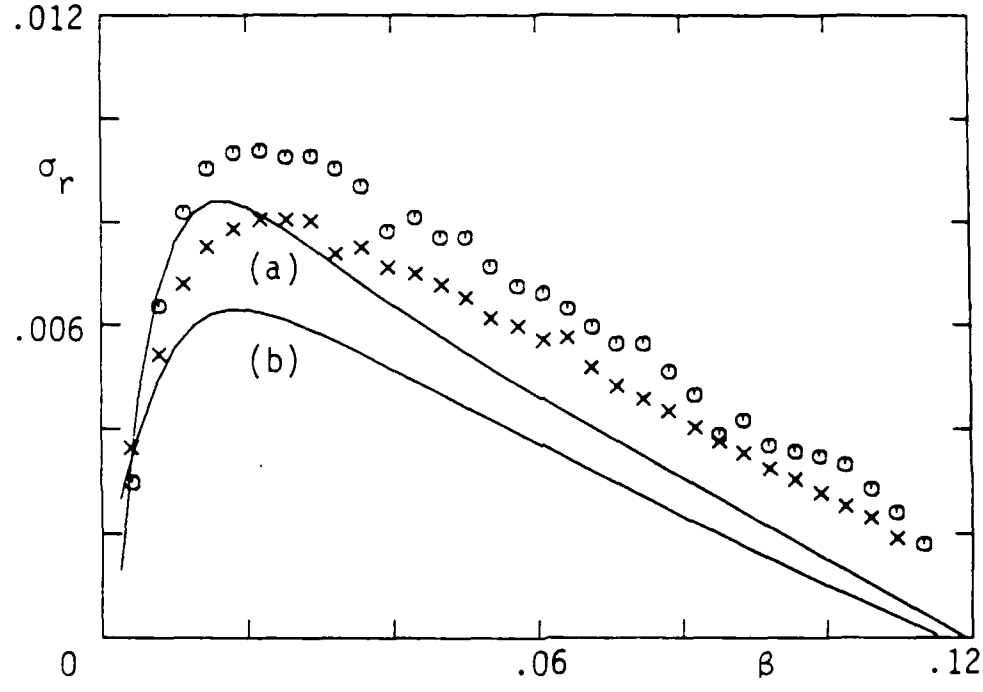

Figure 9 Growth rate of three-dimensional disturbances as a function of the spanwise wavenumber β for $F = 58.8$, $R = 950$, and $A = 0.014$ Theory: (a) subharmonic, (b) fundamental. Computation by Spalart (1986): (o) subharmonic, (x) fundamental.

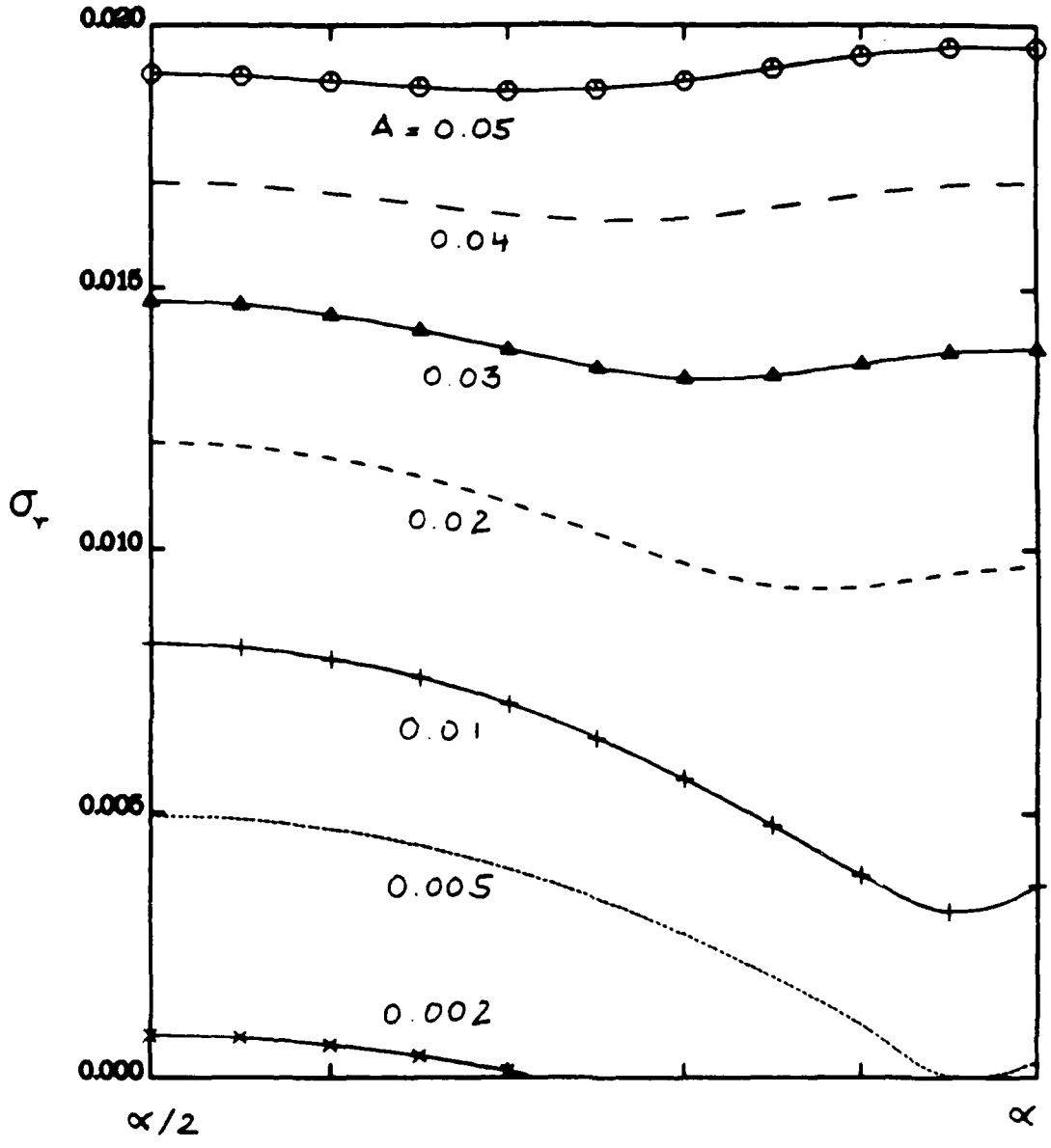

Figure 10 Growth rate σ_r for detuned modes at $F = 124$, $R = 606$, $A = 0.01$, $b = 0.33$. Subharmonic and fundamental modes correspond to $\hat{\alpha} = \alpha/2$ and α, respectively.

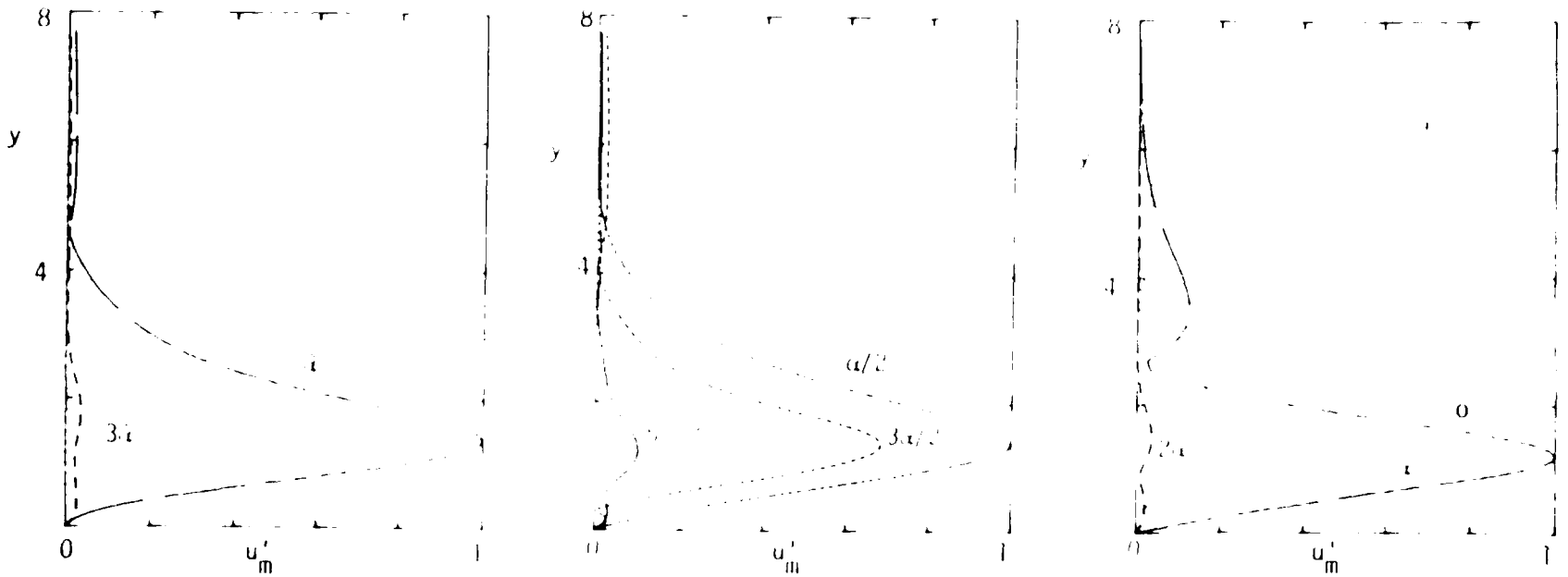

Figure 11 Normalized streamwise velocity components. Subharmonic mode, $c = 1$ (left), detuned mode $c = 0.5$ (middle), fundamental mode $c = 0$ (right). $R = 606$, $\alpha = 0.1017$, $A = 0.01$, $\beta = 0.2$.

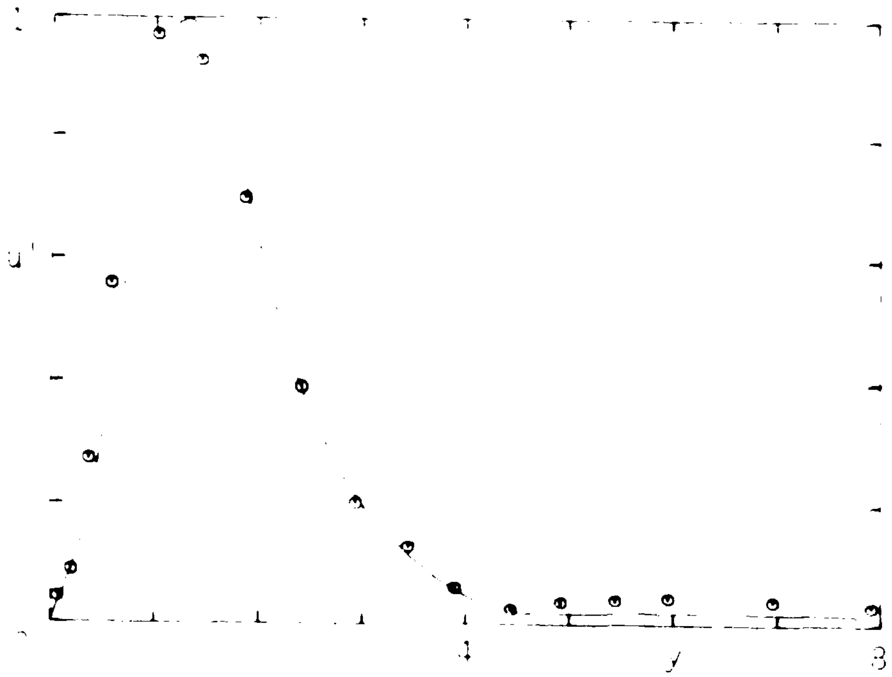

Figure 12 Normalized u' distribution [illegible] harmonic mode at $F = 121$, $R = 608$, $A = 0.0122$, and [illegible] $= 0.38$. Theory —— and experiment [illegible] of Kachanov & Levchenko [illegible].

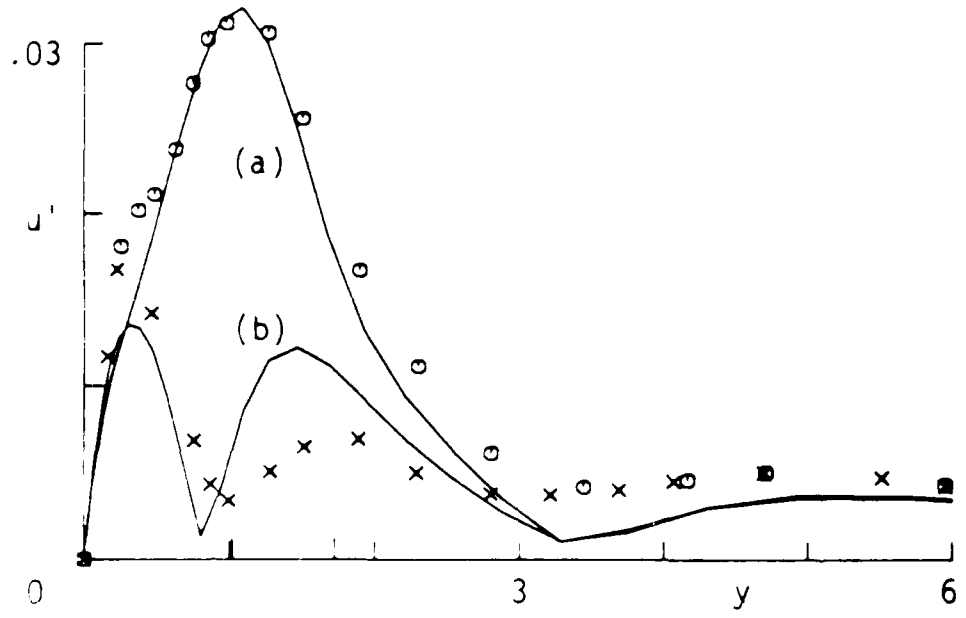

Figure 13 Distribution of u' across the boundary layer for $F = 58.8$, $b = 0.243$, and $R = 960$. Theory: (a) peak, (b) valley. Experiment of Klebanoff et al: (o) peak, (x) valley.

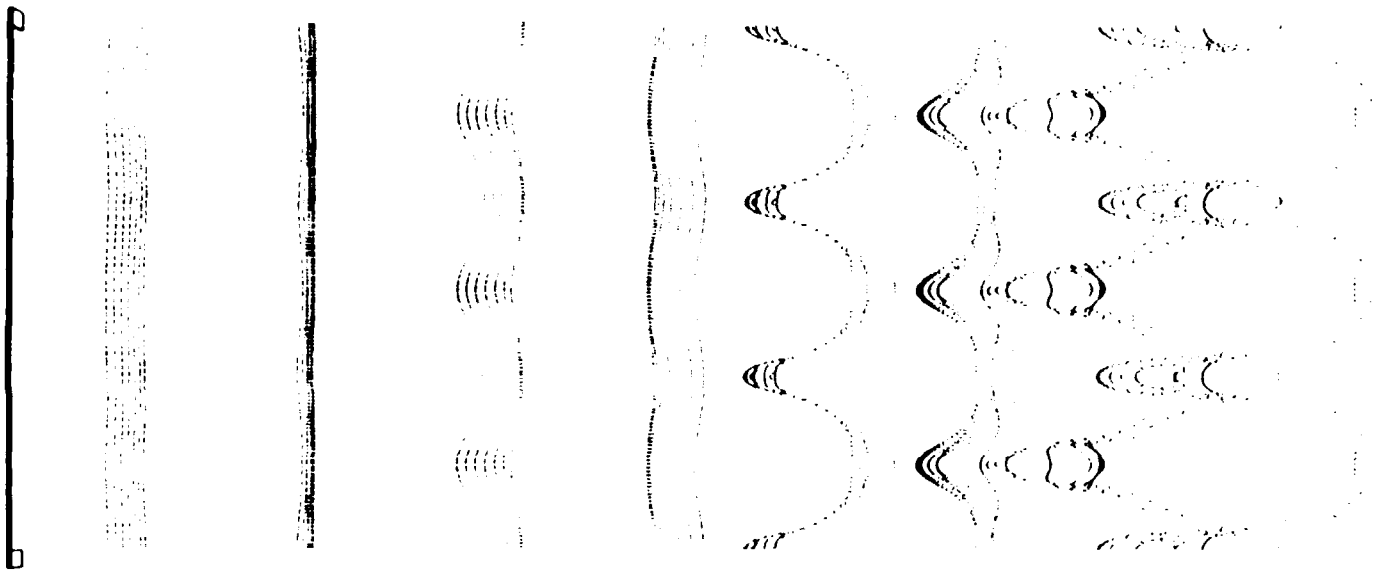

Figure 14 Computer visualization of combination resonance ($\epsilon = \pm 0.3$). Note the change-overs between aligned and staggered arrangement.

(Temporary)

Figure 15 A vortices in plane Poiseuille flow shown by the streamwise vorticity component at $R = 1500$. K-type (left) and H type (right). (Krist & Zang 1987).

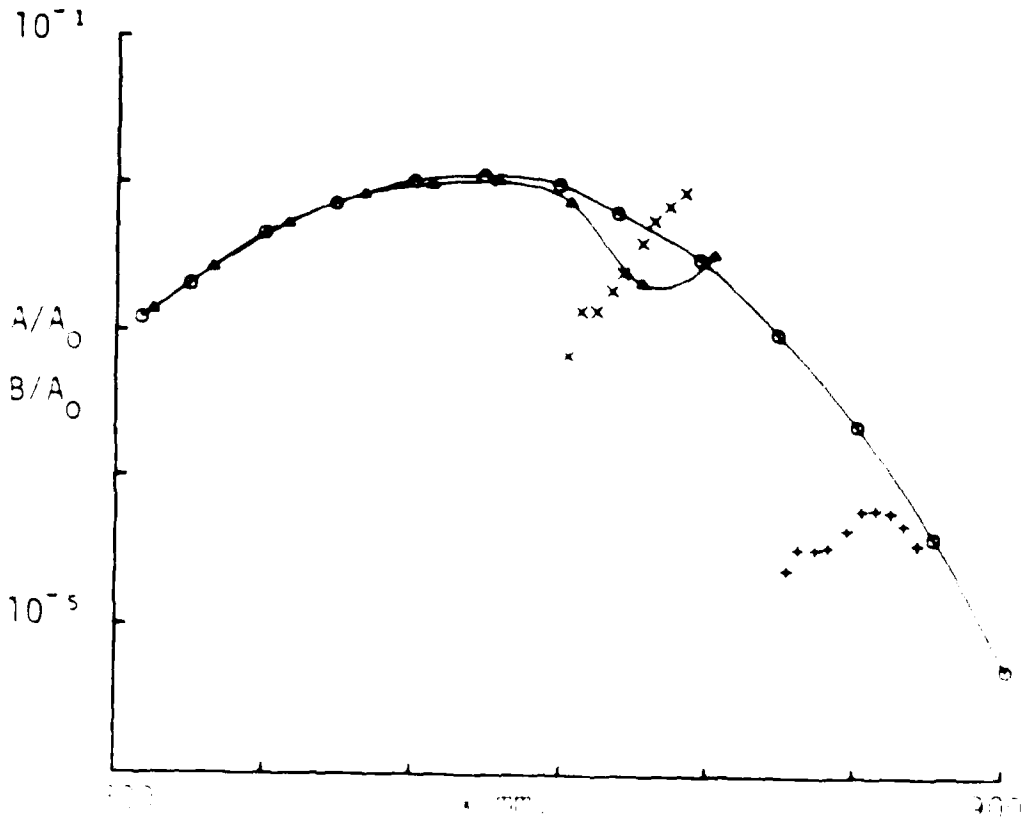

Amplitude growth curves for [illegible]
TS amplitude [illegible]
subharmonic [illegible]
$A_0 = 0.00^{\circ}54$ [illegible]
[illegible]

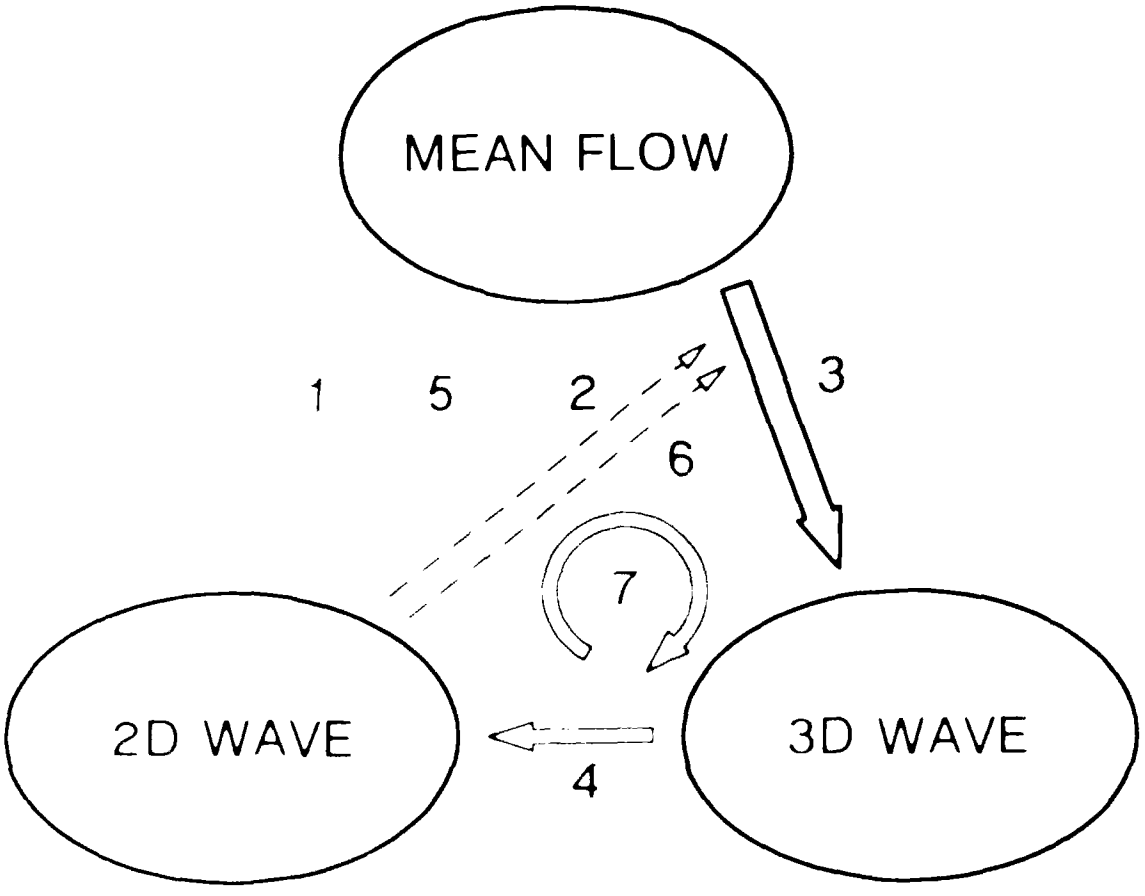
MEAN FLOW
1
5
2
3
6
7
2D WAVE
3D WAVE
4

END

DATE

FILMED

DEC.

1987